

# **Utilization of Waste Biomass Resources for Hydrogen-rich Syngas Production via Steam Co-gasification Process**

**Aisikaer Anniwaer**

**A Dissertation Submitted in Partial Fulfillment of the  
Requirements for the Degree of Doctor of Philosophy in  
Engineering**

**GRADUATE SCHOOL OF SCIENCE AND TECHNOLOGY  
HIROSAKI UNIVERSITY**

**2022**



## **Abstract**

In recent decades, the increasing global energy demand leads to a dramatic increase in the use of fossil fuels, which greatly arises the adverse health effect and irreversible environmental pollution. Fossil fuels such as coal, crude oil, and natural gas are the main energy sources for most of the countries to meet their energy demands. Concerning on depletion of fossil fuels prompts the world to explore renewable sources as the substitute of fossil fuels for energy production, in which biomass is regarded as the most promising one. Thermochemical conversion is considered as a more proper and efficient way to convert biomass wastes into value-added products. Biomass wastes are low-cost biomass energy resources, which can be converted into useful energy products including heat, power, and gaseous or liquid fuels using thermochemical conversion technologies. It is believed that biomass energy can probably be a good substitution of feedstock for hydrogen production via the gasification process. Hydrogen with the highest energy density (122 MJ/kg) is a potential energy carrier due to its cleanness and flexibility. As an alternative way, the renewable and sustainable biomass resource can be used for replacing fossil fuels to produce hydrogen. However, the use of biomass in large-scale industrial applications is restricted due to several disadvantages such as low bulk density, low energy density, wide and thin distribution, and unstable seasonal supply. As such, co-utilization of various kinds of biomass wastes as the mixture feedstock for the gasification process is more practical with relatively low cost. Meanwhile, different types of biomass have different physicochemical characteristics, which directly affect the gasification reactivity and gas production. In particular, some types of biomass containing high content of alkali and alkaline earth metals (AAEM) can be easily gasified at a lower gasification temperature and tend to produce syngas with larger content of hydrogen due to the catalytic effect provided by AAEM species. While some other types of biomass contained large content of lignin or high content of ash enriched in silicon compounds have a low gasification reactivity and tend to produce undesirable tar. More importantly, different synergy behaviors, either synergistic or inhibition effects, on co-gasification reactivity could be obtained from the combination of different kinds of biomass. More syngas production with higher content of hydrogen and less tar production could be obtained by co-gasification of different types of feedstock due to the synergistic effect

compared with gasification of single feedstock, while the inhibition effect would cause lower co-gasification reactivity and lower syngas production yield. Hence, it is necessary to investigate the compatibility and potential synergy effect in various biomass mixtures to provide a better understanding and guidance on biomass selection and corresponding co-gasification conditions for large-scale industrial applications. This dissertation, therefore, focuses on investigating co-gasification reactivity and performances, especially hydrogen production, of mixture feedstock and the potential synergy effect. The different carbon-based solid materials were selected as gasification co-feedstock i.e., biomass/biomass, biomass/biochar, and biomass/coal in order to utilize biomass resources more efficiently and explore the co-gasification behaviors and feasibility of hydrogen-rich syngas production by combination of biomass with different types of carbon-based materials.

Firstly, steam co-gasification behaviors and H<sub>2</sub>-rich gas production of biomass/biomass co-feedstock were studied. Three different types of biomass wastes, i.e., food waste (banana peel), forestry residues (Japanese cedarwood), and agricultural residues (rice husk) were selected as steam gasification feedstock in a fixed-bed reactor. For the co-gasification process, the banana peels were physically mixed with rice husk, Japanese cedarwood and their mixture respectively by different mixing weight ratios. The effects of reaction temperature and the addition amount of banana peel on the gas production yield were investigated by comparing the experimental data with the calculated ones based on the individual biomass gasification at the same condition. It was found that the banana peel with a high content of alkali and alkaline earth metals (AAEM) species exhibited not only high gasification reactivity but also a significant enhancing catalytic effect on the co-gasification process at the low temperature, especially with the biomass containing no silica species. The high content of silica species in the rice husk had a negative effect on the gasification reactivity of banana peel during the co-gasification since it could hinder the release of AAEM from the biomass and/or lead to the possible formation of inactive alkaline silicates. However, the combination of these three samples with the suitable weight ratio could improve the gasification performance at the low temperature due to the synergetic effect provided by high contents of potassium and calcium from banana peel and cedarwood respectively. Moreover, the addition of calcined seashells as the CaO source could further

improve the gas production yield, especially the hydrogen gas yield at a relatively low gasification temperature of 750 °C. This study provided guidance for the utilization of waste biomass for H<sub>2</sub>-rich syngas production via the steam gasification process and the combination of different types of biomass in a proper way to obtain higher gasification reactivity and syngas yields due to the synergistic effect during the co-gasification process.

Secondly, steam gasification and co-gasification of Japanese cedarwood and its commercial biochar were performed to investigate the effect of the carbonization process on gasification reactivity and H<sub>2</sub>-rich syngas production. Ultimate analysis, proximate analysis, Brunauer-Emmett-Teller (BET) surface area analysis, and scanning electron microscopy (SEM) were conducted to understand the changes in physicochemical properties caused by the carbonization process. The effects of gasification temperature and steam flow rate on gas production yield from the steam gasification of the individual samples were investigated at first, which showed larger gas production yield and less tar yield for the steam gasification of the commercial biochar than that of raw cedarwood, indicating that the commercial biochar obtained from the carbonization process was more beneficial for the gasification. The co-gasification of raw Japanese cedarwood and its commercial biochar with different mixing ratios was conducted at different reaction temperatures. The synergistic effect was obviously observed. Especially, the commercial biochar with the highly porous structure and high content of alkali and alkaline earth metal (AAEM) species might provide the catalytic effect on cracking and reforming of tar derived from the raw cedarwood, resulting in a larger H<sub>2</sub> yield. However, the catalytic effect and gasification reactivity of biochar would decrease by increasing the amount of raw-cedarwood in the blends due to the coke deposition on the surface of biochar. This study offered guidance for the efficient use of woody biomass for H<sub>2</sub>-rich syngas production via steam gasification and co-gasification processes.

Lastly, in order to efficiently utilize fruit waste and decrease the usage of low-rank coal as well as GHG emissions, steam co-gasification of banana peel (BP) with brown coal (BC) for H<sub>2</sub>-rich syngas production was studied in a fixed-bed reactor. The results showed that the gasification rate of BC was highly enhanced after mixing it with BP and the obvious synergistic effect was observed in all investigated three mixing ratios (i.e., 1:1, 1:4, 4:1), resulting in a

higher carbon conversion as well as H<sub>2</sub>-rich gas production yield during the co-gasification. However, the extent of promotion by synergistic effect was affected by the reaction temperature, mixing ratio, and steam amount. It was found that the high potassium (K) species content in the BP provided the catalytic effect on promoting not only water-gas shift reaction but also tar reforming/cracking, thereby enhancing the gasification of BC. In addition, it is confirmed that steam should be an important factor to promote the synergistic effect and H<sub>2</sub>-rich gas production. This study provided guidance on improving gasification reactivity and decreasing the reaction temperature of brown coal gasification by utilizing fruit waste to conduct the co-gasification process, producing higher content of H<sub>2</sub> at a lower gasification temperature.

## **Acknowledgments**

Firstly, the deepest gratitude is expressed to Prof. Abuliti Abudula, my supervisor, for kindly giving me the opportunity to conduct my PhD research in his laboratory. His motivation, advice, comments, teaching, and support gave me great support both academically and personally during my life in Japan. It was a great privilege and honor to work and study under his guidance. I am extremely grateful for what he has offered me. I will cherish him all my life.

The sincere thank and gratitude are also expressed to Prof. Guoqing Guan for his great advice and instruction. He has taught me the methodology to carry out the research and to present the research work as clearly as possible. I have benefited greatly from his wealth of knowledge, vision, and meticulous editing. I deeply thank him for providing full support and guidance so that I can solve all the difficulties during my PhD study.

I am also deeply indebted to Associate Professor Yoshida Akihiro and Assistant Professor Tao Yu. I really appreciate their encouragement and I feel very grateful for their guidance that improves me a lot. I also would like to express my gratitude to all the students and researchers e.g., Dr. Suchada, Dr. Irwan, Dr. Yohanes, and Dr. Nichaboon, in our research group for being very helpful during my research and daily life at Hirosaki University, Japan. Thanks for the energy, motivation, advice, care, and friendship that help me keep improving myself. Also, a great appreciation is expressed to Dr. Yutaka Kasai, Industrial Research Institute, Aomori Prefecture Industrial Technology Research Center (AITC), for the technical support of sample analysis.

I deeply acknowledge the Iwatani Naoji Foundation for providing the scholarship during my PhD study at Hirosaki University, Japan. The financial support from the Iwatani Naoji Foundation helped me pass through the stressful time caused by the COVID pandemic so that I can keep concentrating on my research.

I am extremely grateful to all my family members, especially my dear parents, Anwar and Arzigul, my sister and her husband, Hurxida and Elyar, for the endless love and support they have given me. Thank you for the encouragement, understanding, prayers, caring, sacrifices, and continuing support to complete this research work. Thank you for the love that never stops,

I love you all for now and forever. Also, I express my thanks to my friends in Japan and overseas for their love and support.

-Per Aspera, Ad Astra-

Askar Anwar

April, 2022

Hirosaki, Japan

## Table of Contents

|  |    |
|--|----|
| Abstract .....   | i  |
| Acknowledgments.....   | v  |
| List of Tables.....  | x  |
| List of Figures .....  | xi |
| CHAPTER 1: Introduction .....                                | 1  |
| 1.1 Motivation .....   | 1  |
| 1.2 Biomass gasification.....                                | 5  |
| 1.2.1 Biomass resources.....                                 | 5  |
| 1.2.1.1 Woody biomass.....                                   | 5  |
| 1.2.1.2 Agricultural residues.....                           | 6  |
| 1.2.1.3 Food waste.....                                      | 7  |
| 1.2.2 Gasifying agents.....                                  | 8  |
| 1.2.3 Steam gasification process .....                       | 9  |
| 1.2.4 Co-gasification process .....                          | 10 |
| 1.3 Effect of different factors on gasification process..... | 11 |
| 1.3.1 Feedstock type .....                                   | 11 |
| 1.3.2 Reaction temperature .....                             | 13 |
| 1.3.3 Steam amount.....                                      | 14 |
| 1.3.4 Catalyst .....   | 14 |
| 1.4 Objective .....  | 16 |
| Reference .....  | 17 |
| CHAPTER 2: Materials and Characterizations .....             | 27 |
| 2.1 Gasification feedstock .....                             | 27 |
| 2.2 Catalyst.....  | 27 |
| 2.3 Characterization apparatuses .....                       | 28 |
| 2.3.1 GC-TCD.....  | 28 |
| 2.3.2 Elemental analysis .....                               | 28 |
| 2.3.3 Scanning electron microscopy analysis (SEM) .....      | 28 |

|  |    |
|--|----|
| 2.3.4 X-ray diffraction analysis (XRD) .....   | 29 |
| 2.3.5 X-ray fluorescence analysis (XRF).....   | 29 |
| 2.3.6 Thermogravimetric analysis (TGA).....  | 29 |
| CHAPTER 3: Hydrogen-rich gas production from steam co-gasification of banana peel with agricultural residues and woody biomass ..... | 30 |
| 3.1 Introduction .....   | 30 |
| 3.2 Experimental .....   | 32 |
| 3.2.1 Materials .....  | 32 |
| 3.2.2 Steam gasification of biomass .....  | 34 |
| 3.2.3 Estimation of carbon conversion efficiency .....   | 35 |
| 3.3 Results and discussion.....  | 36 |
| 3.3.1 Thermogravimetry analysis .....  | 36 |
| 3.3.2 Steam gasification of individual biomass .....   | 41 |
| 3.3.3 Steam co-gasification of biomass mixture.....  | 45 |
| 3.3.4 Steam co-gasification of BP and RH .....   | 45 |
| 3.3.5 Steam co-gasification of BP and CW .....   | 50 |
| 3.3.6 Steam co-gasification of BP, CW and RH .....   | 54 |
| 3.3.7 Effect of the addition of calcined seashell .....  | 57 |
| 3.4 Conclusions .....  | 63 |
| References.....  | 63 |
| CHAPTER 4: Steam co-gasification of Japanese cedarwood and its commercial biochar for hydrogen-rich gas production .....             | 70 |
| 4.1 Introduction .....   | 70 |
| 4.2 Experimental .....   | 74 |
| 4.2.1 Materials .....  | 74 |
| 4.2.2 Steam gasification processes.....  | 75 |
| 4.2.3 Estimation of carbon conversion efficiency .....   | 76 |
| 4.3 Results and discussion.....  | 76 |
| 4.3.1 Characteristics of raw cedarwood and its biochar samples .....   | 76 |

|  |     |
|--|-----|
| 4.3.2 Steam gasification of individual raw biomass and biochar .....   | 81  |
| 4.3.2.1 Effect of reaction temperature .....   | 81  |
| 4.3.2.2 Effect of water injection rate .....   | 85  |
| 4.3.3 Steam co-gasification of raw biomass and biochar.....  | 89  |
| 4.4 Conclusions .....  | 95  |
| References.....  | 96  |
| CHAPTER 5: Utilization of fruit waste for H <sub>2</sub> -rich syngas production via steam co-gasification<br>with brown coal..... | 103 |
| 5.1 Introduction .....   | 103 |
| 5.2 Materials and methods.....   | 106 |
| 5.2.1 Materials .....  | 106 |
| 5.2.2 Apparatus and procedure.....   | 108 |
| 5.2.3 Carbon conversion efficiency .....   | 109 |
| 5.3 Results and discussion.....  | 109 |
| 5.3.1 Effect of reaction temperature.....  | 109 |
| 5.3.2 Effects of blending ratio and reaction time.....   | 115 |
| 5.3.2.1 Effect of blending ratio.....  | 115 |
| 5.3.2.2 Effect of reaction time .....  | 119 |
| 5.3.3 Effect of steam flow rate.....   | 122 |
| 5.4 Conclusion.....  | 128 |
| References.....  | 129 |
| CHAPTER 6: Conclusions and Future Perspective.....   | 135 |
| 6.1 Conclusions .....  | 135 |
| 6.2 Future perspective .....   | 137 |

## List of Tables

|   |     |
|---|-----|
| <b>Table 1.1</b> Benefits and drawbacks of different gasifying agents.....  | 9   |
| <b>Table 1.2</b> Main reactions in biomass steam gasification. ....   | 10  |
| <b>Table 2.1</b> Gasification feedstock used in this study.....   | 27  |
| <b>Table 3.1</b> Ultimate analysis results of biomass samples. ....   | 33  |
| <b>Table 3.2</b> Main compositions of biomass ash samples and calcined shell (CS). ....   | 33  |
| <b>Table 3.3</b> R50 values at T50 and of different samples based on TG analysis results.....   | 41  |
| <b>Table 4.1</b> Ultimate and proximate analyses of raw cedarwood and its commercial biochar samples.....   | 79  |
| <b>Table 4.2</b> Main compositions of ash residues of raw cedarwood (RCW) and its biochar (CBC). ....   | 80  |
| <b>Table 4.3</b> BET surface area analysis of raw cedarwood and its biochar samples. ....   | 81  |
| <b>Table 4.4</b> Conversion rate, H <sub>2</sub> concentration, and carbon conversion efficiency results from the gasification of the raw cedarwood and its biochar at 650, 750 and 850 °C.....                           | 85  |
| <b>Table 4.5</b> Conversion rate, H <sub>2</sub> concentration, and carbon conversion efficiency results from gasification of raw cedarwood and its biochar at 750 °C with three different water injection rates. ....    | 89  |
| <b>Table 4.6</b> Conversion rate, H <sub>2</sub> concentration, and carbon conversion efficiency results from co-gasification of raw biomass and the biochar at 750 °C and 850 °C with three different mixing ratios..... | 95  |
| <b>Table 5.1</b> Ultimate and proximate analyses of BP and BC. ....   | 107 |
| <b>Table 5.2</b> Main elemental compositions of ash residues of BP and BC.....  | 107 |
| <b>Table 5.3</b> Elemental analysis results of chars derived from pyrolysis of BP, BC, and their mixture sample at 750 °C.....  | 127 |
| <b>Table 5.4</b> Main components of chars derived from pyrolysis of BP, BC, and their mixture sample at 750 °C. ....  | 128 |

## List of Figures

|  |    |
|--|----|
| <b>Fig 1.1</b> Carbon neutral of biomass.....  | 2  |
| <b>Fig 1.2</b> Hydrogen production methods. ....   | 4  |
| <b>Fig 1.3</b> Thermochemical conversion methods of biomass. ....  | 5  |
| <b>Fig 1.4</b> Major sources of biomass.....   | 8  |
| <b>Fig 2.1</b> Preparation of CaO catalyst.....  | 28 |
| <b>Fig 3.1</b> Schematic diagram of a fixed-bed reactor for steam gasification of biomass.....   | 35 |
| <b>Fig 3.2</b> TGA and DTG analyses for the individual samples (a) (b) and blends (c) (d) in N <sub>2</sub> atmosphere at 10 °C/min heating rate. ....   | 40 |
| <b>Fig 3.3</b> Steam gasification of three types of individual biomass at three different temperatures with a water injection rate of 0.15 g/min: (a) gas yield; (b) carbon conversion efficiency to gas. ....   | 44 |
| <b>Fig 3.4</b> Gas yields from steam co-gasification of BP and RH (a): at 750 °C; (b): at 850 °C, and compared with the predicted ones; (c) Carbon conversion efficiency to gas; (d) XRD analysis for the residues after the gasification. ....  | 49 |
| <b>Fig 3.5</b> Gas yields from steam co-gasification of BP and RH (a): at 750 °C; (b): at 850 °C; (c): comparison of experimental results obtained at 750 °C and 850 °C; (d) Carbon conversion efficiencies to gas.....  | 53 |
| <b>Fig 3.6</b> (a) Steam co-gasification of the mixture (BP+CW+RH) samples with different mixing weight ratios; (b) Carbon conversion efficiency to gas for the mixture samples. ....  | 56 |
| <b>Fig 3.7</b> (a) and (b): Effect of the CS addition on the gas yield in different cases at 750 °C with a biomass/CS mixing weight ratio of 1:1; (c): Comparison of the different co-gasification processes with and without CS addition; (d): Comparison of carbon conversion efficiencies to gas by using different mixture samples. .... | 62 |
| <b>Fig 4.1</b> TGA and DTG curves of raw-cedarwood (RCW) and commercial biochar (CBC) samples in N <sub>2</sub> atmosphere.....  | 80 |
| <b>Fig 4.2</b> SEM images of raw cedarwood (a, b) and its biochar (c, d). ....   | 81 |
| <b>Fig 4.3</b> Gas yields from raw biomass (a) and biochar (b) samples at the reaction temperatures of 650, 750, and 850 °C. ....  | 84 |

|  |     |
|--|-----|
| <b>Fig 4.4</b> Gas yields from raw biomass (a) and biochar (b) samples at 750 °C with three different water injection rates. ....  | 88  |
| <b>Fig 4.5</b> Gas yields from the mixture samples of raw biomass and the biochar at 750 °C (a,b,c) and 850 °C (d,e,f) with three different mixing ratios (2:1, 1:1, 1:2).....                   | 93  |
| <b>Fig 4.6</b> TGA and DTG curves of raw-cedarwood (RCW) and commercial biochar (CBC) with the weight ratio of 1:1 in N <sub>2</sub> atmosphere. ....  | 94  |
| <b>Fig 4.7</b> Illustration of possible tar reforming mechanism over biochar in the crucible during the TG analysis. ....  | 94  |
| <b>Fig 5.1</b> Thermogravity analysis (TGA) of BP and BC in N <sub>2</sub> atmosphere. ....  | 108 |
| <b>Fig 5.2</b> Gas yields from steam gasifications of individual samples (a) and mixture sample (b); (c) carbon conversion efficiency to gas. ....   | 115 |
| <b>Fig 5.3</b> Gas yields (a) and carbon conversion efficiencies (b) from co-gasifications of BP and BC with three different blending ratios at 750 °C. ....                                     | 118 |
| <b>Fig 5.4</b> Gas yields (a) and carbon conversion efficiency (b) from co-gasification of BP and BC with three different blending ratios at 750 °C in a shorter reaction time (30 min). ....    | 121 |
| <b>Fig 5.5</b> Gas yields from the steam gasifications of individual samples (a) and mixture sample (b) at 750 °C with different steam flow rates ; (c) carbon conversion efficiency to gas..... | 127 |
| <b>Fig 6.1</b> Utilization of waste biomass for achieving the circular economy.....  | 140 |

# CHAPTER 1: Introduction

## 1.1 Motivation

Energy is an indispensable requirement for modern life. The consumption and dependence on energy have been increasing significantly with the rapid growth of the world population and the global economy. To date, the energy market is still dominated by fossil fuels which contribute 87% of global energy consumption [1]. Although traditional fossil energy occupied most of the energy consumption of the world, the overuse of non-renewable fossil fuels can lead to climate change, environmental pollution, and other issues. The combustion of fossil fuels emitted harmful greenhouse gases (GHG) such as carbon dioxide ( $\text{CO}_2$ ), methane ( $\text{CH}_4$ ), nitrous oxide ( $\text{N}_2\text{O}$ ), etc. The emission of  $\text{CO}_2$  accounts for 76% share of the total GHG emissions which are mostly contributed by fossil fuels and industrial activities [2]. The emission of  $\text{CO}_2$  causes global scale impact which is regarded as the major factor of climate change. Moreover, fossil fuels are limited resources and distributed unevenly around the earth, which means the country that lacks domestic reserves of fossil fuels highly depends on imports from foreign countries to satisfy energy consumption demands. Under such circumstances, the exploration of renewable energy resources which are abundant, environmental-friendly, and have low GHG emissions is becoming more and more urgent. Among all the renewable energy sources such as solar, wind, geothermal, tide, etc. biomass is considered as a promising energy resource due to the environmental benefits such as renewability, carbon-neutrality, and abundant reserve. Compared with biomass resources, other renewable energy resources have some limitations, for example, solar energy cannot be collected during the night, wind energy requires strong and stable wind, geothermal energy depends on location-specific. Therefore, biomass is considered as an organic renewable alternative energy source to fossil fuels for meeting energy demands. Biomass is biodegradable non-fossilized organic material that has obtained and stored energy from the sun such as wood, crops, seagrass, animal wastes, etc. For thousands of years, people have burned wood to cook food and heat homes. Biomass is ranked as the 4<sup>th</sup> largest energy source after coal, natural gas, and crude oil [3]. According to Global Energy Review, biomass contributed about 50% of energy production among the renewable

energy sources and provided 12% of the total final energy consumption in 2020 [4]. Moreover, compared with fossil fuels, biomass contains low content of nitrogen and sulfur and the use of biomass can be considered as carbon-neutral. As shown in **Fig 1.1**, biomass obtains energy from the sun during the process called photosynthesis, the obtained energy helps biomass convert water and CO<sub>2</sub> into oxygen and sugars. Biomass can be converted into biogas or biofuels which can produce heat and power by burning. The produced CO<sub>2</sub> from biomass utilization processes can be adsorbed by biomass via photosynthesis while growing. Thus, the utilization of biomass can not only replace non-renewable fossil fuels for energy production but also can contribute to a net reduction of GHG emissions.

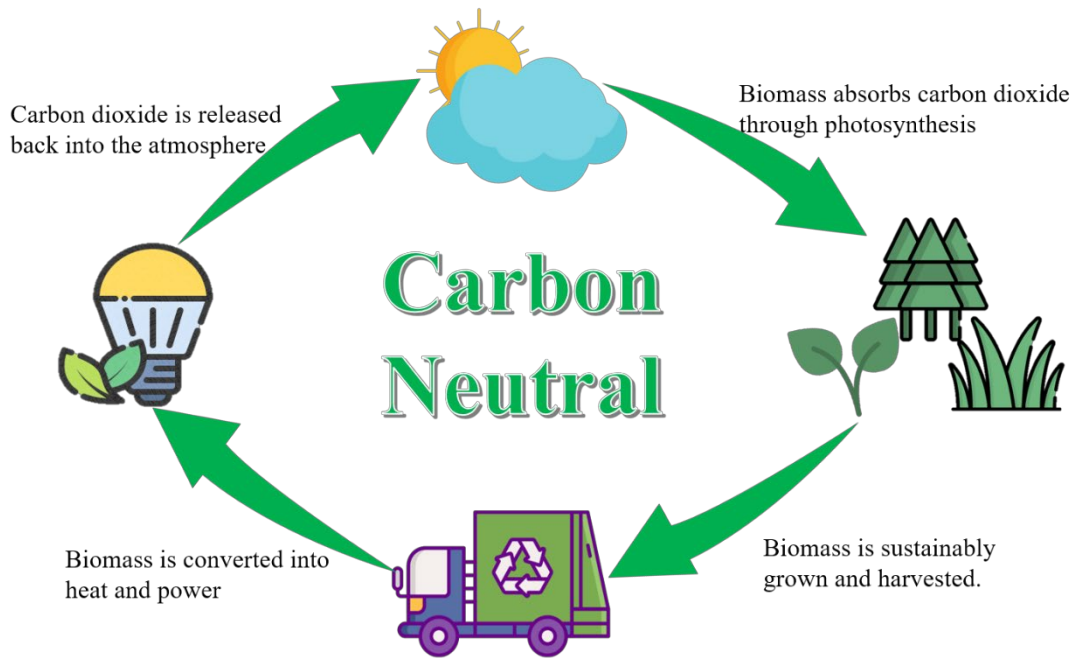


**Fig 1.1** Carbon neutral of biomass.

Japan is the 4<sup>th</sup> largest energy consumer in the world and the energy sector in Japan is also dominated by traditional fossil fuels such as oil, coal, and natural gas, which accounted for 88% of the total primary energy supply [5]. Oil is the largest energy source in Japan followed by coal and natural gas, accounting for 38%, 27%, and 23% of the total primary energy supply respectively in 2019 [5]. However, Japan is short of significant domestic sources of energy and highly depends on importing large amounts of energy resources such as crude oil, natural gas, coal, and uranium. The degree of dependency on fossil fuels increased from 81% to 88% from 2010 to 2019 due to the impacts of the Great East Japan Earthquake. The shutdown of nuclear

power plants led to a decrease in energy self-sufficiency ratio and an increase in dependency on fossil fuels, especially coal and natural gas, which are the largest sources of power generation in Japan. Consequently, the amount of GHG emissions had been increasing and reaching 1.4 billion tons the highest ever in 2013 [6]. The Fukushima accident has pushed Japan to further develop renewable and sustainable energy. Japan launched the Basic Hydrogen Strategy in 2017, becoming the first country to adopt a national hydrogen framework, which aims to make hydrogen play a vital role in the transition to carbon-free societies. Japan aims to build a global hydrogen supply chain by producing 0.8 million fuel cell vehicles and more than 5 million residential fuel cells [7]. At the 2020 Tokyo Olympics, Japan showcased the determination on establishing the hydrogen society and showed on a global scale how hydrogen can be applied in a wide range. The Tokyo 2020 Olympic Village is Japan's first full-scale hydrogen infrastructure, hydrogen was used to provide heat, hot water, and light for 11,000 athletes which the electricity was generated using pure-hydrogen fuel cells.

In the energy sector, hydrogen ( $H_2$ ) energy is regarded as a promising clean energy source and efficient energy storage medium which is expected to play a central role in replacing oil and other resources. Among all the fuels and energy carriers,  $H_2$  has the highest energy density (122 kJ/kg) and the by-product from the combustion of  $H_2$  is only water, which shows a great potential to be an effective alternative to gasoline [8]. Moreover,  $H_2$  is a basic feedstock in various industries such as oil refining industry, fertilizer industry, chemical industry, etc. As shown in **Fig 1.2**,  $H_2$  is a secondary form of energy that has to be artificially generated from some modern process technologies such as water electrolysis, gasification, and steam reforming of coal, natural gas, and oil. To date, industrial-scale  $H_2$  production has been dominated by fossil fuels using the steam reforming process [9]. Due to the concerns on depletion of fossil fuels and environmental impacts caused by the use of fossil fuels, it is necessary to find alternative sources for  $H_2$  generation. Biomass has been considered as the ideal primary source to replace fossil fuels for  $H_2$  production. At present,  $H_2$  can be generated from biomass via thermochemical, biological, and electrolysis methods [10-12]. The thermochemical route is getting more attention since biological and electrolysis routes are difficult to be applied to large-scale production and have low production rates. As shown in

**Fig 1.3**, the thermochemical conversion process of biomass mainly includes direct combustion, pyrolysis, and gasification. Among these three thermochemical conversion technologies, gasification is a promising method for converting solid biomass materials into a more practical and clean fuel called combustible syngas which mainly includes  $H_2$ ,  $CO_2$ , methane ( $CH_4$ ), and carbon monoxide ( $CO$ ). Gasification is a thermochemical conversion process that converts organic or carbonaceous materials into combustible syngas in the presence of a quantity of oxygen less than the combustion process. The produced syngas can be further used in a wide range of applications such as power generation (fuel cells and gas turbine), or as feedstock to produce liquid fuels and chemicals [13, 14].

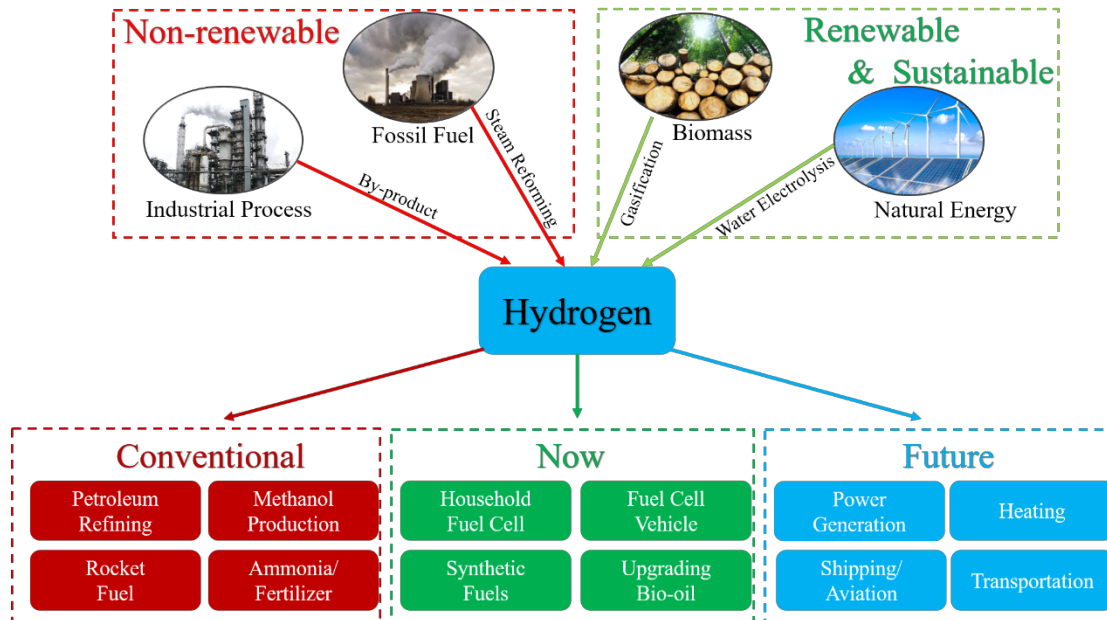


**Fig 1.2** Hydrogen production methods.

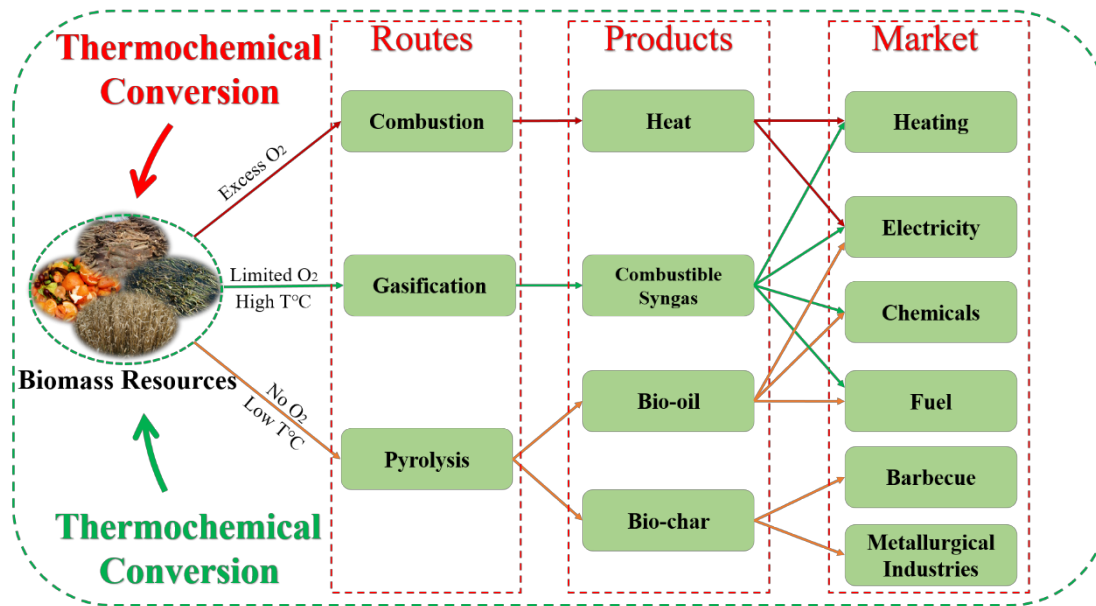


**Fig 1.3** Thermochemical conversion methods of biomass.

## 1.2 Biomass gasification

### 1.2.1 Biomass resources

Biomass is biodegradable non-fossilized organic matter such as plants, algae, and animal wastes, that can be used as an energy source [12, 15]. Biomass is mainly composed of cellulose, hemicellulose, lignin, and minerals (ash), which affect the product composition from biomass steam gasification. As shown in **Fig 1.4**, biomass is available in various forms, including woody biomass from forestry, agricultural crops and residues (such as straw, rice husk, sugarcane bagasse), sewage, municipal solid wastes (MSW), industrial wastes (such as black liquor, food processing wastes), and animal manure. Generally, biomass can be classified into three categories [10]: (1) Natural: the biomass produced without human intervention; (2) Residual: the biomass remains from farming and different kind of industries; (3) Energy Crops: this is the industrial growth of certain types of plants to obtain energy from them. The wide varieties of biomass sources provide sufficient options for each country to utilize the appropriate domestic biomass resources.

#### 1.2.1.1 Woody biomass

Woody biomass has been preferred to be utilized to generate heat and power compared with other biomass sources due to the various advantages of woody biomass such as easy handling,

high energy content, and relative-high fixed carbon content. In 2019, 1.9 billion m<sup>3</sup> of wood fuel, which is used for cooking, heating, or power generation, was produced globally [15, 16]. Woody biomass contains three main components: cellulose, hemicellulose, and lignin. Cellulose is the main component of cell walls and hemicellulose is also present in cell walls, while lignin with an aromatic structure acts as a binding agent [16]. Wood can be classified into softwood (like spruce) and hardwoods (like birch). Different kinds of woody biomass contain different contents of hemicellulose, cellulose, and lignin. Generally, softwoods contain a larger content of lignin and less holocellulose (cellulose + hemicellulose) as compared to hardwood types [17]. The pelletizing process is an important pre-treatment for woody biomass, which can increase the heating value by increasing the bulk density and volatile matter of woody biomass [18]. European countries (e.g., Austria, Denmark, Finland, Germany) show the highest wood pellet demand in the world (15.8 million tons in 2018) [16]. Many types of woody biomass have been used as steam gasification feedstock for H<sub>2</sub>-rich gas production, some of them are: pine sawdust [19], cedar wood [20], beech wood [21], apple tree branch [22], waste wood [23].

#### **1.2.1.2 Agricultural residues**

Agriculture residues as one type of non-woody biomass are lignocellulosic (contains cellulose, hemicellulose, and lignin) which have a lower lignin content than woody biomass. Typical agricultural residues are rice husk, rice straw, sugarcane bagasse, etc., which are abundant, readily available, and inexpensive. It is estimated that agricultural residues account for 30% of the total agricultural production in the world. About 5 million tons of biomass are produced from agricultural land. It is estimated that 667.6 million tons of rice straw, 8.9 million tons of cereal waste, and 8.8 million metric tons of sugar beet waste are produced in Asia and Europe [4]. However, in most of developing countries, the agricultural residues are generally directly burned in the farmlands to avoid weeds, pests and to reduce the time between harvests [24]. Hydrogen production from different types of agricultural waste via the gasification process has been extensively studied, which is a promising approach for the utilization of agricultural waste. Recent studies have demonstrated the potential of H<sub>2</sub>-rich syngas production from rice husk [25], rice straw [26], corn straw [27], cotton stalk [28], and wheat straw [29].

### 1.2.1.3 Food waste

Food waste is one of the largest sources of municipal solid waste, which was more than plastic and paper. One-third of food waste generates during the food supply chain from harvesting to consumption. It is estimated that 1.3 billion tons of food waste is generated annually around the world and most of them are discarded in landfills, which has significant potential to cause air, land, and water pollution [30-32]. Food waste contains a large content of reusable organic compounds such as carbohydrates, proteins, and oils, which can be sustainably converted into value-added products (i.e., H<sub>2</sub>-rich syngas) via the gasification process [33]. Tanaka et al. [34] investigated the feasibility of mixed food waste collected from the kitchen for biomass gasification, clarifying that the gasification process can efficiently reduce the generation of food waste. Ahmad and Gupta [35] compared pyrolysis and gasification performances of mixed food waste. Both of these two works concluded that the mixture of food waste could be a good feedstock for the steam gasification process and that the inherent inorganic compounds in food waste ash could provide a catalytic effect during the reaction. Raizada [36] collected the real food waste from the university dining hall to use as steam gasification feedstock. The results showed that high syngas and hydrogen production could be obtained at a low reaction temperature (700), indicating the great potential of food waste for H<sub>2</sub>-rich syngas production.

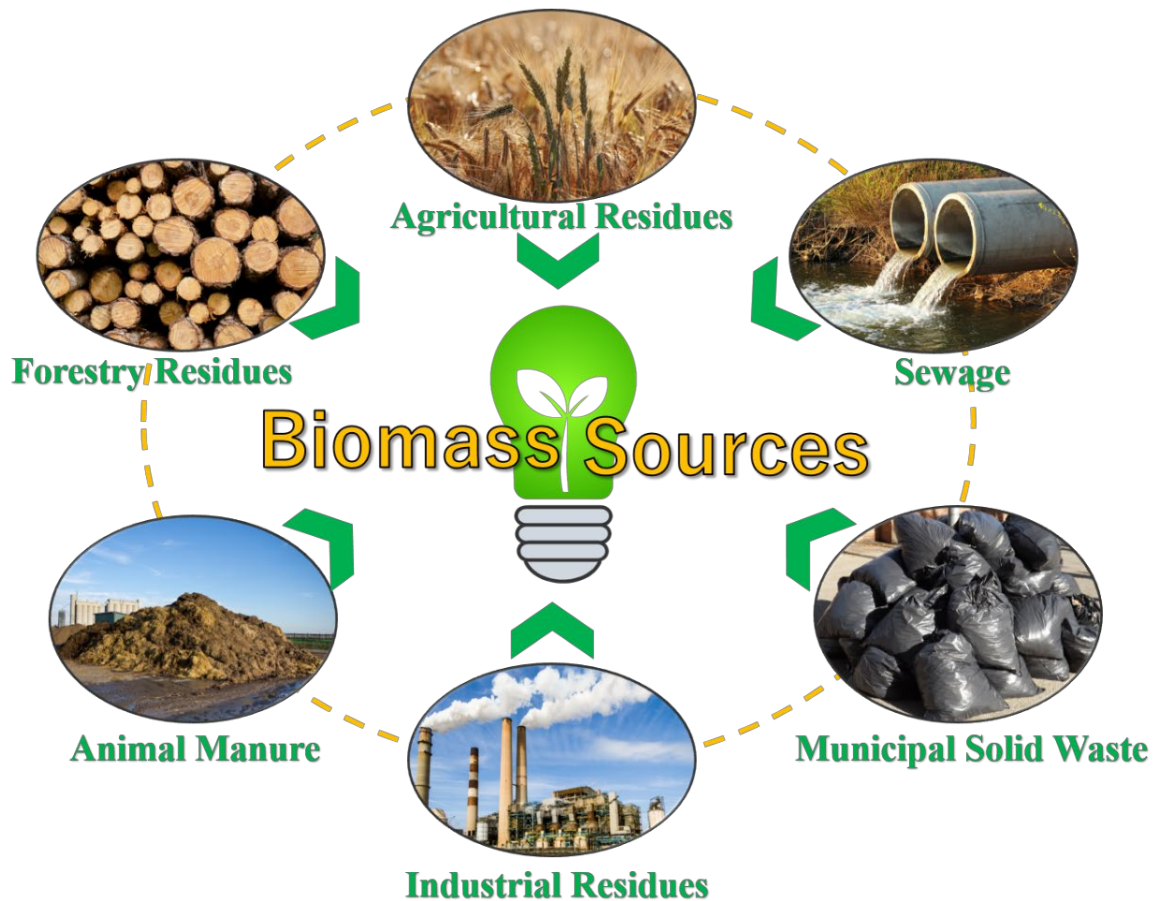


**Fig 1.4** Major sources of biomass.

### 1.2.2 Gasifying agents

Generally, biomass gasification is carried out at a temperature between 700-1200 °C, using a controlled amount of gasifying agent, which leads to syngas products mainly formed by H<sub>2</sub>, CO, CO<sub>2</sub>, CH<sub>4</sub>, and. Air, oxygen, CO<sub>2</sub>, steam, or their mixture are generally used as the gasifying agent, which depends on the desired syngas composition and energy considerations [37]. Air is the most common gasifying agent used in the gasification process due to the low cost. However, the heating value of produced syngas from the air gasification is low due to the high content of nitrogen. The use of pure oxygen or oxygen-rich air as gasifying agent can produce syngas with higher heating value, but the operating cost increases consequently. Compared with other gasifying agents, steam is regarded as the most promising gasifying agent since it can enhance H<sub>2</sub> formation and produce a high heating value syngas with no nitrogen. Steam gasification of biomass can produce 53-55 vol.% of H<sub>2</sub> in the syngas product which is

5 times larger than air gasification. The gasification performance and results from steam gasification are generally better than oxygen gasification since oxygen would consume some of the combustible gases in the syngas, resulting in a decrease in the heating value of syngas [10]. **Table 1.1** shows a summary of the benefits and drawbacks of various gasifying agents.

**Table 1.1** Benefits and drawbacks of different gasifying agents.

| <b>Gasifying agent</b> | <b>Benefits</b>  | <b>Drawbacks</b>                                 |
|------------------------|--|--|
| Air                    | Abundant and low-cost<br>Autothermal process   | Nitrogen dilution of syngas<br>Low heating value |
| Oxygen                 | Autothermal process<br>N <sub>2</sub> free product gas<br>High heating value                   | High cost  |
| Steam                  | N <sub>2</sub> free product gas<br>H <sub>2</sub> -rich syngas<br>High heating value           | Endothermic process                              |
| Carbon dioxide         | N <sub>2</sub> free product gas<br>Low CO <sub>2</sub> content in syngas<br>High heating value | Low reaction rate<br>Endothermic process         |

### 1.2.3 Steam gasification process

Steam gasification is a well-proven and well-established process that can produce the highest yield of renewable H<sub>2</sub> from biomass and provide a cleaner product with minimal environmental impact [11]. The biomass steam gasification process mainly includes three stages. Drying is the initial step that the moisture contained in the biomass is removed as much as possible at low temperatures (100-200 °C) before biomass is fed into the gasifier. Pyrolysis step occurs with further increasing temperature above 300 °C, dried biomass is thermally decomposed into volatiles (mixture gas of H<sub>2</sub>, CO, CO<sub>2</sub>, CH<sub>4</sub>), solid char (residue mainly composed of solid

carbon), a few condensable unsaturated hydrocarbons, e.g., tar (a complex mixture of oxygenates composed of heavy organic and inorganic molecules). The tar can be further cracked or reformed into small molecules with increasing temperature and/or adding catalyst. The steam gasification process starts at a temperature above 500 °C, which involves homogeneous reactions (among gases and steam) and heterogeneous reactions (among char and gases as well as steam) [37]. The char formed in the pyrolysis step is gasified by heterogeneous reactions including steam-char gasification, Boudouard reaction, and Methanation reaction. The homogeneous reactions include water-gas shift reaction and steam-methane reforming reaction. **Table 1.2** lists the main reactions during the steam gasification process [38].

**Table 1.2** Main reactions in biomass steam gasification.

| No. | Reaction   | Name of reaction        |
|-----|--|-------------------------|
| 1   | $\text{Biomass} \rightarrow \text{Tar} + \text{Char} + \text{Volatiles}$               | Pyrolysis               |
| 2   | $\text{Tar} \rightarrow \text{Gas (H}_2, \text{CO, CO}_2, \text{CH}_4, \text{others)}$ | Tar reforming           |
| 3   | $\text{Char (mainly C)} + \text{H}_2\text{O} \rightarrow \text{CO} + \text{H}_2$       | Water-gas               |
| 4   | $\text{Char (mainly C)} + \text{CO}_2 \rightarrow 2\text{CO}$                          | Boudouard               |
| 5   | $\text{Char (mainly C)} + 2\text{H}_2 \rightarrow \text{CH}_4$                         | Methanation             |
| 6   | $\text{CO} + \text{H}_2\text{O} \rightarrow \text{CO}_2 + \text{H}_2$                  | Water-gas shift         |
| 7   | $\text{CH}_4 + \text{H}_2\text{O} \rightarrow \text{CO} + 3\text{H}_2$                 | Steam-methane reforming |

#### 1.2.4 Co-gasification process

Although H<sub>2</sub>-rich syngas can be produced from the steam gasification process, the use of biomass in large-scale industrial applications is restricted due to several disadvantages such as low bulk density, low energy density, wide and thin distribution, physical characteristics, pre-

process handling, transportation, and unstable seasonal supply. The combination of different types of biomass feedstock used in the co-gasification process is an important technology that ensures the continuity of biomass feedstock throughout the year as well as enhances gasification performances [39]. The co-gasification of renewable biomass with coal is believed to be a promising way to overcome the shortcomings and has been widely investigated in recent years [40-42]. Generally, even partial replacement of coal by biomass can reduce the dependence on fossil fuels and reduce the GHG emissions while co-utilization of biomass with coal can overcome the regional or seasonal availability issue of biomass. The recent studies on co-gasification of coal and biomass are focused on utilizing low-rank coal since half of the coal reserves are in the low-rank state (brown coal and sub-bituminous) [29, 43-45]. Furthermore, more gas production with less tar content can be obtained by co-gasification of different types of feedstock such as biomass/biomass or biomass/coal due to the synergistic effect.

### **1.3 Effect of different factors on gasification process**

#### **1.3.1 Feedstock type**

Biomass is mainly composed of biopolymers such as cellulose, hemicellulose, and lignin as well as three basic elements (C, H, O) [9]. The compositions of biomass vary with the sources of biomass, and even the different parts of a biomass (e.g, tree bark and tree branch) may have different compositions and characteristics. The heterogeneity of biomass can be considered as one of the disadvantages of biomass gasification since the optimum operating conditions and the final products are always different [11, 38, 40]. The compositions of biomass are generally determined by proximate analysis and ultimate analysis. Fixed carbon, moisture, ash, and volatile matter contents can be determined by proximate analysis, whereas the compositions of main chemical elements (C, H, O, N, S) can be determined by ultimate analysis. The volatile matter includes gases and organic vapors containing paraffinic and aromatic hydrocarbons, which are produced from the thermal degradation of biomass in the absence of air. The fixed carbon is the non-vaporized solid carbon in the biomass which remains in the biochar after the thermal degradation process in the absence of air. The ash is the solid residue after the complete combustion of biomass, which contains mineral compounds. The ash-derived in biomass

normally contains alkali and alkaline earth metal (AAEM) species such as sodium (Na), potassium (K), magnesium (Mg), and calcium (Ca), which are reported to have high catalytic activity during the biomass gasification process [46]. The catalytic effect of inherent AAEM in biomass shows a high potential for co-gasifying with coal to enhance coal reactivity [47, 48]. The ash content and ash compositions of biomass have a strong influence on gasification performance, but the extremely high ash content tends to cause sintering and agglomeration problems during the gasification process. Thus, it is important to conduct kinds of analyses on biomass feedstock to understand the physicochemical properties of the feedstock before the gasification process.

Many types of biomass have been investigated the feasibility of H<sub>2</sub>-rich syngas production via steam gasification process. Some of them are: apple tree branch [49], seaweed [50], Japanese cedar [20], knotweed stem [8], palm kernel shells [51], rice husk [52], municipal solid waste [53], mushroom substrate [54], wheat straw [29], citrus peel [55], banana peel [56].

Co-gasification of different types of feedstock has attracted more attention than gasification of a single type of feedstock to address the issues related to the seasonal availability and supply continuity of biomass. Different synergy behavior (synergistic effect and inhibition effect) can be obtained from co-gasification due to the interaction of different types of feedstock. The higher syngas production and less tar production can be obtained by mixing different types of feedstock due to the synergistic effect [29]. Currently, co-gasification of coal with different types of biomass has been widely studied since the advantages of reduction of GHG emission and fossil fuels dependency. Biomass has a higher volatile matter content and tends to produce tar in gasification process, whereas coal has higher fixed carbon content but a lower gasification rate than biomass. By co-gasification process, the tar produced from biomass can be cracked due to the higher heat provided from the coal char, resulting in larger syngas yield and less tar yield [57-59]. Furthermore, most researchers reported that synergy behaviors in co-gasification were mainly attributed to the content and transformation of AAEM in biomass ash. AAEMs as the common inherent mineral species in biomass have been identified to provide a good catalytic effect on enhancing gasification kinetics [40, 42]. The catalytic effect provided by inherent AAEM can increase char reactivity, generating more combustible syngas and

increasing the co-gasification efficiency compared to the gasification of single feedstock. K is the dominant AAEM species in biomass and commonly has a higher catalytic activity than Na, Ca, and Mg [60]. Zou et al. [61] studied co-gasification performances of coal with different daily food wastes, and found that lettuce (high ash and K) provided the highest co-gasification reactivity which was followed by fishbone (high ash and Ca) and rice (low ash). Zhang et al. [62] studied the co-gasification behaviors of different coal/biomass blends by selecting three types of coal (bituminous coal, high-ash lignite, low-ash lignite) and four kinds of biomass feedstock (Chinese redwood, soybean stalk, orange peel, and peanut shells), and the results showed that K species in biomass ash played a catalytic role in enhancing gasification reactivity of coal char, which was considered as the main reason of synergistic effect. Fernandes et al. [63] proposed K transfer route and catalytic mechanism during the co-gasification process which was mainly attributed to the interparticle K mobility. However, the content of inherent Si should also be considered in the co-gasification process since the catalytic effect of inherent AAEM species would be weakened due to the formation of silicate. Thus, it is important to conduct various kinds of analyses on biomass feedstock to understand the physicochemical properties of the feedstock before the gasification process.

### **1.3.2 Reaction temperature**

Temperature is regarded as the most important factor in the gasification process since the producer gas composition, gas heating value, carbon conversion efficiency, and yields of syngas, char, and tar are all affected by gasification temperature. The effect of gasification temperature on H<sub>2</sub>-rich syngas production has been studied by many researchers, and it is widely reported that higher carbon conversion rates and syngas production with less tar content can be achieved at a high gasification temperature [64]. Moreover, Boudouard and steam gasification are endothermic reactions, requiring a large amount of heat supply to destruct the particles, convert the tar molecules into gaseous products, and promote the complete gasification reactions. Li et al. (2015) [65] investigated the steam gasification of sludge at different reaction temperatures. The results showed that the gas yield and H<sub>2</sub> concentration increased significantly with reaction temperature from 600 °C to 900 °C, and the highest gas yield and H<sub>2</sub> concentration were 49.4 wt% and 46.4 vol% obtained at 900 °C, respectively. On

the other hand, Niu et al. [66] studied the steam gasification of sawdust for H<sub>2</sub>-rich syngas production. They found that the H<sub>2</sub> content in the syngas increased at first and then decreased with the increase of gasification temperature. The increase in the reaction temperature would hinder the water-gas shift reaction since it is an exothermic reaction, resulting in a decrease of H<sub>2</sub> concentration in producer gas. Therefore, the determination of reaction temperature is vital for the gasification process.

### **1.3.3 Steam amount**

Steam as a promising gasifying agent has a strong influence on the composition of syngas and energy input. Theoretically, higher H<sub>2</sub>-rich syngas production can be obtained by introducing more steam into the reactor since solid char, hydrocarbons (tar), and CH<sub>4</sub> are reformed to CO<sub>2</sub> and H<sub>2</sub>, whereas CO yield reduces due to the promotion of water-gas shift reaction. Thus, H<sub>2</sub> production highly depends on the steam amount in the biomass gasification process. However, the excess steam would cause high energy consumption which is not economically applicable, and the presence of excess steam is found to have a negative effect due to the reduction of temperature in the reactor. Kalinci et al. [11] reported that the water gas and reforming reactions of hydrocarbons could be enhanced by increasing the steam amount. Feng et al. [67] studied the effects of gasification temperature and steam on H<sub>2</sub> yield and syngas composition from the steam gasification of biochar derived from pine sawdust. The results indicated that gas yield and carbon conversion efficiency increased first as the steam flow rate increased from 0 to 0.165 g/min, and then decreased with further increasing the steam flow rate. Malinee et al. [50] found that the excess steam reduced the H<sub>2</sub> production yield from the steam gasification of brown seaweed. Iovane et al. [68] reported that the syngas yield from palm shells could not be further increased by increasing the steam-biomass ratio higher than 0.6. Based on these studies, it can be concluded that the steam amount is as important as the reaction temperature. The optimum steam amount for gasification of different types of biomass should be considered in order to obtain the highest H<sub>2</sub> yield without excess energy consumption.

### **1.3.4 Catalyst**

Although steam gasification of biomass is regarded as a promising pathway for sustainable H<sub>2</sub> production, the process is inevitably problematic with undesirable CO<sub>2</sub> production due to the

water-gas shift reaction and unwanted tar formation during the reaction. Tar is a complex mixture of aromatics, alcohols, phenols, and aldehydes compounds which is an undesirable by-product from the gasification process since it is easy to condense, causing problems such as blockage and corrosion of the pipeline [69]. The use of catalysts can decrease the gasification temperature and enhance the carbon conversion efficiency as well as  $H_2$  production from biomass [70]. Nevertheless, tar can be cracked or reformed into  $H_2$  and CO with the addition of a proper catalyst. Thus, the introduction of the proper catalyst to the gasification process can potentially increase  $H_2$  yield and reduce the yields of unwanted tar and  $CO_2$ . Catalysts commonly used in the steam gasification process include AAEM catalysts, metal-based catalysts, and mineral catalysts.

Alkali metals such as sodium (Na), potassium (K), Lithium (Li), rubidium (Rh), and other monovalent element-based catalysts are regarded as the most active catalyst for the gasification process, which are found to be able to reduce tar content and improve syngas quality [71]. These catalysts have good resistance for carbon deposition and can increase syngas yield by increasing the reaction rate of water-gas shift through the formation of salt [72]. Among these catalysts, potassium (K) has been studied extensively since it is abundant (low cost) and active. K species have high mobility in catalytic gasification which can diffuse rapidly on the surface area of the carbon, leading to micropore formation and increasing the reaction rate [60]. K species deposit at different sites on the carbon surface and create channels that can bring the gasifying agent ( $H_2O$ ,  $CO_2$ ,  $O_2$ ) into contact with the carbon atoms [73]. Moreover, biomass ash also contains alkali metals, which also can provide catalytic effects during the gasification process to increase gasification rate and syngas yield. However, the problems of alkali metals are evaporation and agglomeration, resulting in the deactivation of catalysts.

Calcium oxide (CaO) is well known as a  $CO_2$  absorbent and a good catalyst for steam gasification process. The use of CaO on adsorption-enhanced steam gasification of biomass (AESGB) has attracted great attention for  $H_2$ -rich syngas production in recent years [74-76]. It was reported that CaO adsorbs  $CO_2$  during the gasification reaction can enhance water-gas shift reaction, resulting in high  $H_2$  production and low CO production [77].  $CO_2$  from the gasification reaction is removed as soon as it is generated which can alter the chemical

equilibrium of the reaction, as a result, more  $H_2$  was generated [78]. Moreover, CaO is found to have good catalytic activity on tar cracking due to the alkaline property [79], further increasing the concentration of desirable products (i.e.  $H_2$ ). Udomsirichakorn et al. [80] applied CaO as a catalyst to the steam gasification of pine sawdust and found that CaO could significantly increase the concentration and yield of  $H_2$  and reduce 67% of tar content within the temperature of 550 – 700 °C. Thus, the use of CaO to enhance  $H_2$  yield with in-process  $CO_2$  capture and tar reduction in the biomass steam gasification process is considered as a promising option for sustainable  $H_2$  production.

Biochar as one of the by-products of pyrolysis and gasification of biomass is recently utilized as the catalyst to decompose tar [81-83]. The biochar or biochar-supported catalysts show the high potential to be utilized in the large-scale biomass gasification process since they can be easily gasified and recover the inherent energy of the biochar without regeneration after deactivation. Biochar has relatively high surface area and porous structure that can not improve not only the dispersion of supported catalyst species but also the transport of reactant molecules into the internal active sites. The major mechanisms of tar conversion over biochar are adsorption, dehydrogenation (soot formation), and soot gasification, which are comparable with those common catalysts such as calcined dolomite, olivine, and commercial nickel catalyst [84, 85]. Mun et al. [86] reported that the high surface area and large pore size of biochar can provide higher reactivity for tar removal. Moreover, the presence of AAEM species in the biochar can further improve the reforming reactions. Wang et al. [83] prepared catalyst by doping Ni on biochar derived from sawdust and found that more than 97% of tar in syngas could be removed in the presence of Ni/biochar, resulting in a significant increase in  $H_2$  and CO concentrations. Shen et al. [87] reported that tar yield and  $CO_2$  concentration could be greatly decreased by using the rice husk char and char-supported catalysts.

## **1.4 Objective**

The utilization of biomass in large-scale industrial applications is restricted due to several disadvantages such as low bulk density, low energy density, wide and thin distribution, and unstable seasonal supply. In order to overcome such issues, combination of different types of biomass or combination of biomass with other carbon-based solid materials to use as co-

feedstock for gasification process are considered as a promising solution. Moreover, different synergy behaviors, either synergistic or inhibition effects, on co-gasification reactivity may occur by mixing different kinds of feedstock due to the different physicochemical characteristics and thermal degradation behaviors. Hence, it is necessary to investigate the compatibility and potential synergy effect in various biomass mixtures to provide a better understanding and guidance on biomass selection and corresponding co-gasification conditions for large-scale industrial applications. This dissertation, therefore, focuses on investigating co-gasification reactivity and performances, especially hydrogen production, of mixture feedstock and the potential synergy effect. The different carbon-based solid materials were selected as gasification co-feedstock i.e., biomass/biomass, biomass/biochar, and biomass/coal in order to utilize biomass resources more efficiently and explore the co-gasification behaviors and feasibility of hydrogen-rich syngas production by combination of biomass with different types of carbon-based materials.

Moreover, this study also aims to utilize the local waste biomass resources and investigate the proper methods to convert waste into value-added products (e.g., H<sub>2</sub>-rich syngas). Aomori Prefecture is located in the northeast of Japan, rice husk and cedarwood are the most common local biomass sources. However, both of them have a low gasification reactivity, which means high reaction temperature and catalyst are required in order to have a high conversion rate and high H<sub>2</sub> production. The co-gasification method is applied in this study to improve the gasification reactivity of local biomass feedstock and decrease the reaction temperature to reduce energy consumption by obtaining the potential synergistic effect during the co-gasification process. The experimental results of this study are expected to contribute to the development of regional renewable energy and waste utilization. Besides, the investigation of hydrogen production from the different biomass feedstock is expected to provide solutions for producing hydrogen in a renewable and sustainable way instead of using fossil fuels, contributing to the Basic Hydrogen Strategy and increasing the energy self-sufficient ratio in Japan.

## Reference

- [1] Zhou S, Dai F, Chen Y, Dang C, Zhang C, Liu D, et al. Sustainable hydrothermal self-

assembly of hafnium–lignosulfonate nanohybrids for highly efficient reductive upgrading of 5-hydroxymethylfurfural. *Green Chemistry*. 2019;21:1421-31.

[2] Chen W, Geng W. Fossil energy saving and CO<sub>2</sub> emissions reduction performance, and dynamic change in performance considering renewable energy input. *Energy*. 2017;120:283-92.

[3] Rizkiana J, Guan G, Widayatno WB, Hao X, Huang W, Tsutsumi A, et al. Effect of biomass type on the performance of cogasification of low rank coal with biomass at relatively low temperatures. *Fuel*. 2014;134:414-9.

[4] Sansaniwal SK, Rosen MA, Tyagi SK. Global challenges in the sustainable development of biomass gasification: An overview. *Renewable and Sustainable Energy Reviews*. 2017;80:23-43.

[5] IEA. Global Energy Review. Paris: IEA; 2021. <https://www.iea.org/reports/global-energy-review-2021>

[6] Japan's Energy 2020; <https://www.enecho.meti.go.jp/en/category/brochures/>.

[7] Basic Hydrogen Strategy. METI; [https://www.meti.go.jp/english/press/2017/1226\\_003.html](https://www.meti.go.jp/english/press/2017/1226_003.html)

[8] Situmorang YA, Zhao Z, Chaihad N, Wang C, Anniwaer A, Kasai Y, et al. Steam gasification of co-pyrolysis chars from various types of biomass. *International Journal of Hydrogen Energy*. 2021;46:3640-50.

[9] Kalamaras CM, Efstathiou AM. Hydrogen Production Technologies: Current State and Future Developments. *Conference Papers in Energy*. 2013;2013:690627.

[10] Balat H, Kirtay E. Hydrogen from biomass – Present scenario and future prospects. *International Journal of Hydrogen Energy*. 2010;35:7416-26.

[11] Kalinci Y, Hepbasli A, Dincer I. Biomass-based hydrogen production: A review and analysis. *International Journal of Hydrogen Energy*. 2009;34:8799-817.

[12] Cao L, Yu IKM, Xiong X, Tsang DCW, Zhang S, Clark JH, et al. Biorenewable hydrogen production through biomass gasification: A review and future prospects. *Environmental Research*. 2020;186:109547.

[13] Gai C, Guo Y, Liu T, Peng N, Liu Z. Hydrogen-rich gas production by steam gasification

of hydrochar derived from sewage sludge. *International Journal of Hydrogen Energy*. 2016;41:3363-72.

[14] Shahbaz M, yusup S, Inayat A, Patrick DO, Ammar M. The influence of catalysts in biomass steam gasification and catalytic potential of coal bottom ash in biomass steam gasification: A review. *Renewable and Sustainable Energy Reviews*. 2017;73:468-76.

[15] Global bioenergy statistics 2020. <http://www.worldbioenergy.org/global-bioenergy-statistics/>.

[16] Solarte-Toro JC, González-Aguirre JA, Poveda Giraldo JA, Cardona Alzate CA. Thermochemical processing of woody biomass: A review focused on energy-driven applications and catalytic upgrading. *Renewable and Sustainable Energy Reviews*. 2021;136:110376.

[17] Börcsök Z, Páztory Z. The role of lignin in wood working processes using elevated temperatures: an abbreviated literature survey. *European Journal of Wood and Wood Products*. 2021;79:511-26.

[18] Pradhan P, Mahajani SM, Arora A. Production and utilization of fuel pellets from biomass: A review. *Fuel Processing Technology*. 2018;181:215-32.

[19] Zribi M, Lajili M, Escudero-Sanz FJ. Hydrogen enriched syngas production via gasification of biofuels pellets/powders blended from olive mill solid wastes and pine sawdust under different water steam/nitrogen atmospheres. *International Journal of Hydrogen Energy*. 2019;44:11280-8.

[20] Aljbour SH, Kawamoto K. Bench-scale gasification of cedar wood – Part I: Effect of operational conditions on product gas characteristics. *Chemosphere*. 2013;90:1495-500.

[21] Reyes L, Abdelouahed L, Campusano B, Buvat J-C, Taouk B. Exergetic study of beech wood gasification in fluidized bed reactor using CO<sub>2</sub> or steam as gasification agents. *Fuel Processing Technology*. 2021;213:106664.

[22] Yu T, Abudukeranmu A, Anniwaer A, Situmorang YA, Yoshida A, Hao X, et al. Steam gasification of biochars derived from pruned apple branch with various pyrolysis temperatures. *International Journal of Hydrogen Energy*. 2020;45:18321-30.

[23] Hwang I-H, Kobayashi J, Kawamoto K. Characterization of products obtained from

pyrolysis and steam gasification of wood waste, RDF, and RPF. *Waste Management*. 2014;34:402-10.

[24] Widjaya ER, Chen G, Bowtell L, Hills C. Gasification of non-woody biomass: A literature review. *Renewable and Sustainable Energy Reviews*. 2018;89:184-93.

[25] Zeng X, Fang M, Lv T, Tian J, Xia Z, Cen J, et al. Hydrogen-rich gas production by catalytic steam gasification of rice husk using CeO<sub>2</sub>-modified Ni-CaO sorption bifunctional catalysts. *Chemical Engineering Journal*. 2022:136023.

[26] Umeki K, Namioka T, Yoshikawa K. The effect of steam on pyrolysis and char reactions behavior during rice straw gasification. *Fuel Processing Technology*. 2012;94:53-60.

[27] Pang Y, Yu D, Chen Y, Jin G, Shen S. Hydrogen production from steam gasification of corn straw catalyzed by blast furnace gas ash. *International Journal of Hydrogen Energy*. 2020;45:17191-9.

[28] Karatas H, Olgun H, Akgun F. Experimental results of gasification of cotton stalk and hazelnut shell in a bubbling fluidized bed gasifier under air and steam atmospheres. *Fuel*. 2013;112:494-501.

[29] Zhao S, Yang P, Liu X, Zhang Q, Hu J. Synergistic effect of mixing wheat straw and lignite in co-pyrolysis and steam co-gasification. *Bioresource Technology*. 2020;302:122876.

[30] Lorenz BA-S, Hartmann M, Langen N. What makes people leave their food? The interaction of personal and situational factors leading to plate leftovers in canteens. *Appetite*. 2017;116:45-56.

[31] Xu Z, Zhang Z, Liu H, Zhong F, Bai J, Cheng S. Food-away-from-home plate waste in China: Preference for variety and quantity. *Food Policy*. 2020;97:101918.

[32] Su G, Ong HC, Fattah IMR, Ok YS, Jang J-H, Wang C-T. State-of-the-art of the pyrolysis and co-pyrolysis of food waste: Progress and challenges. *Science of The Total Environment*. 2021:151170.

[33] Xu Z, Qi H, Yao D, Zhang J, Zhu Z, Wang Y, et al. Modeling and comprehensive analysis of food waste gasification process for hydrogen production. *Energy Conversion and Management*. 2022;258:115509.

[34] Tanaka M, Ozaki H, Ando A, Kambara S, Moritomi H. Basic Characteristics of Food

Waste and Food Ash on Steam Gasification. *Industrial & Engineering Chemistry Research*. 2008;47:2414-9.

[35] Ahmed II, Gupta AK. Pyrolysis and gasification of food waste: Syngas characteristics and char gasification kinetics. *Applied Energy*. 2010;87:101-8.

[36] Raizada A, Yadav S. Hydrogen rich syngas production from food waste via an integrated two-stage process of in-situ steam gasification after fast pyrolysis. *Energy Sources, Part A: Recovery, Utilization, and Environmental Effects*. 2022;44:1608-19.

[37] Dhyani V, Bhaskar T. A comprehensive review on the pyrolysis of lignocellulosic biomass. *Renewable Energy*. 2018;129:695-716.

[38] Parthasarathy P, Narayanan KS. Hydrogen production from steam gasification of biomass: Influence of process parameters on hydrogen yield – A review. *Renewable Energy*. 2014;66:570-9.

[39] Inayat M, Sulaiman SA, Inayat A, Shaik NB, Gilal AR, Shahbaz M. Modeling and parametric optimization of air catalytic co-gasification of wood-oil palm fronds blend for clean syngas ( $H_2+CO$ ) production. *International Journal of Hydrogen Energy*. 2021;46:30559-80.

[40] Mariyam S, Shahbaz M, Al-Ansari T, Mackey HR, McKay G. A critical review on co-gasification and co-pyrolysis for gas production. *Renewable and Sustainable Energy Reviews*. 2022;161:112349.

[41] Shahbaz M, Al-Ansari T, Inayat M, Sulaiman SA, Parthasarathy P, McKay G. A critical review on the influence of process parameters in catalytic co-gasification: Current performance and challenges for a future prospectus. *Renewable and Sustainable Energy Reviews*. 2020;134:110382.

[42] Wang B, Li W, Ma C, Yang W, Pudasainee D, Gupta R, et al. Synergistic effect on the co-gasification of petroleum coke and carbon-based feedstocks: A state-of-the-art review. *Journal of the Energy Institute*. 2022;102:1-13.

[43] Faki E, Üzden ŞT, Seçer A, Hasanoğlu A. Hydrogen production from low temperature supercritical water Co-Gasification of low rank lignites with biomass. *International Journal of Hydrogen Energy*. 2022;47:7682-92.

[44] Liu X, Hu J, Zhao S, Wang W, Zhang Q, Yan X. Chemical looping co-gasification of wheat

straw and lignite with calcium-enhanced iron-based oxygen carrier for syngas production. *Fuel Processing Technology*. 2022;227:107108.

[45] Beagle E, Wang Y, Bell D, Belmont E. Co-gasification of pine and oak biochar with sub-bituminous coal in carbon dioxide. *Bioresource Technology*. 2018;251:31-9.

[46] McKee DW. Mechanisms of the alkali metal catalysed gasification of carbon. *Fuel*. 1983;62:170-5.

[47] Nzihou A, Stanmore B, Sharrock P. A review of catalysts for the gasification of biomass char, with some reference to coal. *Energy*. 2013;58:305-17.

[48] Wei J, Wang M, Wang F, Song X, Yu G, Liu Y, et al. A review on reactivity characteristics and synergy behavior of biomass and coal Co-gasification. *International Journal of Hydrogen Energy*. 2021;46:17116-32.

[49] Yu T, Abudukeranmu A, Anniwaer A, Situmorang YA, Yoshida A, Hao X, et al. Steam gasification of biochars derived from pruned apple branch with various pyrolysis temperatures. *International Journal of Hydrogen Energy*. 2019.

[50] Kaewpanha M, Guan G, Hao X, Wang Z, Kasai Y, Kusakabe K, et al. Steam co-gasification of brown seaweed and land-based biomass. *Fuel Processing Technology*. 2014;120:106-12.

[51] Barco-Burgos J, Carles-Bruno J, Eicker U, Saldana-Robles AL, Alcántar-Camarena V. Hydrogen-rich syngas production from palm kernel shells (PKS) biomass on a downdraft allothermal gasifier using steam as a gasifying agent. *Energy Conversion and Management*. 2021;245:114592.

[52] Zhai M, Zhang Y, Dong P, Liu P. Characteristics of rice husk char gasification with steam. *Fuel*. 2015;158:42-9.

[53] He M, Hu Z, Xiao B, Li J, Guo X, Luo S, et al. Hydrogen-rich gas from catalytic steam gasification of municipal solid waste (MSW): Influence of catalyst and temperature on yield and product composition. *International Journal of Hydrogen Energy*. 2009;34:195-203.

[54] Koido K, Ogura T, Matsumoto R, Endo K, Sato M. Spent mushroom substrate performance for pyrolysis, steam co-gasification, and ash melting. *Biomass and Bioenergy*. 2021;145:105954.

- [55] Prestipino M, Chiodo V, Maisano S, Zafarana G, Urbani F, Galvagno A. Hydrogen rich syngas production by air-steam gasification of citrus peel residues from citrus juice manufacturing: Experimental and simulation activities. *International Journal of Hydrogen Energy*. 2017;42:26816-27.
- [56] He J, Yang Z, Xiong S, Guo M, Yan Y, Ran J, et al. Experimental and thermodynamic study of banana peel non-catalytic gasification characteristics. *Waste Management*. 2020;113:369-78.
- [57] Habibi R, Kopyscinski J, Masnadi MS, Lam J, Grace JR, Mims CA, et al. Co-gasification of Biomass and Non-biomass Feedstocks: Synergistic and Inhibition Effects of Switchgrass Mixed with Sub-bituminous Coal and Fluid Coke During CO<sub>2</sub> Gasification. *Energy & Fuels*. 2013;27:494-500.
- [58] Jeong HJ, Park SS, Hwang J. Co-gasification of coal–biomass blended char with CO<sub>2</sub> at temperatures of 900–1100°C. *Fuel*. 2014;116:465-70.
- [59] Kerkkaiwan S, Fushimi C, Tsutsumi A, Kuchonthara P. Synergetic effect during co-pyrolysis/gasification of biomass and sub-bituminous coal. *Fuel Processing Technology*. 2013;115:11–8.
- [60] Kopyscinski J, Rahman M, Gupta R, Mims CA, Hill JM. K<sub>2</sub>CO<sub>3</sub> catalyzed CO<sub>2</sub> gasification of ash-free coal. Interactions of the catalyst with carbon in N<sub>2</sub> and CO<sub>2</sub> atmosphere. *Fuel*. 2014;117:1181-9.
- [61] Zou X, Ding L, Gong X. Study on the Co-gasification Reactivity and Interaction Mechanism of Coal with Different Components of Daily Food Waste. *Energy & Fuels*. 2020;34:1728-36.
- [62] Zhang Y, Zheng Y, Yang M, Song Y. Effect of fuel origin on synergy during co-gasification of biomass and coal in CO<sub>2</sub>. *Bioresource Technology*. 2016;200:789-94.
- [63] Fernandes R, Hill JM, Kopyscinski J. Determination of the Synergism/Antagonism Parameters during Co-gasification of Potassium-Rich Biomass with Non-biomass Feedstock. *Energy & Fuels*. 2017;31:1842-9.
- [64] Kumar A, Jones DD, Hanna MA. Thermochemical Biomass Gasification: A Review of the Current Status of the Technology. *Energies*. 2009;2.

- [65] Li H, Chen Z, Huo C, Hu M, Guo D, Xiao B. Effect of bioleaching on hydrogen-rich gas production by steam gasification of sewage sludge. *Energy Conversion and Management*. 2015;106:1212-8.
- [66] Niu Y, Han F, Chen Y, Lyu Y, Wang L. Experimental study on steam gasification of pine particles for hydrogen-rich gas. *Journal of the Energy Institute*. 2017;90:715-24.
- [67] Yan F, Luo S-y, Hu Z-q, Xiao B, Cheng G. Hydrogen-rich gas production by steam gasification of char from biomass fast pyrolysis in a fixed-bed reactor: Influence of temperature and steam on hydrogen yield and syngas composition. *Bioresource Technology*. 2010;101:5633-7.
- [68] Iovane P, Donatelli A, Molino A. Influence of feeding ratio on steam gasification of palm shells in a rotary kiln pilot plant. Experimental and numerical investigations. *Biomass and Bioenergy*. 2013;56:423-31.
- [69] Guan G, Chen G, Kasai Y, Lim EWC, Hao X, Kaewpanha M, et al. Catalytic steam reforming of biomass tar over iron- or nickel-based catalyst supported on calcined scallop shell. *Applied Catalysis B: Environmental*. 2012;115-116:159-68.
- [70] Kaewpanha M, Karnjanakom S, Guan G, Hao X, Yang J, Abudula A. Removal of biomass tar by steam reforming over calcined scallop shell supported Cu catalysts. *Journal of Energy Chemistry*. 2017;26:660-6.
- [71] Arnold RA, Hill JM. Catalysts for gasification: a review. *Sustainable Energy & Fuels*. 2019;3:656-72.
- [72] Brown RC, Liu Q, Norton G. Catalytic effects observed during the co-gasification of coal and switchgrass. *Biomass and Bioenergy*. 2000;18:499-506.
- [73] Lobo LS. Intrinsic kinetics in carbon gasification: Understanding linearity, “nanoworms” and alloy catalysts. *Applied Catalysis B: Environmental*. 2014;148-149:136-43.
- [74] Gao N, Śliz M, Quan C, Bieniek A, Magdziarz A. Biomass CO<sub>2</sub> gasification with CaO looping for syngas production in a fixed-bed reactor. *Renewable Energy*. 2021;167:652-61.
- [75] Wu Y, Liao Y, Liu G, Ma X. Syngas production by chemical looping gasification of biomass with steam and CaO additive. *International Journal of Hydrogen Energy*. 2018;43:19375-83.

- [76] Udomsirichakorn J, Basu P, Abdul Salam P, Acharya B. CaO-based chemical looping gasification of biomass for hydrogen-enriched gas production with in situ CO<sub>2</sub> capture and tar reduction. *Fuel Processing Technology*. 2014;127:7-12.
- [77] Udomsirichakorn J, Salam PA. Review of hydrogen-enriched gas production from steam gasification of biomass: The prospect of CaO-based chemical looping gasification. *Renewable and Sustainable Energy Reviews*. 2014;30:565-79.
- [78] Jordan CA, Akay G. Effect of CaO on tar production and dew point depression during gasification of fuel cane bagasse in a novel downdraft gasifier. *Fuel Processing Technology*. 2013;106:654-60.
- [79] Li B, Yang H, Wei L, Shao J, Wang X, Chen H. Absorption-enhanced steam gasification of biomass for hydrogen production: Effects of calcium-based absorbents and NiO-based catalysts on corn stalk pyrolysis-gasification. *International Journal of Hydrogen Energy*. 2017;42:5840-8.
- [80] Udomsirichakorn J, Basu P, Salam PA, Acharya B. Effect of CaO on tar reforming to hydrogen-enriched gas with in-process CO<sub>2</sub> capture in a bubbling fluidized bed biomass steam gasifier. *International Journal of Hydrogen Energy*. 2013;38:14495-504.
- [81] Abu El-Rub Z, Bramer EA, Brem G. Experimental comparison of biomass chars with other catalysts for tar reduction. *Fuel*. 2008;87:2243-52.
- [82] Gilbert P, Ryu C, Sharifi V, Swithenbank J. Tar reduction in pyrolysis vapours from biomass over a hot char bed. *Bioresource Technology*. 2009;100:6045-51.
- [83] Wang D, Yuan W, Ji W. Char and char-supported nickel catalysts for secondary syngas cleanup and conditioning. *Applied Energy*. 2011;88:1656-63.
- [84] Hosokai S, Kumabe K, Ohshita M, Norinaga K, Li C-Z, Hayashi J-i. Mechanism of decomposition of aromatics over charcoal and necessary condition for maintaining its activity. *Fuel*. 2008;87:2914-22.
- [85] Sueyasu T, Oike T, Mori A, Kudo S, Norinaga K, Hayashi J-i. Simultaneous Steam Reforming of Tar and Steam Gasification of Char from the Pyrolysis of Potassium-Loaded Woody Biomass. *Energy & Fuels*. 2012;26:199-208.
- [86] Mun T-Y, Kim J-W, Kim J-S. Air gasification of dried sewage sludge in a two-stage

gasifier: Part 1. The effects and reusability of additives on the removal of tar and hydrogen production. *International Journal of Hydrogen Energy*. 2013;38:5226-34.

[87] Shen Y, Zhao P, Shao Q, Ma D, Takahashi F, Yoshikawa K. In-situ catalytic conversion of tar using rice husk char-supported nickel-iron catalysts for biomass pyrolysis/gasification. *Applied Catalysis B: Environmental*. 2014;152-153:140-51.

## CHAPTER 2: Materials and Characterizations

### 2.1 Gasification feedstock

As shown in **Table 2.1**, different types of carbonaceous materials such as agricultural residues (rice husk), food waste (banana peel), woody biomass (Japanese cedar), biochar, and brown coal were selected as gasification and co-gasification feedstock in this study in order to investigate the feasibility for H<sub>2</sub>-rich syngas production as well as the potential synergistic effect. The details of each sample will be introduced in the following Chapters.

**Table 2.1** Gasification feedstock used in this study.

| Feedstock                    | Source   |
|------------------------------|--|
| Rice husk                    | Aomori, Japan  |
| Banana peel                  | Ecuador  |
| Japanese cedarwood           | Aomori, Japan  |
| Commercial cedarwood biochar | Aomori National Land Conservation Association, Japan |
| Brown coal                   | Adaro, Indonesia                                     |

### 2.2 Catalyst

CaO is well known as a CO<sub>2</sub> absorbent and has a good catalytic effect on enhancing the water-gas shift reaction during the steam gasification process to produce H<sub>2</sub>-rich syngas. Therefore, one kind of small parasitic seashell discarded in the Mutsu Gulf in Japan was utilized as the CaO source. As shown in **Fig 2.1**, the seashells were calcinated in a muffle furnace at 900 °C for 2 h to convert the main component of the seashells CaCO<sub>3</sub> into CaO. Then the calcined seashells (CS) were ground to the fine powder and stored in a closed container to prevent carbonation and humidification prior to use.

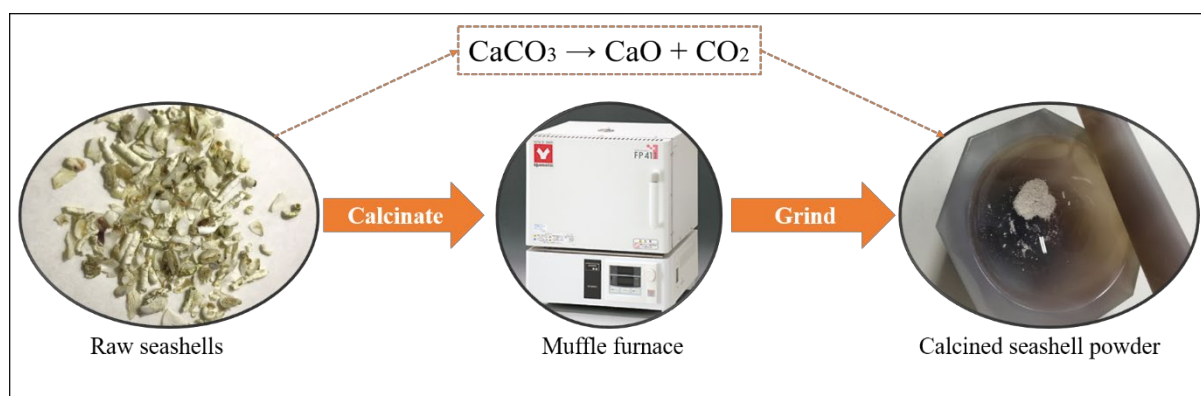


**Fig 2.1** Preparation of CaO catalyst.

## 2.3 Characterization apparatuses

### 2.3.1 GC-TCD

The syngas produced from gasification or co-gasification processes was firstly collected in the gas bag and the compositions of syngas were then analyzed using a gas chromatograph with two thermal conductivity detectors (GC-TCD, Agilent 7890A GC system), in which one TCD is connected to three columns (2 molecular sieve 5A columns and 1 HayeSep Q column) using He as a carrier gas to separate CO, CH<sub>4</sub>, and CO<sub>2</sub>, while the other TCD is connected with molecular sieve 5A and HayeSep Q columns to detect H<sub>2</sub> using Ar as carrier gas. The operating temperatures of the front inlet and back inlet were both 150 °C, while the front and back TCDs were operated at 200 °C with carrier gases (He and Ar) flow rate of 30 ml/min.

### 2.3.2 Elemental analysis

The elemental compositions (C, N, H, S) of each sample were determined using a Vario EL cube elemental analyzer which connected with a standard PC for accurate results. For each test, about 2 mg of sample was weighed into tin boats and tungsten trioxide powder was added to the sample for binding alkaline ions. All gasification feedstock used in this study were analyzed 3 times by the standard method.

### 2.3.3 Scanning electron microscopy analysis (SEM)

The surface morphology of the sample was examined by a scanning electron microscope (SEM, SU8010, Hitachi) connected with an energy dispersive spectrometer (EDS, EMAX x-act, Horiba) which could analyze the elemental composition at the same time. The dried sample was put on a conductive carbon tape which was attached to the specimen stub and then sputter-

coated with a thin layer of platinum (Pt) at 15 mA for 20 seconds using an ion sputter coater (Hitachi E-1045) before the analysis.

#### **2.3.4 X-ray diffraction analysis (XRD)**


The crystalline structures of the solid residues obtained from gasification and co-gasification processes were determined by X-ray diffraction analysis using a Rigaku Smartlab X-ray diffractometer with Cu K $\alpha$  radiation ( $\lambda = 0.15418$  nm). The operating voltage was 45 kV and the current was 200 mA. The sample was ground to the fine powder and packed horizontally on the glass sample holder for analysis. The spectra were recorded between the 2-theta ranges from 10° to 80° with a scanning speed of 10° min<sup>-1</sup>.

#### **2.3.5 X-ray fluorescence analysis (XRF)**

The qualitative and quantitative elements of the ash derived from gasification feedstock were determined by XRF analysis using an Energy Dispersive X-ray fluorescence spectrometer (EDX-800HS, Shimadzu) with a detection range from carbon to uranium. The ash sample was placed in the analysis chamber and irradiated with X-rays emitted by an X-ray tube, and then the resulted characteristic X-rays generated in the sample were detected and analyzed.

#### **2.3.6 Thermogravimetric analysis (TGA)**

TGA analyses were performed using a thermogravimetric analyzer (DTG-60H, Shimadzu) in order to understand the thermal decomposition behaviors and the thermal stability of different samples. For each test, about 10 mg of sample was put into a crucible and heated from ambient temperature to 900 °C with a heating rate of 10 °C/min. All samples were carried out in the nitrogen atmosphere with a flow rate of 50 cm<sup>3</sup>/min.



# **CHAPTER 3: Hydrogen-rich gas production from steam co-gasification of banana peel with agricultural residues and woody biomass**

## **3.1 Introduction**

Recently, the increasing global energy demand leads to a dramatic increase in the use of fossil fuels, which greatly arises the adverse health effect and irreversible environmental pollution. Hydrogen ( $H_2$ ) with the highest energy density ( $122 \text{ MJ kg}^{-1}$ ) is regarded as a potential energy carrier due to its cleanness and flexibility [1, 2]. However,  $H_2$  production is still dominated by using non-renewable sources such as natural gas and coal [3]. As an alternative way, the sustainable biomass resource can be used for replacing the fossil ones to produce  $H_2$  via thermochemical and biochemical routes [4-8]. Among various biomass thermochemical conversion processes, biomass steam gasification is considered as a promising one for hydrogen-rich syngas production. In this route, the use of steam as the gasifying agent can not only provide  $H_2$ -rich syngas but also cause the minimal environmental impact, especially prevent  $NO_x$  formation with low generation of  $CO_2$  [9-11]. However, the wide varieties of biomass have different physical characteristics and chemical compositions, which always result in different steam gasification efficiencies. Biomass can be characterized based on (i) chemical component (cellulose, hemicelluloses, and lignin); (ii) elemental composition; (iii) inherent mineral content; (iv) volatile content; (v) moisture content; and (vi) physical properties (particle size, shape, and density). The effects of these parameters on the composition of syngas and gas yield during the biomass steam gasification have been widely investigated [12]. In particular, alkali and alkaline earth metals (AAEMs) as the common inherent mineral species

in biomass have been identified to provide good catalytic effect on enhancing biomass gasification kinetics, and the alkali metals are reported to be more active than the alkaline earth metals with the following order,  $K > Na > Ca > Mg$  [13-15]. The catalytic ability of those AAEM species present in the biomass feed should be vital in applications where the catalysts are hard to be added. Recently, extensive studies have been focused on the co-gasification of coal with biomass [16-20], and found that the gasification rate was enhanced by increasing the biomass proportion in the blends owing to the inherent AAEMs compounds in the biomass [21-25]. The AAEM species present in biomass ash were also reported to promote the conversion of solid char into gaseous products by enhancing the char reactivity and porosity during the gasification [26-28].

In 2017, the worldwide production of banana was 114 million tonnes with India ranking as the predominant producer (29 Mt) followed by China (11 Mt), Philippines (7.5 Mt), Brazil (7 Mt), and Ecuador (7 Mt) [29]. Moreover, the latest data from Japanese Ministry of Agriculture, Forestry and Fisheries (MAFF) indicates that 1.62 Mt of fresh fruit was imported in 2017 in Japan, where banana accounted for over 60.9% share [30]. Banana peel is the major residue from banana which accounts for 30-40% of the total weight of banana. Several studies have been conducted to investigate the potential of BP for the production of syngas, biochar, and bio-oil via the pyrolysis, digestion, and supercritical gasification processes [31-35]. Nevertheless, to the best of our knowledge, the researches on the utilization of BP in the steam gasification or steam co-gasification processes are very limited. He et al. [36] reported the gasification performance of BP and investigated the effect of temperature, steam to carbon ratio on the hydrogen production. However, the effect and utilization viability of AAEM species in

BP ash on the steam gasification and co-gasification have not been explored. Large quantities of AAEM species especially K contained in the BP may provide potential sources of inexpensive catalysts for the promoting of steam co-gasification with other biomass. In this study, the steam co-gasification of banana peel with the agricultural residue (rice husk), woody biomass (Japanese cedarwood), or their mixture was carried out, and the effects of different gasification operating parameters on H<sub>2</sub>-rich gas production yield were investigated and discussed. The aim was to enhance the gasification reactivity and the hydrogen production yields of rice husk and Japanese cedar wood by the addition of banana peel.

## **3.2 Experimental**

### **3.2.1 Materials**

Banana peel (BP, Ecuador), rice husk (RH) and Japanese cedarwood (CW, Aomori, Japan) were used as feedstocks. All the samples were dried in an oven at 105 °C for 24 h before cut and sieved into a size of  $0 < d_p < 1$  mm. The moisture content of sample after drying was analyzed by a MX50 moisture content analyzer (AND, Japan). A kind of small parasitic seashell discarded in the Mutsu Gulf in Japan was utilized as the CaO source, which was calcinated in a muffle furnace at 900 °C for 2 h and ground to the fine powder and stored in a closed container to prevent carbonation and humidification prior to use. The ultimate analysis was conducted by using a Vario El cube elemental analyzer (Germany). The compositions of biomass ash obtained from the calcination of biomass at 800 °C for 2 h in the air were analyzed by an Energy Dispersive X-ray Spectrometer (XRF, EDX-800HS, Shimadzu). Herein, the ultimate and XRF analyses for each sample were performed for 3 times and the average value are shown in **Tables 3.1** and **3.2**. The crystalline structures of the solid residues were determined by an X-ray

diffractor (XRD, Rigaku Smartlab, Japan) with a Cu-K $\alpha$  radiation ( $\lambda = 0.15418$  nm) in a range of 10°–80° with a scanning speed of 10° min<sup>−1</sup>.

**Table 3.1** Ultimate analysis results of biomass samples.

| Ultimate analysis ( wt%, daf basis <sup>a</sup> ) |     |      |     |     |                |
|---|-----|------|-----|-----|----------------|
|   | N   | C    | H   | S   | O <sup>b</sup> |
| <b>BP</b>   | 1.3 | 44.3 | 4.9 | n.d | 49.5           |
| <b>RH</b>   | 0.2 | 40.3 | 5.4 | n.d | 54.1           |
| <b>CW</b>   | 1.4 | 48.8 | 6.6 | 0.2 | 43.0           |

<sup>a</sup> Dry and ash-free.

<sup>b</sup> By difference.

n.d: not detected.

**Table 3.2** Main compositions of biomass ash samples and calcined shell (CS).

| XRF Analysis ( wt% ) |      |      |     |      |      |       |
|----------------------|------|------|-----|------|------|-------|
|                      | Ca   | K    | Na  | Si   | Cl   | Other |
| <b>BP ash</b>        | 3.5  | 67.3 | 2.4 | 2.8  | 21.8 | 2.2   |
| <b>RH ash</b>        | 1.6  | 7.8  | n.d | 88.4 | n.d  | 2.2   |
| <b>CW ash</b>        | 50.7 | 4.0  | n.d | 6.8  | n.d  | 38.5  |
| <b>CS</b>            | 94.7 | 0.3  | n.d | n.d  | n.d  | 2.6   |

### 3.2.2 Steam gasification of biomass

As shown in **Fig 3.1**, the steam gasification experiment was conducted by using a vertical fixed-bed reactor with an inner diameter of 18 mm and a length of 350 mm. For each experimental run of gasification or co-gasification, 1 g of biomass or biomass mixture sample was loaded into the middle section of the reactor. The reactor was placed inside of an electrical furnace, and heated from ambient temperature to the target temperature with a heating rate of 10 °C/min and held at the desired temperature. The peristaltic pump was used to introduce distilled water into a vaporization furnace (250 °C) and then flowed into the reactor with the carrier gas (Ar) at a gas flow rate of 50 cm<sup>3</sup>/min. The steam was introduced into the reactor as the reactor temperature reached 200 °C and the total reaction time was 2 h for each experiment. The steam gasification experiment was conducted at atmospheric pressure with a preset temperature in the range of 650-850 °C. The products carried by Ar gas were passed through two ice-cold bottles without any solution addition and a dry cylinder filter filled up with CaCl<sub>2</sub> particles, where the tar and steam were condensed and adsorbed, and then the gas product with the carrier gas was collected by a 10 L gas bag for 2 h. The main gas compositions of CO, CO<sub>2</sub>, CH<sub>4</sub>, and H<sub>2</sub> in the product were analyzed using a gas chromatograph (GC-TCD, Agilent 7890-USA) and shown as mmol per gram of biomass sample in dry and ash-free basis (mmol/g-biomass d.a.f.).

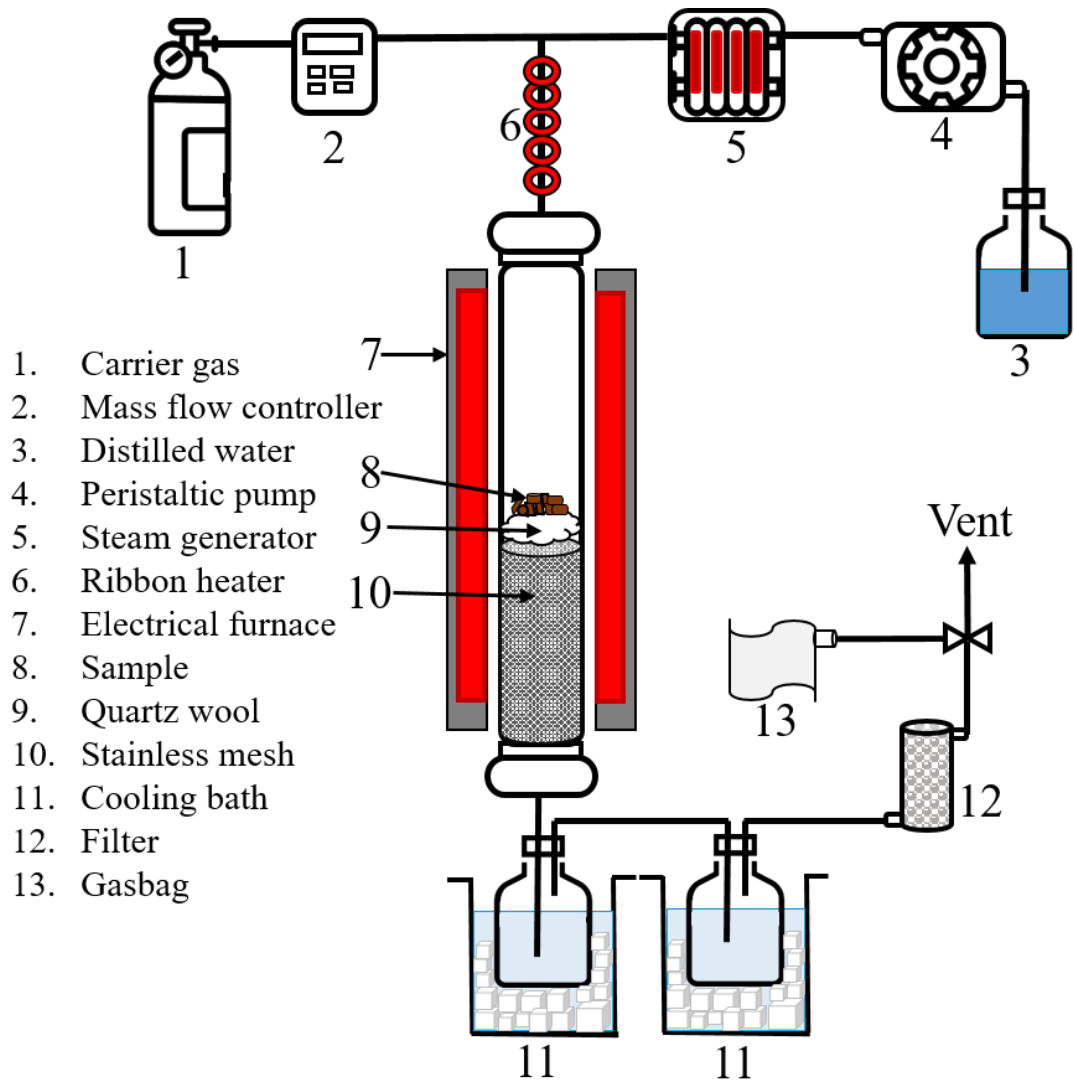


**Fig 3.1** Schematic diagram of a fixed-bed reactor for steam gasification of biomass.

### 3.2.3 Estimation of carbon conversion efficiency

Carbon conversion efficiency (CCE) to gas was calculated by Eq. (1):

$$\text{CCE}(\%) = (\text{C content Produced} / \text{C Supplied}) \times 100 \quad (1)$$

where the “C content produced” is the product gases detected by the GC that contain carbon (i.e., CO, CO<sub>2</sub>, CH<sub>4</sub>). “C supplied” is the total carbon content in dry biomass feedstock which was determined from the ultimate analysis.

### 3.3 Results and discussion

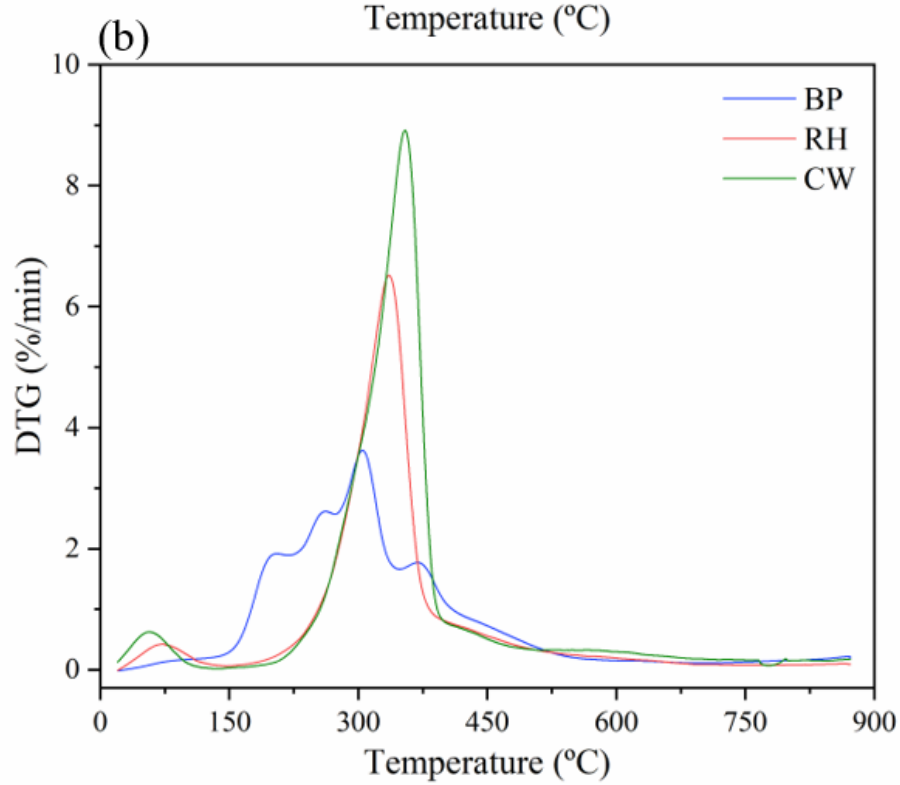
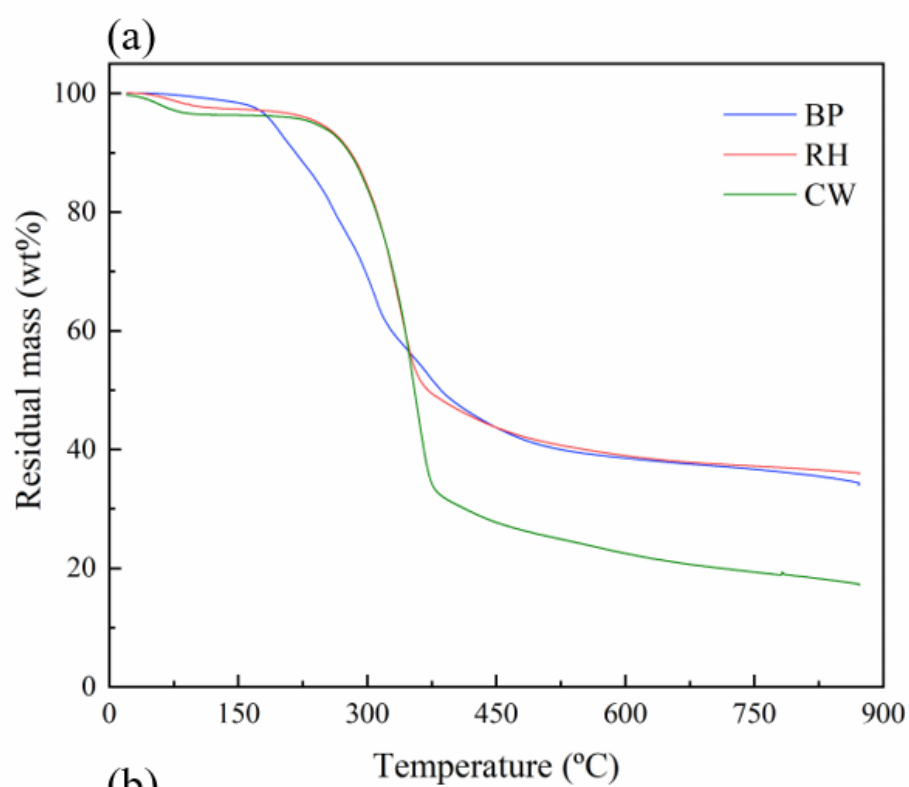
#### 3.3.1 Thermogravimetry analysis

Thermogravimetry analyses (TGA) with the thermogravimetric (DTG) curves of BP, RH CW, and their mixture samples were conducted by heating the sample from ambient temperature to 900 °C with a heating rate of 10 °C/min in the N<sub>2</sub> atmosphere. **Fig 3.2a** shows the TGA results for the three individual biomass samples. It is obvious that the weight loss behaviors of the three biomass samples were different. Herein, the fast weight loss was mainly caused by the volatilization and/or decomposition of hemicellulose and cellulose and the slow weight loss was attributed to lignin decomposition. Meanwhile, the different structures of biochars formed during the thermal decomposition of different biomass feedstocks also affected the decomposition rate [37, 38]. Different types of biomass always contain different amounts of hemicellulose, cellulose and lignin with different molecular structures, resulting different decomposition performances. It is reported that the banana peel contains 7.04% cellulose, 7.94% hemicellulose and 9.70% lignin [39], rice husk contains 31.12% cellulose, 22.48% hemicellulose and 22.34% lignin [40], and Cedar wood contains more contents of cellulose, hemicellulose and lignin (i.e., 39.3%, 12.0%, and 28.8%, respectively (Fayoud et al., 2015)) when compared with them. In **Fig 3.2a**, the first weight-loss stage occurred at a temperature lower than 160 °C with a small amount of weight loss should be attributed to the removal of moisture and the volatilization and/or decomposition of some light volatile matters. The second and third weight-loss stages should associate with the major thermal decompositions of hemicellulose and cellulose at the temperature range of 160-380 °C and lignin mainly at 380-600 °C. The sharp decrease within a narrow temperature range at the second weight-loss stage

for the three individual biomass samples belonged to the decomposition of hemicellulose and cellulose. One can see that the decomposition rate at the third stage, which mainly corresponded to the decomposition of lignin, was slower than that at the second stage since lignin consists of various functional groups and aromatic compounds which can be only decomposed slowly [41]. The thermal decomposition behaviors of three individual samples can be observed more clearly from the DTG curves (**Fig 3.2b**). The thermal decomposition of BP initiated at around 150 °C whereas RH and CW started from 225 °C. The sharp peaks obtained at 304.8 °C, 336.0 °C, and 354.8 °C for BP, RH, and CW respectively should belong to the degradation of hemicellulose and cellulose. The R50 value, which indicates the reactivity of biomass at its T50, was obtained from the TG curve. As summarized in **Table 3.3**, R50 values of BP, RH, and CW were found to be 1.33%/min (at 386.1 °C), 1.12%/min (at 370.7 °C), and 6.34%/min (at 353.6 °C), respectively, and CW had the highest R50 value with the lowest T50 due to the high decomposition rate. The final residual weights of BP, RH, and CW were 33.9 wt%, 35.8%, and 17.1 wt%, respectively.

**Figs 3.2c** and **d** show the TGA and DTG results for the samples of the BP blending with RH and CW respectively with a weight ratio of 1:1. In order to investigate the potential synergetic effects on the decomposition behavior, the predicted results (dot lines) calculated by the TGA results of the three individual samples were also plotted in **Figs 3.2c** and **d**. From the TGA results of BP and RH blends, no significant differences were observed between the measured and predicted results. While, in the case of BP and CW blends, the main difference from the predicted result occurred at around 600 °C, where the decomposition rate was higher than the predicted one. The DTG curves of mixture samples (**Fig 3.2d**) also showed similar trends. It

can be seen that the BP and CW blends decomposed continuously after 500 °C with an increase after 750 °C. In comparison, the decomposition of the BP and RH blends almost finished after 600 °C. Johansen et al. [42] investigated the release patterns of inorganic species (i.e., K, Cl, and S) under the pyrolysis and combustion condition, and found that the release of KCl began as the reaction temperature was higher than 700 °C but the Si-rich sample was able to hinder K releasing. Kowalski et al. [43] also studied alkali release from various types of biomass during the pyrolysis and found that the evaporation of inorganic salt, namely KCl, occurred at a temperature above 600 °C. In the present study, it can be seen from **Table 3.1** that the BP ash contained larger contents of K and Cl while the RH ash contained larger content of Si than the CW ash. Hence, in the case of BP and CW blend, the small peak obtained at 750 °C might be the release of inorganic compounds such as KCl. However, for the BP and RH blend, no obvious peak was observed at the temperature higher than 700 °C due to the alkali retention by the high content of Si from RH. As a result, the R50 values of BP and RH blend and BP and CW blend were almost identical with predicted ones (**Table 3.3**). That is, 1.10%/min (at 380.9 °C) and 5.05%/min (at 356.1 °C) experimental results vs. 1.38%/min (at 379.4 °C) and 5.14%/min (at 359.8 °C) predicted results, respectively. In addition, the final residual weights for the BP and RH blend and BP and CW blend were 34.0% and 20.7% whereas the predicted results were 34.9% and 25.6%, respectively. These results indicated that the mixing of BP and CW exhibited the synergetic effect with an enhanced conversion rate.



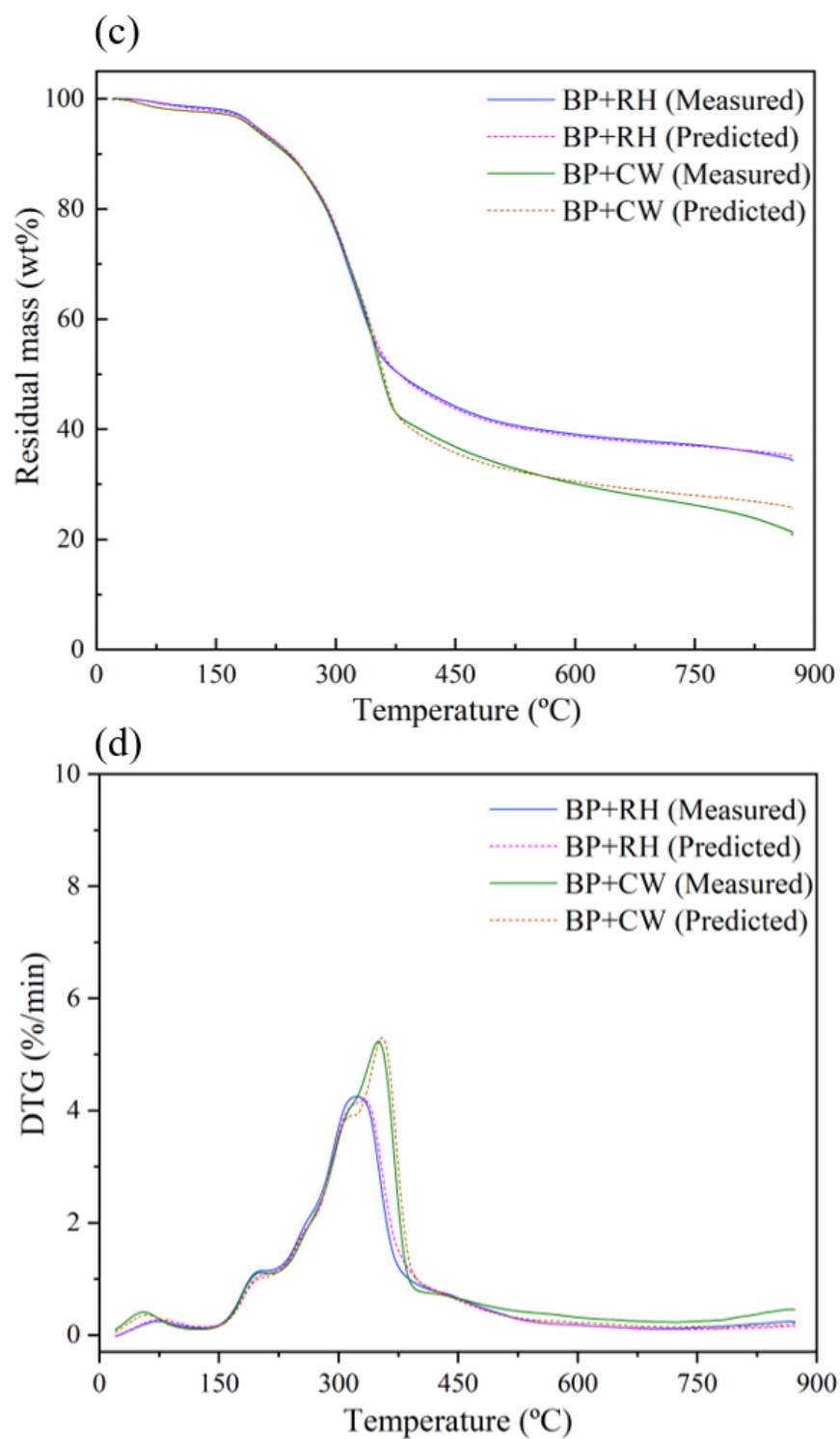


**Fig 3.2** TGA and DTG analyses for the individual samples (a) (b) and blends (c) (d) in N<sub>2</sub> atmosphere at 10 °C/min heating rate.

**Table 3.3** R50 values at T50 and of different samples based on TG analysis results.

|          | BP    | RH    | CW    | BP+RH    | BP+RH     | BP+CW    | BP+CW     |
|----------|-------|-------|-------|----------|-----------|----------|-----------|
|          |       |       |       | Measured | Predicted | Measured | Predicted |
| T50 (°C) | 386.1 | 370.7 | 353.6 | 380.9    | 379.4     | 356.1    | 359.8     |
| R50      | 1.33  | 1.12  | 6.34  | 1.10     | 1.38      | 5.05     | 5.14      |
| (%/min)  |       |       |       |          |           |          |           |

### 3.3.2 Steam gasification of individual biomass

For comparison, the steam gasifications of individual samples of BP, RH and CW were conducted at three different temperatures 650 °C, 750 °C, and 850 °C for 2 h, respectively. In our previous study [44] and the preliminary experiments, it was found that the 0.15 g/min was the optimal water injection rate and the higher water injection rate than it resulted in a decrease in the total gas production yield, which might be attributed to the decrease of inner temperature and lack of feedstock to react with more steam. Therefore, the water injection rate was fixed at 0.15 g/min for all gasification and co-gasification experiments in this study. As shown in **Fig 3.3a**, the steam gasification of BP gave the largest amount of gas product mainly including H<sub>2</sub> and CO<sub>2</sub> with a small amount of CH<sub>4</sub> at all the three reaction temperatures. Comparing to the agricultural residue and the woody biomass, BP contains less cellulose, hemicellulose and lignin but with a large amount of carbohydrates (sugar), protein and simple lipids. Schumacher et al. [45] reported that the gasification of carbohydrates(sugar) was easier than that of lignocellulosic biomass at 200-400 °C in a supercritical water gasification condition. In the

present study, it is also found that the gasification reactivity of BP and the gas production yield from BP were much higher than those of RH and CW. On the one hand, the carbohydrates (sugar) were also easier to be gasified in the steam atmosphere at ambient pressure than cellulose, hemicellulose and lignin. On the other hand, a large amount of AAEM species, especially potassium species (K), was also contained in BP, which could *in-situ* promote tar cracking and char reforming during the pyrolysis and steam gasification, thereby increasing the gas product from the steam reforming of carbon species. Several studies have also proven that the AAEM catalysts such as  $K_2CO_3$  and CaO had high activity for the tar decomposition and steam biomass gasification [46-48].

Temperature is one of the most vital operating parameters for the thermochemical conversion of biomass, especially, for the endothermic steam gasification reactions. In general, high temperature can promote the initial pyrolysis process, the steam char gasification and the secondary tar cracking and hydrocarbon reforming [49]. As shown in **Figs 3.3a** and **3b**, the temperature had great effect on the yield and concentration of  $H_2$  from the steam gasification as well as the carbon conversion efficiency (CCE) to gas product for all the three samples. One can see that the steam gasification of CW and RH showed identical gasification performance at lower temperatures and the  $H_2$  production at 850 °C increased three times higher than those at 750 °C. Moreover, the  $H_2$  concentrations from CW and RH rose from 35.8% and 35.3% to 69.8% and 66.8% respectively when the gasification temperature was increased from 650 °C to 850 °C. Meanwhile, the CCEs of RH and CW increased significantly with the increasing of reaction temperature. Herein, although both CW and RH showed low total gas yields at lower temperatures, the reasons might be different. One can see that the conversion rate of CW at

750 °C was around 92% while that of RH was around 88%, indicating that fewer solid residue was obtained from the gasification of CW. As shown in **Table 3.1**, CW contained the highest carbon content, however, the CCE of CW was the lowest in **Fig 3.3b**. Herein, the total tar amount from the gasification of woody biomass could be increased with the reducing of reaction temperature and the increasing of the initial moisture content of the feedstock [50]. As shown in **Fig 3.2a**, CW contained a higher moisture content when compared with the other two kinds of biomass. Therefore, more liquid product (tar) should be produced from the gasification of CW at a lower temperature when compared with that of RH.

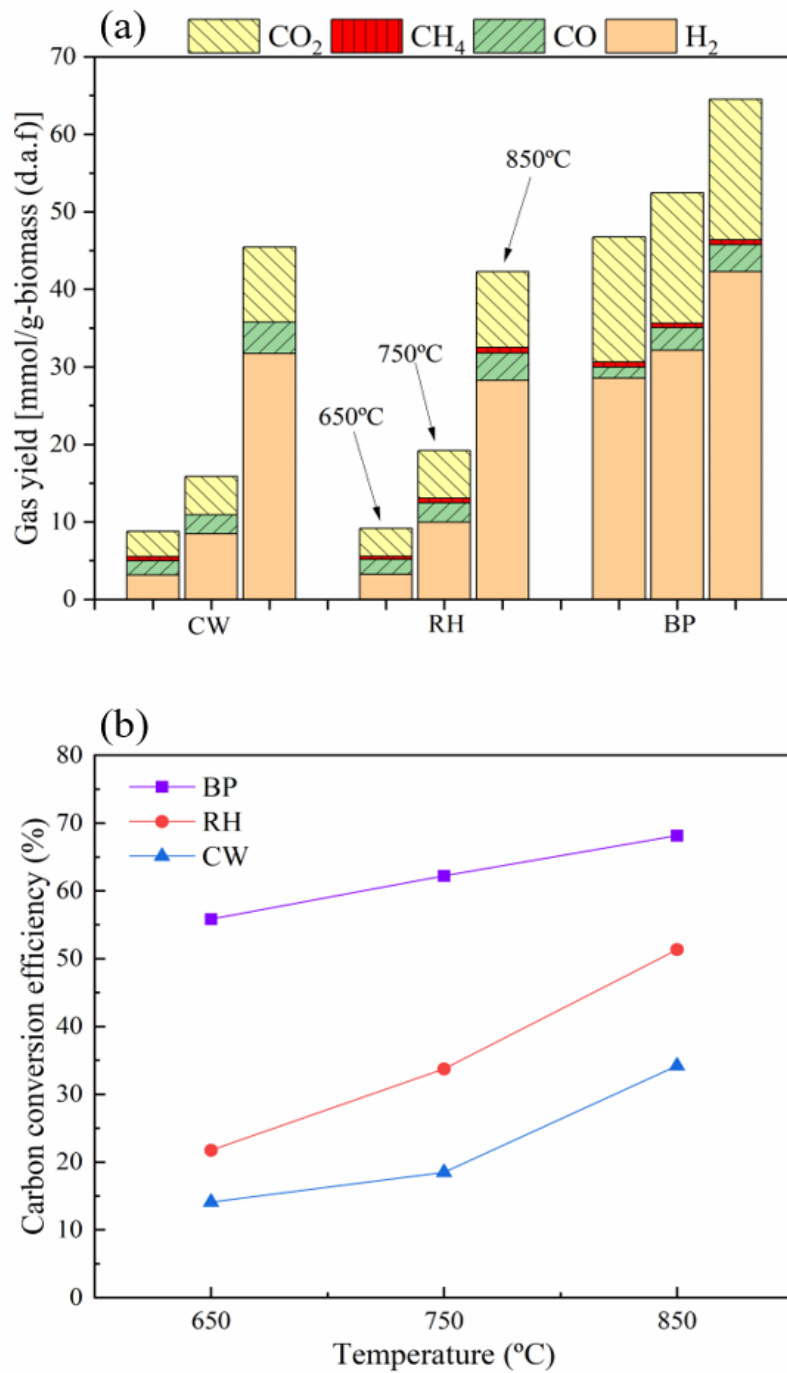


**Fig 3.3** Steam gasification of three types of individual biomass at three different temperatures with a water injection rate of 0.15 g/min: (a) gas yield; (b) carbon conversion efficiency to gas.

### 3.3.3 Steam co-gasification of biomass mixture

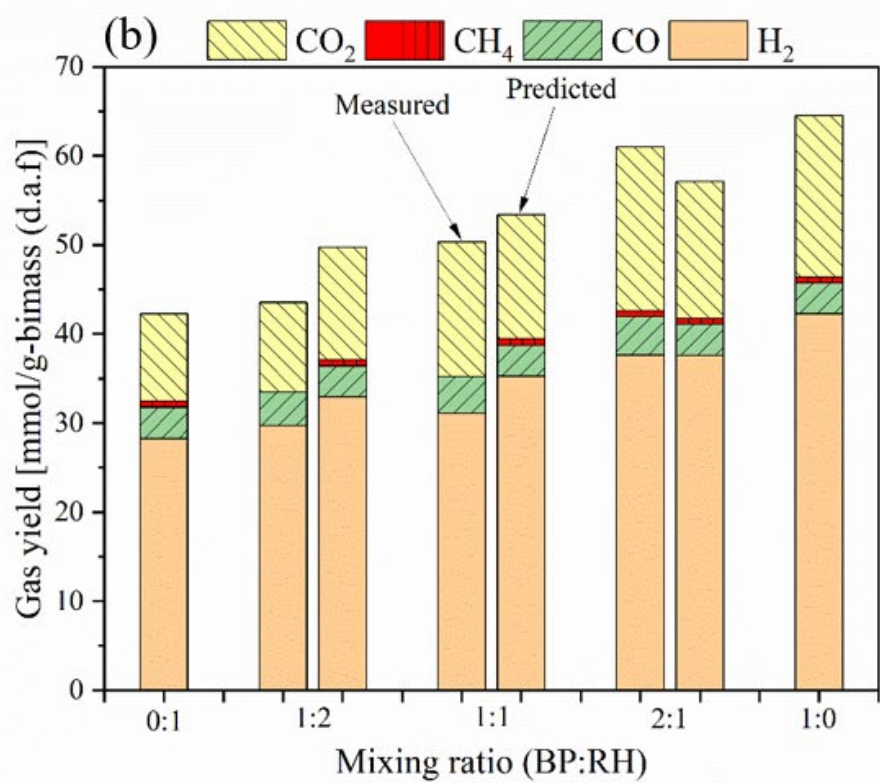
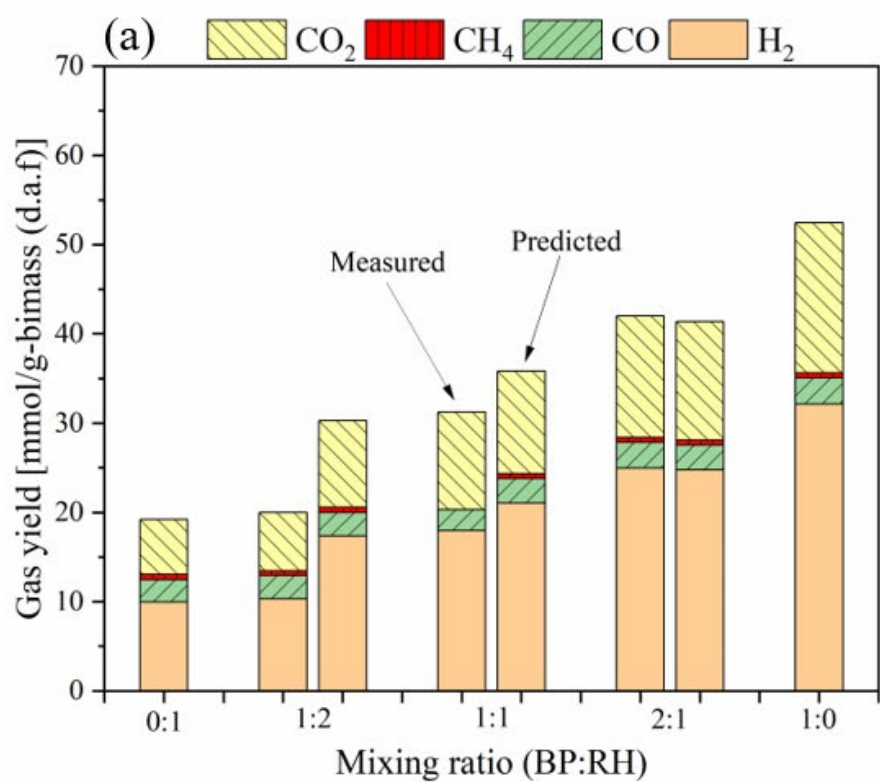
As described above, due to the higher inherent K content in BP, the steam gasification of BP showed higher gasification reactivity as well as higher H<sub>2</sub> production yield. In recent years, the catalytic effect of K species on the steam gasification of biomass has been studied extensively [51-53]. K species could act as the Lewis acid, depositing at different sites of the carbon surface and creating channels during gasification to bring the gasifying agent into contact with the carbon, thereby increasing the reaction rate [54]. The high mobility of the K species in catalytic gasification always leads to a high dispersion on the surface of the carbon and the micropore [21, 55, 56]. In the present study, the catalytic effect of the inherent K from the BP on the steam gasification of RH and CW by mixing BP with them was investigated. The BP was physically mixed with RH and CW respectively by the different weight ratios and gasified at 750 °C and 850 °C. By using the results from the steam gasification of individual samples of BP and RH, the predicted gas yields were calculated, which were compared with the experimental results of the co-gasification.

### 3.3.4 Steam co-gasification of BP and RH

**Fig 3.4** shows the gas yields from the steam co-gasification of BP and RH at 750 °C **(a)** and 850 °C **(b)** with different BP/RH weight ratios (0:1, 1:1, 1:2, 2:1, 1:0) at a water injection rate of 0.15 g/min for 2 h. The results were also compared with the predicted ones based on the results from the steam gasification of individual samples of BP and RH. Obviously, more gas products, especially H<sub>2</sub> yield, increased at higher gasification temperature. However, the enhancement effect only occurred in the case of more BP existed in the biomass mixture, for example, the case with a BP/RH weight ratio of 2:1, in which the gas yield was higher than

that from the predicted result. Herein, although the difference was not so obvious, it can be seen that the synergetic effect appeared when the BP/RH weight ratio was increased to a suitable value. While, the CCE to gas (**Fig 3.3c**) had the similar trend, which increased with the increasing of reaction temperature as well as the increasing of weight ratio of BP in the blend. The main reason for the negative effect on the gas yield during the co-gasification of BP and RH with more RH content should be attributed to the large content of Si species in the RH. It is reported that the devolatilization rate of biomass could be inhibited and the degradation temperature of biomass increased in the presence of large amount of Si species in the biomass [51, 57]. As indicated in the XRF analysis results (**Table 3.2**), the RH ash was dominated by Si species (88.4 wt%). Correspondingly, the high content of Si in RH might delay the release of volatiles and K species from BP, resulting in the disappearance of the promoting effect of BP on the gasification of RH. Furthermore, K species in the BP could react with Si species in RH to form stable and unreactive potassium aluminosilicates and/or silicates, leading the losing of the catalytic effect of some K species in the BP for the gasification [51, 58, 59]. Rizkiana et al. [60] reported that the presence of Si in the biomass ash also inhibited the reactivity of the low-rank coal during the steam gasification. To confirm whether the alkali silicate was formed or not during the gasification, XRD analysis was conducted for the ash residues from the co-gasification of BP and RH at 750 °C with different mixing weight ratios. As shown in **Fig 3.4d**, the broad peak between 20° and 33° in the 2θ scale was assigned to the disordered carbons. The crystalline peaks corresponding to SiO<sub>2</sub> were observed between 21° and 23° in each case. In addition, the diffraction peaks corresponding to KCl (PDF#41-1476) located at around 28° and 40° were also found in the cases of the mixing weight ratios of BP and RH at 1:1 and 2:1.

The ashes from co-gasification of BP and RH at 750 °C were dominated by SiO<sub>2</sub> and KCl. However, the alkali silicate peaks were difficult to be determined accurately due to the overlap of the peaks. However, the disappearance of the KCl in the case of the mixing weight ratio of 1:2 might be the evidence of the formation of potassium silicate. Zhao et al. [61] investigated the release and transformation of K<sub>2</sub>CO<sub>3</sub> and KCl during the biomass thermal conversion, and found that KCl could react with SiO<sub>2</sub> to form insoluble K silicates in the presence of steam. The increase in Si content could increase the possibility of the alkali silicate formation, resulting in a decrease in the mass concentration of KCl. Thus, when BP is mixed with other biomass containing Si species, its amount should be over a value so that the negative effect of Si species is offset. Therefore, in this study, the gas yield from the steam co-gasification of BP and RH with a BP/RH weight ratio of 2:1 exhibited a promoting effect for the production of H<sub>2</sub>-rich gas product.



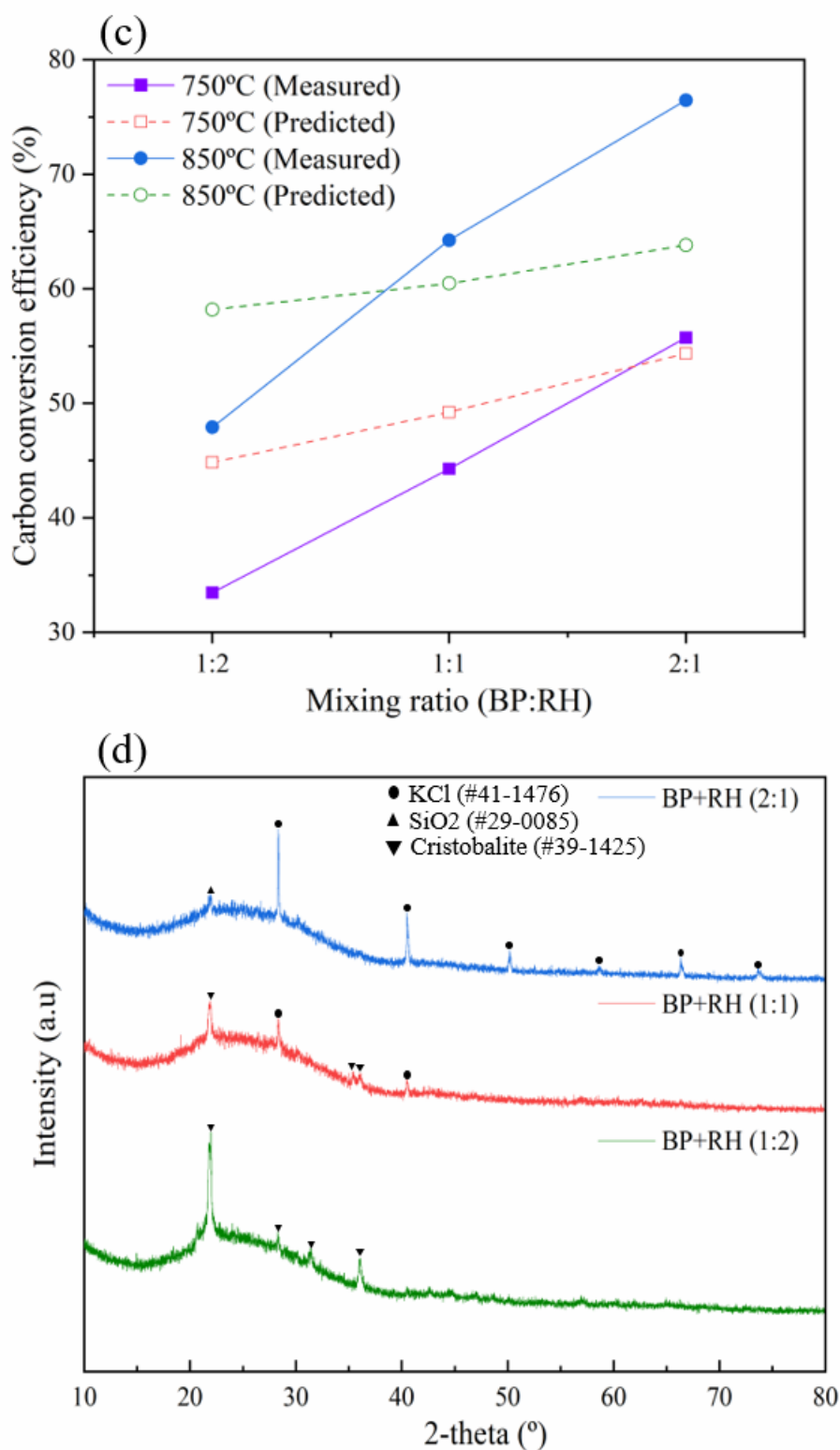
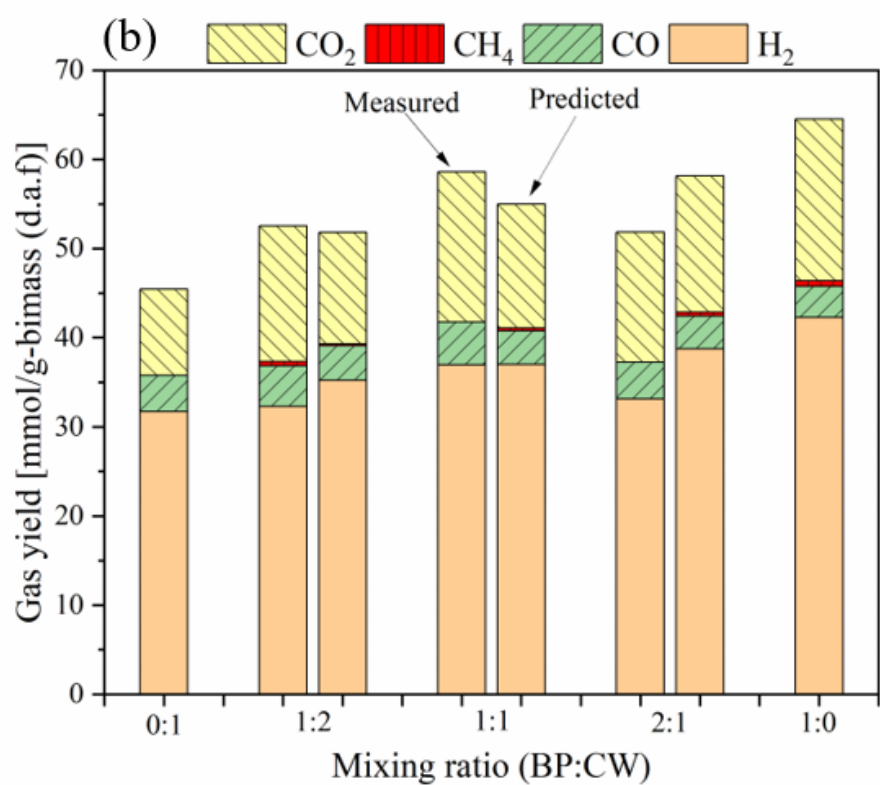
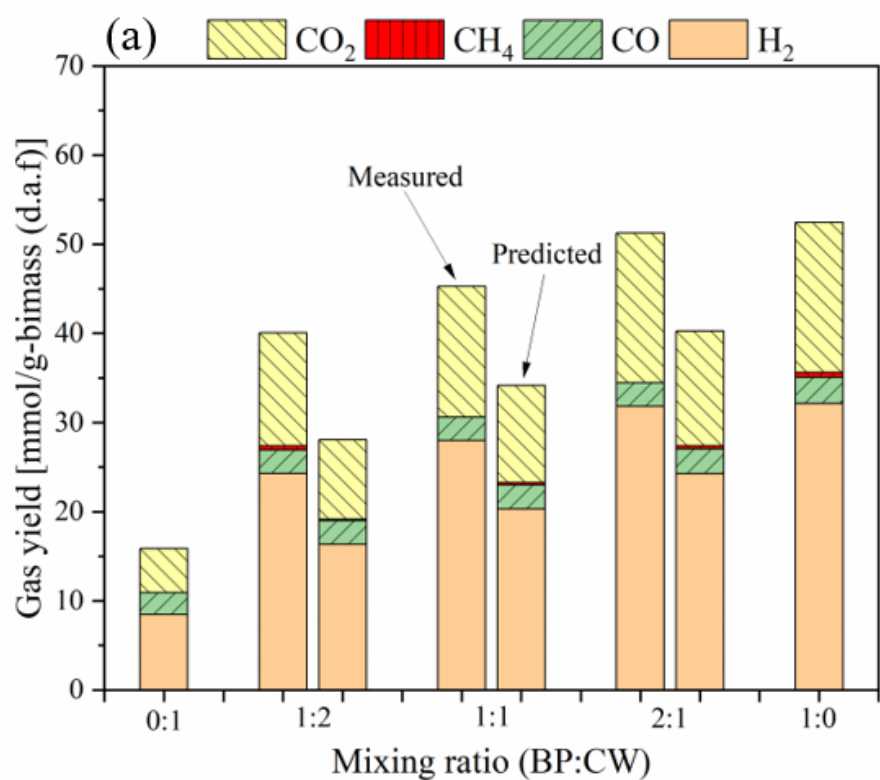


**Fig 3.4** Gas yields from steam co-gasification of BP and RH (a): at 750 °C; (b): at 850 °C, and compared with the predicted ones; (c) Carbon conversion efficiency to gas; (d) XRD analysis for the residues after the gasification.

### 3.3.5 Steam co-gasification of BP and CW

**Figs 3.5a and b** show the gas yields from the steam co-gasification of BP with another biomass without Si species in it, i.e., CW, at 750 °C and 850 °C respectively with different BP/CW weight ratios (0:1, 1:1, 1:2, 2:1, 1:0) at a water injection rate of 0.15 g/min for 2 h. The results were also compared with the predicted ones based on the results from the steam gasification of individual samples of BP and CW. Unlike the results from the co-gasification of BP and RH, in which the promoting effect was hindered due to the high content of Si in the RH, the synergetic effect by the mixing BP of CW was obviously observed, especially at the relatively lower gasification temperature of 750 °C (**Fig 3.5a**). As shown in **Fig 3.5a**, the total gas production yields and especially the H<sub>2</sub> yield in the co-gasification cases were much higher than those predicted ones. It was also obvious that the amount of BP in the blend greatly affected the gas production yield. Moreover, the gas production yield from the steam gasification of the individual CW at 750 °C was very low. However, after adding more BP into the blend, the gas production yield, especially the H<sub>2</sub> and CO<sub>2</sub> yields, increased significantly, which could be mainly attributed to the promoting catalytic effect of AAEM species in the BP for the gasification of CW. As a common woody-biomass, CW only contains a small content of ash species (0.2 wt%) while BP contains a larger content of ash species (11 wt%) enriched in K species. As such, in the case of co-gasification of CW with BP, a part of AAEM species in the BP could promote the catalytic activity for the CW gasification. In addition, as a woody-biomass, CW tends to generate more tar at the early stage of gasification while the K species could be evaporated from the BP. As such, the generated tar from the CW might be catalytically converted into syngas by the evaporated K species in the BP via the steam reforming reaction

during the steam co-gasification of BP and CW. Moreover, as shown in **Fig 3.3**, BP was much easier to be gasified than CW. During the co-gasification process, more H and OH radicals could be released from BP at first, which could further promote the cracking of heavy tar to light tar as well as syngas [62]. However, as shown in **Fig 3.5b**, the synergetic effect decreased after the co-gasification temperature was increased to 850 °C. Herein, although the total gas yields based on the experiments were slightly higher than those predicted ones at the BP/CW mixing ratios of 1:1 and 1:2, it should be noted that the increases were accounted for the CO<sub>2</sub> production. At high gasification temperature, K species in the BP could be evaporated into the gas phase, reducing its catalytic effect on the gasification of solid residues of CW. Thus, the synergetic effect between BP and CW only appeared at a relatively lower gasification temperature. **Fig 3.5c** compares the experimental results of the steam co-gasification of BP and CW with three weight mixing weight ratios at 750 °C and 850 °C. At the BP/CW mixing weight ratio of 2:1, it was observed that the total gas production yield at 750 °C was almost identical to that at 850 °C, also indicating that the suitable mixing ratio could effectively achieve the best co-gasification result even at lower gasification temperatures. The CCEs to gas of co-gasifications of BP and CW at 750 °C and 850 °C are shown in **Fig 3.5d**. It can be seen that the CCEs of the measured results were all higher than those of predicted ones. The co-gasification of BP and CW at 850 °C with a mixing weight ratio of 1:1 showed the highest CCE (around 60%). Moreover, the CCE of the mixing weight ratio of BP and CW at 2:1 showed a higher value at 750 °C than that at 850 °C due to the synergistically catalytic effect as mentioned above.



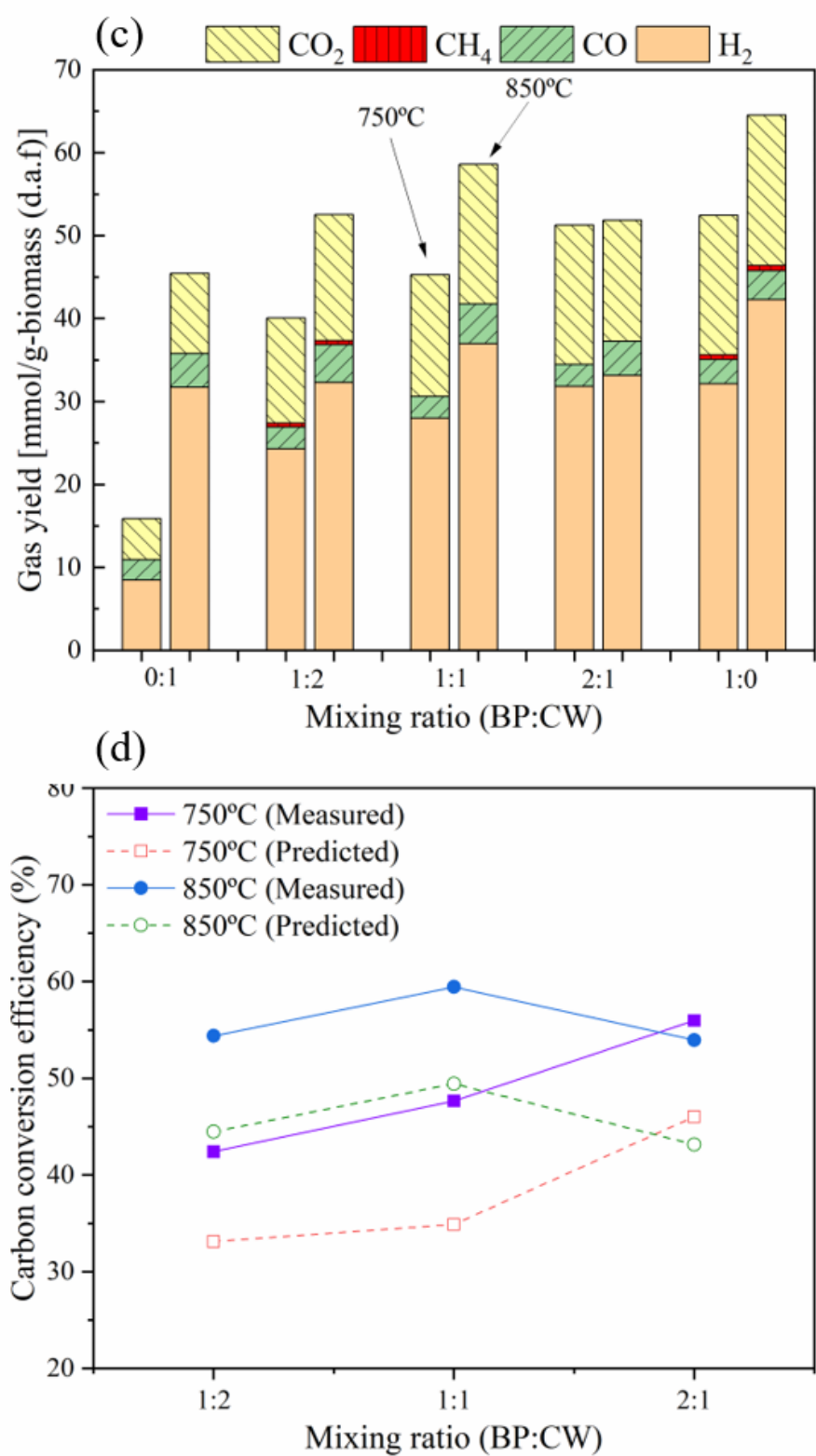


**Fig 3.5** Gas yields from steam co-gasification of BP and RH (a): at 750 °C; (b): at 850 °C; (c): comparison of experimental results obtained at 750 °C and 850 °C; (d) Carbon conversion efficiencies to gas.

### 3.3.6 Steam co-gasification of BP, CW and RH

As indicated above, the high content of Si in RH could offset the catalytic effect of K from BP, thereby decreasing the reaction rate during the steam co-gasification of BP and RH. In contrast, the steam co-gasification of BP and CW showed a positive synergetic effect at lower gasification temperature due to no Si species in them and meanwhile rich K and Ca species in BP and CW respectively. Also, it is reported that Ca species can react with Si species to form aluminosilicates and/or silicates preferentially, which potentially deactivate the AAEM catalysis performance [63-65]. Herein, the steam co-gasification of BP, RH and CW together was conducted to investigate the synergetic effect of K and Ca species from BP and CW and the negative effect of Si species from the RH. **Fig 3.6a** shows the gas yields from the steam co-gasification of BP with CW without Si species but with rich Ca species in its ash and RH with rich Si species in its ash at 750 °C with different BP/CW/RH weight ratios (1:2:1, 1:1:1, 2:2:1 and 2:1:1) at a water injection rate of 0.15 g/min for 2 h. The results were also compared with the predicted ones based on the results from the steam gasification of individual samples of BP, CW and RH. One can see that the synergetic effect occurred when the weight ratio of CW in the mixture was the same or higher than that of BP. Comparing with the co-gasification results shown in **Fig 3.4a**, the Ca species provided from CW could greatly affect the gasification performance of the mixture. However, the ash content of CW was much lower than those of BP and RH, the Ca species amount from CW might be not enough to react with the large amount of Si from RH to avoid its negative effect on the K species in BP when the same or little more amount of CW was added in the mixture. As a result, the improvement of the synergetic effect on the gas production yields was not so significant as shown in **Fig 3.6a** or

even a negative effect was still exhibited when less amount of CW was mixed (e.g., with a BP/CW/RH weight ratio of 2:1:1). As shown in **Fig 3.6b**, the CCEs of mixture samples showed identical trends with the gas yield, and the highest CCE of the mixture sample was obtained at the mixing ratio of 1:1:1 which was also higher than the predicted result.

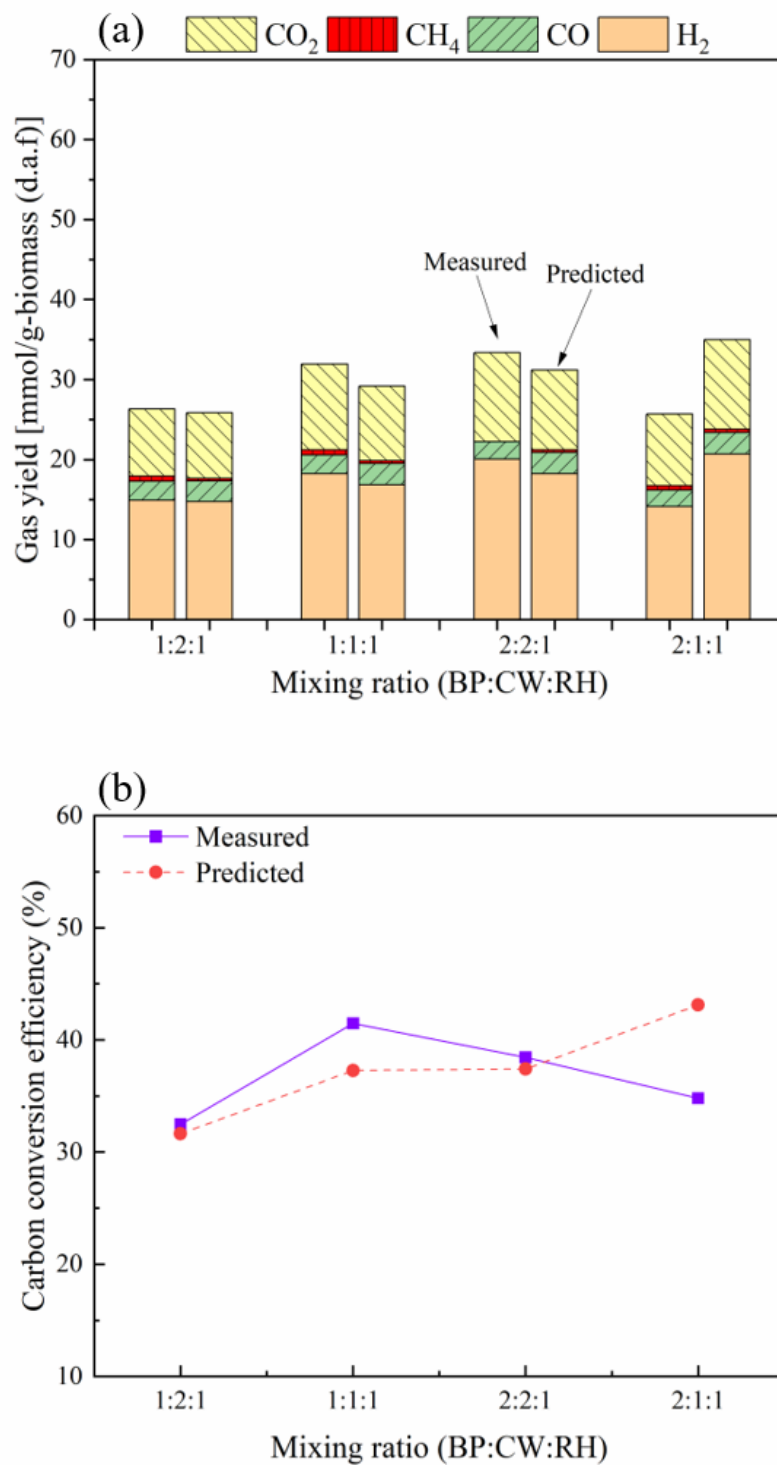


**Fig 3.6** (a) Steam co-gasification of the mixture (BP+CW+RH) samples with different mixing weight ratios; (b) Carbon conversion efficiency to gas for the mixture samples.

### 3.3.7 Effect of the addition of calcined seashell

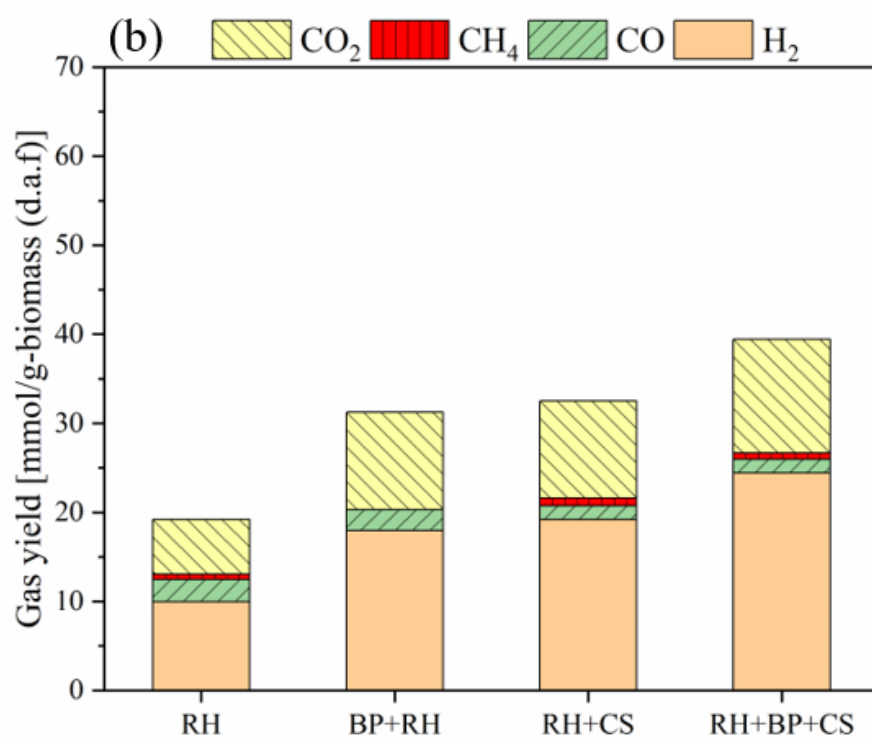
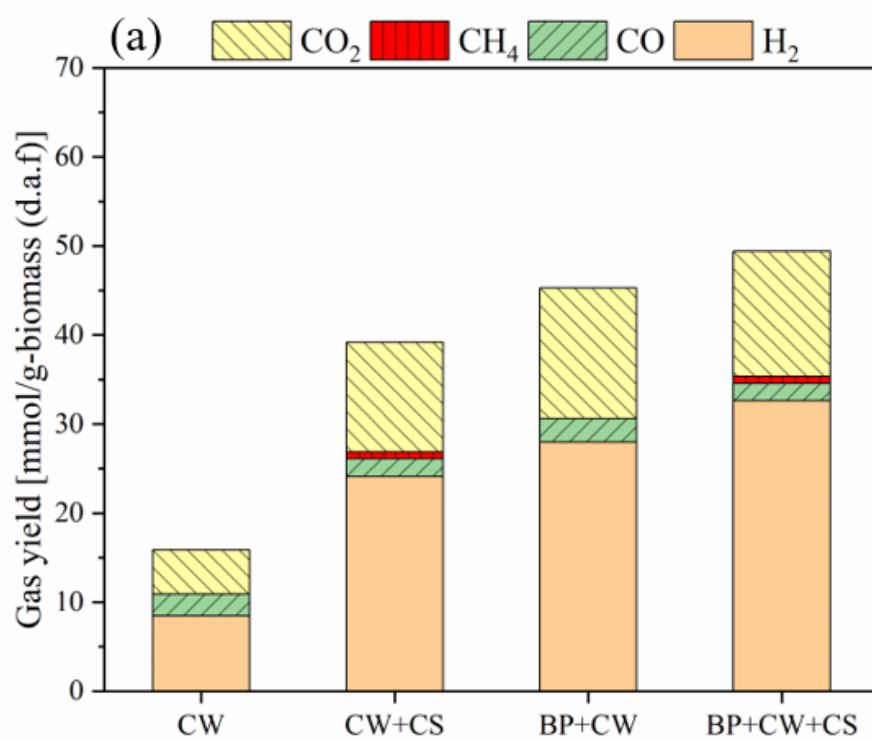
In order to further improve the gasification performance and provide more content of Ca species to avoid the negative effect of Si species in the RH, calcined seashell (CS), whose main component is CaO, was also introduced into the mixture in this study. Calcium-based (e.g., CaO) adsorption-enhanced steam gasification of biomass (AESGB) has attracted great attention for H<sub>2</sub> production in recent years. It was reported that CaO introduced in the steam gasification process as an in-situ CO<sub>2</sub> absorbent could effectively absorb the CO<sub>2</sub> in syngas since it can shift the chemical reaction equilibrium of the gasification process to produce more H<sub>2</sub> with a higher concentration. In our previous studies, it was also found that the addition of CS can be not only utilized as a CO<sub>2</sub> sorbent but also acted as a catalyst for enhancing hydrogen production [44, 66]. **Figs 3.7a** and **b** show the effect of the CS addition on the gas production yields in different cases of gasification at 750 °C with a biomass/CS mixing weight ratio of 1:1. Obviously, the gas production yields, especially H<sub>2</sub> and CO<sub>2</sub>, from the gasification of CW or RH in the presence of CS increased significantly when compared with those without CS addition. Meanwhile, the CO yields decreased in both cases. One possible reason is that the shift in the chemical equilibrium of the water gas shift (WGS) reaction due to CO<sub>2</sub> absorption. However, the increase in H<sub>2</sub> yield was higher than the decrease in CO yield since the addition of CS not only affected the chemical equilibrium but also provided catalytic effect during the gasification process, resulting in H<sub>2</sub>-rich production. In **Fig 3.7a**, the gas yield from the co-gasification of BP and CW with a mixing weight ratio of 1:1 was higher than that from the catalytic gasification of CW in the presence of CS due to the high gasification reactivity of BP and the synergetic effect of inherent AAEM species from BP and CW. However, the co-

gasification performance for the mixture of BP and CW was further improved by the addition of CS. Meanwhile, although the high content of Si species in RH would react with AAEM species in other biomass to form alkaline silicates and decrease the gasification reaction rate, as shown in **Fig 3.7c**, the gas production yield from the steam gasification of RH in the addition of CS was slightly higher than that from the co-gasification of RH and BP. Herein, the catalytic gasification of RH in the presence of CS was performed in a CaO-rich condition. As such, the CaO content in the reaction system was sufficient to catalyze the gasification of the organic components in the RH even though the Si species in it could result in the formation of calcium silicate during the reaction. Moreover, it should be noted that the total carbon content in the catalytic gasification of RH was much lower than that in the co-gasification of RH and BP, but the gas yields were almost the same in the both cases, indicating the conversion and gasification reactivity of RH were enhanced significantly by the addition of CS. In addition, the gas yield from the steam co-gasification of BP and RH with a mixing weight ratio of 1:1 was also improved after the addition of the same weight amount of CS. These results indicated that the additional CaO played an important catalytic function on the co-gasification of biomass with high Si species and other biomass.

**Fig 3.7c** compares gas yields from the co-gasification of different mixture samples in the presence and absence of CS with the predicted ones. Herein, for the co-gasification of two biomass, the same amount of two biomass samples were physically mixed (1:1), while in the case of the co-gasification of three biomass (BP+CW+RH), the mixing weight ratio of BP/CW/RH of 2:2:1 was used since the highest H<sub>2</sub> production yield was obtained from this mixing ratio (**Fig 3.6a**). In the case of CS addition, the weight ratio of biomass/CS was also

(1:1). As shown in **Fig 3.7c**, the co-gasification of BP and CW in the presence of CS gave the highest gas production yield. Meanwhile, the co-gasification of BP+CW+RH in the presence of CS also resulted in a high gas production yield. Especially, in this case, the experimental results were all better than the predicted ones, indicating the synergetic effect occurred during the co-gasification. In addition, it should be mentioned that in the case of the co-gasification of BP and RH with or without CS addition, the experimental results were worse than the predicted ones. However, after adding the CW, the gas production yield increased significantly and also was higher than that of predicted ones, suggesting that the addition of CW could improve the synergetic effect. **Fig 3.7d** compares the CCEs to gas in the co-gasifications of the different mixture samples in the absence and presence of CS. It can be seen that all the CCEs of measured results were higher than those of predicted ones except the co-gasification of BP and RH without CS addition, whereas the highest CCE was obtained after the adding of CS for the co-gasification of BP and RH. In the co-gasification of the mixture sample (BP+CW+RH) in the presence of CS, the Si species from RH could react with Ca from CW preferentially, avoiding the reacting with K from BP and CaO from CS. As such, the K from BP and CaO from CS can maintain their catalytic activity for the gasification of organic components in the biomass mixture. However, it was difficult to determine the formation of alkali or alkaline silicates from the further XRD analysis on the residues obtained from gasification and co-gasification of individual samples and mixture samples in such a CaO-rich condition and the diffraction patterns were dominated by the CaO and Ca(OH)<sub>2</sub> peak signals. Wang et al. [67] investigated the steam gasification of coal char in the presence of K<sub>2</sub>CO<sub>3</sub> for hydrogen-rich gas production and the enhanced catalytic effect in the steam gasification of coal char by utilizing Ca(OH)<sub>2</sub>

for char preparation. It was found that  $\text{Ca}(\text{OH})_2$  played a significant role in suppressing the interactions between  $\text{K}_2\text{CO}_3$  and acidic minerals in coal during the gasification, which mitigated the deactivation of the  $\text{K}_2\text{CO}_3$  catalyst. Hence, in the present study, the introduction of the CS could not only improve the WGS reaction and reduce the tar formation but also prevent the deactivation of the K compounds, resulting in a higher gas yield from the mixture sample.



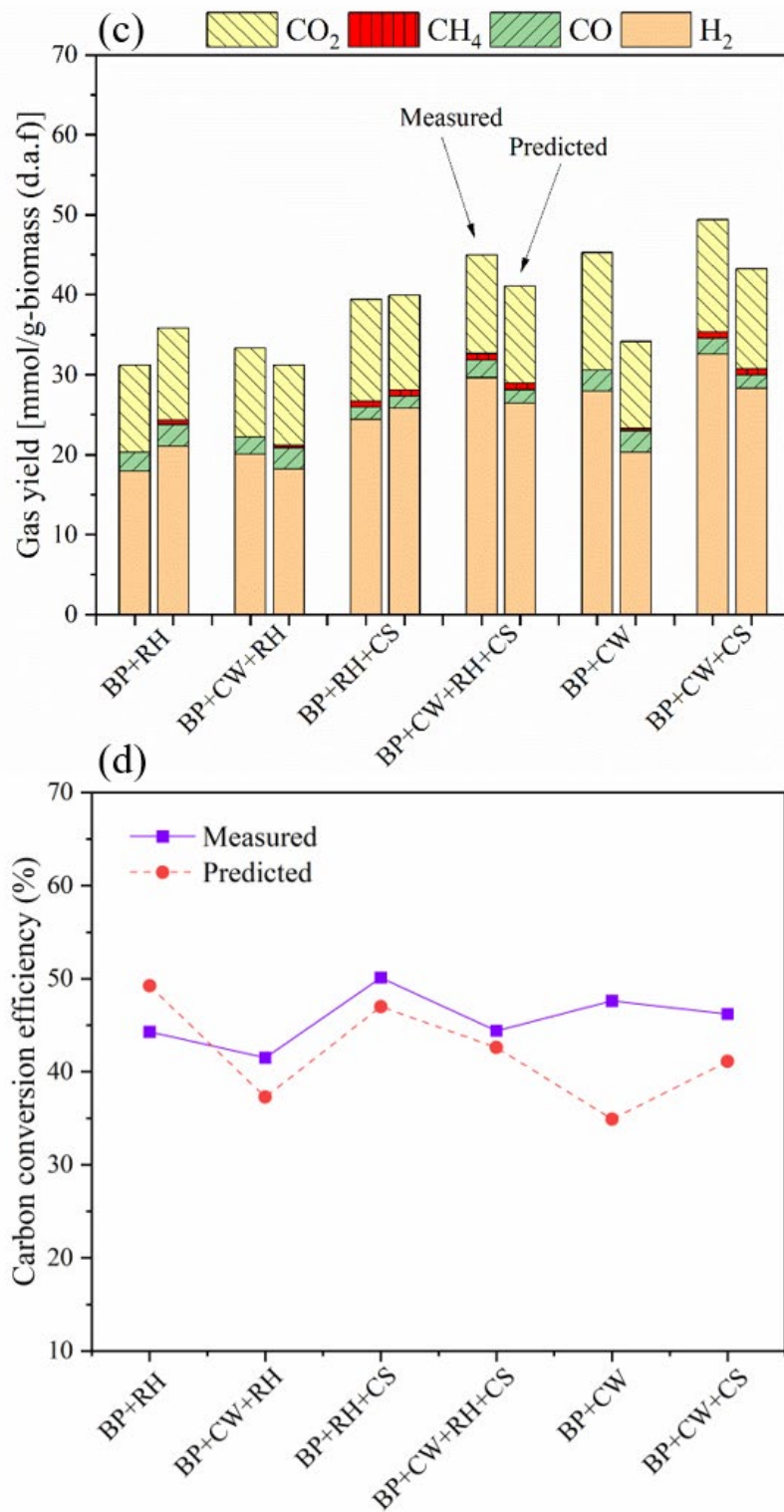


**Fig 3.7** (a) and (b): Effect of the CS addition on the gas yield in different cases at 750 °C with a biomass/CS mixing weight ratio of 1:1; (c): Comparison of the different co-gasification processes with and without CS addition; (d): Comparison of carbon conversion efficiencies to gas by using different mixture samples.

### 3.4 Conclusions

Steam co-gasification of banana peel with other biomass with different properties were performed in order to investigate the synergistic effect of different biomass with different inorganic species, and the following conclusions were obtained:

- (1) It is found that BP with a high content of K species in its ash was easier to be gasified at relatively low gasification temperature when compared with RH with high Si species and CW with a low ash content but high Ca species in its ash.
- (2) The high content of Si species in RH obviously hindered the gasification rate during the co-gasification with BP, resulting in a low total gas production yield. Herein, it is considered that the high content of silica species in the RH had a negative effect on the gasification reactivity of BP during the co-gasification since it could hinder the release of AAEM from the biomass and/or lead to the possible formation of inactive alkaline silicates. However, the synergistic effect can be still achieved by addition of suitable amount of BP.
- (3) The synergetic effect was found in the co-gasification of these three different types of biomass and a higher gas production yield was obtained since the high content of Ca species in the CW ash could preferentially react with the Si species from RH, avoiding the potential hindrance of the catalytic activity of K from BP.
- (4) The addition of calcined seashell (CS) as the CaO resource was found to be an effective way to offset the negative effect of Si species in the RH, resulting in an improved H<sub>2</sub>-rich gas production yield.

### References

- [1] Nowicki L, Markowski M. Gasification of pyrolysis chars from sewage sludge. Fuel.

2015;143:476-83.

[2] Kang K, Azargohar R, Dalai AK, Wang H. Systematic screening and modification of Ni based catalysts for hydrogen generation from supercritical water gasification of lignin. *Chemical Engineering Journal*. 2016;283:1019-32.

[3] Kalamaras CM, Efstathiou AM. Hydrogen Production Technologies: Current State and Future Developments. *Conference Papers in Energy*. 2013;2013:690627.

[4] Huang A-N, Hsu C-P, Hou B-R, Kuo H-P. Production and separation of rice husk pyrolysis bio-oils from a fractional distillation column connected fluidized bed reactor. *Powder Technology*. 2018;323:588-93.

[5] Loy ACM, Yusup S, Lam MK, Chin BLF, Shahbaz M, Yamamoto A, et al. The effect of industrial waste coal bottom ash as catalyst in catalytic pyrolysis of rice husk for syngas production. *Energy Conversion and Management*. 2018;165:541-54.

[6] Cai W, Dai L, Liu R. Catalytic fast pyrolysis of rice husk for bio-oil production. *Energy*. 2018;154:477-87.

[7] Minh Loy AC, Yusup S, Fui Chin BL, Wai Gan DK, Shahbaz M, Acda MN, et al. Comparative study of in-situ catalytic pyrolysis of rice husk for syngas production: Kinetics modelling and product gas analysis. *Journal of Cleaner Production*. 2018;197:1231-43.

[8] Zhang S, Zhang H, Liu X, Zhu S, Hu L, Zhang Q. Upgrading of bio-oil from catalytic pyrolysis of pretreated rice husk over Fe-modified ZSM-5 zeolite catalyst. *Fuel Processing Technology*. 2018;175:17-25.

[9] Qadi NMN, Zaini IN, Takahashi F, Yoshikawa K. CO<sub>2</sub> Cogasification of Coal and Algae in a Downdraft Fixed-Bed Gasifier: Effect of CO<sub>2</sub> Partial Pressure and Blending Ratio. *Energy & Fuels*. 2017;31:2927-33.

[10] AlNouss A, McKay G, Al-Ansari T. A comparison of steam and oxygen fed biomass gasification through a techno-economic-environmental study. *Energy Conversion and Management*. 2020;208:112612.

[11] Shayan E, Zare V, Mirzaee I. Hydrogen production from biomass gasification; a theoretical comparison of using different gasification agents. *Energy Conversion and Management*. 2018;159:30-41.

- [12] Florin NH, Harris AT. Enhanced hydrogen production from biomass with in situ carbon dioxide capture using calcium oxide sorbents. *Chemical Engineering Science*. 2008;63:287-316.
- [13] Huang Y, Yin X, Wu C, Wang C, Xie J, Zhou Z, et al. Effects of metal catalysts on CO<sub>2</sub> gasification reactivity of biomass char. *Biotechnology Advances*. 2009;27:568-72.
- [14] Yip K, Tian F, Hayashi J-i, Wu H. Effect of Alkali and Alkaline Earth Metallic Species on Biochar Reactivity and Syngas Compositions during Steam Gasification. *Energy & Fuels*. 2010;24:173-81.
- [15] Zhang Y, Ashizawa M, Kajitani S, Miura K. Proposal of a semi-empirical kinetic model to reconcile with gasification reactivity profiles of biomass chars. *Fuel*. 2008;87:475-81.
- [16] Zhang Y, Zheng Y. Co-gasification of coal and biomass in a fixed bed reactor with separate and mixed bed configurations. *Fuel*. 2016;183:132-8.
- [17] Tursun Y, Xu S, Wang C, Xiao Y, Wang G. Steam co-gasification of biomass and coal in decoupled reactors. *Fuel Processing Technology*. 2016;141:61-7.
- [18] Massoudi Farid M, Jeong HJ, Hwang J. Kinetic study on coal–biomass mixed char co-gasification with H<sub>2</sub>O in the presence of H<sub>2</sub>. *Fuel*. 2016;181:1066-73.
- [19] Massoudi Farid M, Jeong HJ, Hwang J. Co-gasification of coal–biomass blended char with CO<sub>2</sub> and H<sub>2</sub>O: Effect of partial pressure of the gasifying agent on reaction kinetics. *Fuel*. 2015;162:234-8.
- [20] Krerkkaiwan S, Fushimi C, Tsutsumi A, Kuchonthara P. Synergetic effect during co-pyrolysis/gasification of biomass and sub-bituminous coal. *Fuel Processing Technology*. 2013;115:11-8.
- [21] Sadhwani N, Adhikari S, Eden MR, Wang Z, Baker R. Southern pines char gasification with CO<sub>2</sub>—Kinetics and effect of alkali and alkaline earth metals. *Fuel Processing Technology*. 2016;150:64-70.
- [22] Mahadevan R, Adhikari S, Shakya R, Wang K, Dayton D, Lehrich M, et al. Effect of Alkali and Alkaline Earth Metals on in-Situ Catalytic Fast Pyrolysis of Lignocellulosic Biomass: A Microreactor Study. *Energy & Fuels*. 2016;30:3045-56.
- [23] Zhu W, Song W, Lin W. Catalytic gasification of char from co-pyrolysis of coal and

biomass. *Fuel Processing Technology*. 2008;89:890-6.

[24] Xu Q, Pang S, Levi T. Reaction kinetics and producer gas compositions of steam gasification of coal and biomass blend chars, part 1: Experimental investigation. *Chemical Engineering Science*. 2011;66:2141-8.

[25] Miccio F, Ruoppolo G, Kalisz S, Andersen L, Morgan TJ, Baxter D. Combined gasification of coal and biomass in internal circulating fluidized bed. *Fuel Processing Technology*. 2012;95:45-54.

[26] Lv D, Xu M, Liu X, Zhan Z, Li Z, Yao H. Effect of cellulose, lignin, alkali and alkaline earth metallic species on biomass pyrolysis and gasification. *Fuel Processing Technology*. 2010;91:903-9.

[27] Matsuoka K, Yamashita T, Kuramoto K, Suzuki Y, Takaya A, Tomita A. Transformation of alkali and alkaline earth metals in low rank coal during gasification. *Fuel*. 2008;87:885-93.

[28] Lee WJ, Kim SD. Catalytic activity of alkali and transition metal salt mixtures for steam-char gasification. *Fuel*. 1995;74:1387-93.

[29] Food wastage footprint: impacts on natural resources. 2013.

[30] Japanese Fresh Fruit Market Overview 2018. 2018.

[31] Nanda S, Isen J, Dalai AK, Kozinski JA. Gasification of fruit wastes and agro-food residues in supercritical water. *Energy Conversion and Management*. 2016;110:296-306.

[32] Tahir MH, Zhao Z, Ren J, Rasool T, Naqvi SR. Thermo-kinetics and gaseous product analysis of banana peel pyrolysis for its bioenergy potential. *Biomass and Bioenergy*. 2019;122:193-201.

[33] Tock JY, Lai CL, Lee KT, Tan KT, Bhatia S. Banana biomass as potential renewable energy resource: A Malaysian case study. *Renewable and Sustainable Energy Reviews*. 2010;14:798-805.

[34] Housagul S, Sirisukpoka U, Boonyawanich S, Pisutpaisal N. Biomethane Production from Co-digestion of Banana Peel and Waste Glycerol. *Energy Procedia*. 2014;61:2219-23.

[35] Kabenge I, Omulo G, Banadda N, Seay J, Zziwa A, Kiggundu N. Characterization of Banana Peels Wastes as Potential Slow Pyrolysis Feedstock. *Journal of Sustainable Development*. 2018;11:14.

- [36] He J, Yang Z, Xiong S, Guo M, Yan Y, Ran J, et al. Experimental and thermodynamic study of banana peel non-catalytic gasification characteristics. *Waste Management*. 2020;113:369-78.
- [37] Feng D, Guo D, Zhang Y, Sun S, Zhao Y, Shang Q, et al. Functionalized construction of biochar with hierarchical pore structures and surface O-/N-containing groups for phenol adsorption. *Chemical Engineering Journal*. 2020:127707.
- [38] Feng D, Zhang Y, Zhao Y, Sun S, Wu J, Tan H. Mechanism of in-situ dynamic catalysis and selective deactivation of H<sub>2</sub>O-activated biochar for biomass tar reforming. *Fuel*. 2020;279:118450.
- [39] Rehman S-u, Nadeem M, Ahmad F, Mushtaq Z. Biotechnological Production of Xylitol from Banana Peel and Its Impact on Physicochemical Properties of Rusks. *Journal of Agricultural Science and Technology*. 2013;15.
- [40] Ponnusamy SK, Ramakrishnan K, Kirupha S, Sivanesan S. Thermodynamic and kinetic studies of cadmium adsorption from aqueous solution onto rice husk. *Brazilian Journal of Chemical Engineering - BRAZ J CHEM ENG*. 2010;27.
- [41] Sharma RK, Wooten JB, Baliga VL, Lin X, Geoffrey Chan W, Hajaligol MR. Characterization of chars from pyrolysis of lignin. *Fuel*. 2004;83:1469-82.
- [42] Johansen JM, Jakobsen JG, Frandsen FJ, Glarborg P. Release of K, Cl, and S during Pyrolysis and Combustion of High-Chlorine Biomass. *Energy & Fuels*. 2011;25:4961-71.
- [43] Kowalski T, Ludwig C, Wokaun A. Qualitative Evaluation of Alkali Release during the Pyrolysis of Biomass. *Energy & Fuels*. 2007;21:3017-22.
- [44] Anniwaer A, Yu T, Chaihad N, Situmorang YA, Wang C, Kasai Y, et al. Steam gasification of marine biomass and its biochars for hydrogen-rich gas production. *Biomass Conversion and Biorefinery*. 2020.
- [45] Schumacher M, Yanik J, Sinağ A, Kruse A. Hydrothermal conversion of seaweeds in a batch autoclave. *The Journal of Supercritical Fluids*. 2011;58:131-5.
- [46] Acharya B, Dutta A, Basu P. Gasification of biomass in a circulating fluidized bed based calcium looping gasifier for hydrogen-enriched gas production: experimental studies. *Biofuels*. 2017;8:643-50.

- [47] Jiang L, Hu S, Syed-Hassan SSA, Xu K, Shuai C, Wang Y, et al. Hydrogen-Rich Gas Production from Steam Gasification of Lignite Integrated with CO<sub>2</sub> Capture Using Dual Calcium-Based Catalysts: An Experimental and Catalytic Kinetic Study. *Energy & Fuels*. 2018;32:1265-75.
- [48] Kuchonthara P, Vitidsant T, Tsutsumi A. Catalytic effects of potassium on lignin steam gasification with  $\gamma$ -Al<sub>2</sub>O<sub>3</sub> as a bed material. *Korean Journal of Chemical Engineering*. 2008;25:656-62.
- [49] Yang S, Zhang X, Chen L, Sun L, Xie X, Zhao B. Production of syngas from pyrolysis of biomass using Fe/CaO catalysts: Effect of operating conditions on the process. *Journal of Analytical and Applied Pyrolysis*. 2017;125:1-8.
- [50] Kuba M, Hofbauer H. Experimental parametric study on product gas and tar composition in dual fluid bed gasification of woody biomass. *Biomass and Bioenergy*. 2018;115:35-44.
- [51] Dahou T, Defoort F, Jeguirim M, Dupont C. Towards understanding the role of K during biomass steam gasification. *Fuel*. 2020;282:118806.
- [52] Arnold RA, Hill JM. Catalysts for gasification: a review. *Sustainable Energy & Fuels*. 2019;3:656-72.
- [53] Mitsuoka K, Hayashi S, Amano H, Kayahara K, Sasaoaka E, Uddin MA. Gasification of woody biomass char with CO<sub>2</sub>: The catalytic effects of K and Ca species on char gasification reactivity. *Fuel Processing Technology*. 2011;92:26-31.
- [54] Kopyscinski J, Rahman M, Gupta R, Mims CA, Hill JM. K<sub>2</sub>CO<sub>3</sub> catalyzed CO<sub>2</sub> gasification of ash-free coal. Interactions of the catalyst with carbon in N<sub>2</sub> and CO<sub>2</sub> atmosphere. *Fuel*. 2014;117:1181-9.
- [55] Bhatia SK, Perlmutter DD. A random pore model for fluid-solid reactions: I. Isothermal, kinetic control. *AIChE Journal*. 1980;26:379-86.
- [56] Hurt RH, Dudek DR, Longwell JP, Sarofim AF. The phenomenon of gasification-induced carbon densification and its influence on pore structure evolution. *Carbon*. 1988;26:433-49.
- [57] Bartels M, Lin W, Nijenhuis J, Kapteijn F, van Ommen JR. Agglomeration in fluidized beds at high temperatures: Mechanisms, detection and prevention. *Progress in Energy and Combustion Science*. 2008;34:633-66.

- [58] Lang RJ. Anion effects in alkali-catalysed steam gasification. *Fuel*. 1986;65:1324-9.
- [59] Yang H, Kudo S, Norinaga K, Hayashi J-i. Steam–Oxygen Gasification of Potassium-Loaded Lignite: Proof of Concept of Type IV Gasification. *Energy & Fuels*. 2016;30:1616-27.
- [60] Rizkiana J, Guan G, Widayatno WB, Hao X, Huang W, Tsutsumi A, et al. Effect of biomass type on the performance of cogasification of low rank coal with biomass at relatively low temperatures. *Fuel*. 2014;134:414-9.
- [61] Zhao H-b, Xu W-t, Song Q, Zhuo J-k, Yao Q. Effect of Steam and SiO<sub>2</sub> on the Release and Transformation of K<sub>2</sub>CO<sub>3</sub> and KCl during Biomass Thermal Conversion. *Energy & Fuels*. 2018;32:9633-9.
- [62] Blesa MJ, Miranda JL, Moliner R, Izquierdo MT, Palacios JM. Low-temperature co-pyrolysis of a low-rank coal and biomass to prepare smokeless fuel briquettes. *Journal of Analytical and Applied Pyrolysis*. 2003;70:665-77.
- [63] Qi X, Song G, Yang S, Yang Z, Lyu Q. Exploration of effective bed material for use as slagging/agglomeration preventatives in circulating fluidized bed gasification of high-sodium lignite. *Fuel*. 2018;217:577-86.
- [64] Tang J, Wang J. Catalytic steam gasification of coal char with alkali carbonates: A study on their synergic effects with calcium hydroxide. *Fuel Processing Technology*. 2016;142:34-41.
- [65] Zha J, Huang Y, Xia W, Xia Z, Liu C, Dong L, et al. Effect of mineral reaction between calcium and aluminosilicate on heavy metal behavior during sludge incineration. *Fuel*. 2018;229:241-7.
- [66] Guan G, Chen G, Kasai Y, Lim EWC, Hao X, Kaewpanha M, et al. Catalytic steam reforming of biomass tar over iron- or nickel-based catalyst supported on calcined scallop shell. *Applied Catalysis B: Environmental*. 2012;115-116:159-68.
- [67] Wang J, Jiang M, Yao Y, Zhang Y, Cao J. Steam gasification of coal char catalyzed by K<sub>2</sub>CO<sub>3</sub> for enhanced production of hydrogen without formation of methane. *Fuel*. 2009;88:1572-9.

## **CHAPTER 4: Steam co-gasification of Japanese cedarwood and its commercial biochar for hydrogen-rich gas production**

### **4.1 Introduction**

Hydrogen ( $H_2$ ) has been regarded as the most promising and clean energy carrier due to its highest weight energy density ( $122 \text{ MJ kg}^{-1}$ ) and only water generation during its application. Currently,  $H_2$  is mainly produced from conventional fossil fuels such as natural gas and coal. Considering the impacts on climate change and environmental pollution caused by the use of fossil fuels, the exploration of renewable and sustainable resources such as biomass for  $H_2$  generation has attracted great interest in recent years [1-3].  $H_2$  production from biomass is considered as an efficient and environmentally friendly route since biomass is a renewable natural resource and can be easily gasified. While, biomass is available in various forms such as forest wastes, agricultural wastes and municipal wastes at various scales [4]. At present, the technologies of  $H_2$  generation from biomass mainly include thermochemical, biological and electrolysis methods. Gasification and pyrolysis are the two main routes for the thermochemical conversion of biomass. Compared with pyrolysis, biomass steam gasification is regarded as a promising thermal conversion method to produce  $H_2$ -rich gas [5]. Especially, the applying of steam as a gasifying agent also prevents the formation of  $NO_x$  and produces low  $CO_2$  emissions [6].

Any biomass can be considered as the potential feedstock for hydrogen production via the gasification process. However, compared with other biomass sources, woody biomass has been preferred to generate heat and power due to its high energy content and relatively high fixed carbon content [7]. In 2019, 1.9 billion  $m^3$  of wood fuel, which is used for cooking, heating, or

power generation, was produced globally [8]. The total forest area in Japan is approximately 25 million ha, which corresponds to about two-thirds of the total land area [9]. Moreover, most of the buildings in Japan are built by wood, resulting in about 5 Mt of architectural waste wood production per year [10]. Considering the abundant wood resources in Japan, woody biomass has a high potential to be utilized as the steam gasification feedstock. Aljbour and Kawamoto [11] investigated the gasification of Japanese cedarwood in a bench-scale updraft gasifier. They found that the syngas contained 30-50 vol.% of  $H_2$  could be produced. Kaewpanha et al. [12] compared the gasification behaviors of brown seaweed with two kinds of woody biomass, i.e., Japanese cedarwood and apple branch under the steam atmosphere. They found that higher gas production and higher conversion rate could be obtained from the brown seaweed than that of two types of woody biomass samples. However, in the further co-gasification process, the gas yield from Japanese cedarwood was significantly enhanced with the addition of brown seaweed. In a partial or absence of oxygen, thermal degradation of biomass (pyrolysis) is operated to yield carbon-rich biochar[3, 13-17]. In the past few years, biochars have gained more and more attention due to the high carbon content and low content of volatile matters. Compared to raw biomass, most of the volatiles have been removed from biomass during the pyrolysis process, resulting in lower tar production during the gasification of biochar. Moreover, the calorific value of biochar is notably higher than that of raw biomass due to the larger content of fixed carbon. Therefore, the steam gasification of biochar is considered as a clean way to produce  $H_2$ -rich syngas and various studies of steam gasification of biochars have been reported [6, 14, 18, 19]. López et al. [20] studied the gasification performance of biochars from the pyrolysis of three different types of woody biomass samples. They found that the AAEM compounds in

the ash could provide the catalytic effect during the gasification reaction, resulting in higher  $H_2$  and CO gas production. Duman et al. [21] studied the reactivity of different types of biochars in  $CO_2$  gasification. The results showed that woody biochars had higher reactivity compared with the biochar derived from agricultural biomass. They also found that the gasification reactivity highly depended on the surface area of the biochar.

As a promising alternative, biochar has been applied as a cheaper catalyst or catalyst supports for tar conversion because of its highly porous textural structure [22-25]. The macroporous and mesoporous structures of biochar can improve not only the dispersion of supported catalyst species but also the transferring of the reactants into the inner active sites. Compared with other catalysts, the woody biochar based ones also exhibited higher catalytic activity for tar reduction with more resistance ability to poisoning [26-29]. Tar is a complex mixture of aromatics and undesirable liquid by-products from the gasification process since it is easy to condense, causing plugging, fouling, and corrosion of the pipeline [5]. Therefore, it is important to remove tar from the syngas before the application of syngas. Usually, the adsorption ability of biochar is benefit for the adsorption of light tar compounds. While, heavy tar can be removed by chemical methods, such as catalytic and non-catalytic thermal conversion [30]. The main mechanisms of tar conversion over carbonaceous materials are deposition, dehydrogenation (soot formation on the char surface), and soot gasification [28, 31-33], which are identical with the processes of tar conversion over porous catalysts [34-36]. In particular, the AAEM species in the char could greatly improve the soot gasification rate [32, 33]. Abu El-Rub [37] considered that tar can be absorbed on the active sites of char, subsequently converted into CO and  $H_2$  by steam gasification reactions. Meanwhile, coke can be formed from tar decomposition

and deposited on the char surface. However, the coke could be further gasified to CO and H<sub>2</sub> so that the active surface of char is refreshed at a reaction temperature higher than 800 °C. Nestler et al. [38] investigated the catalytic decomposition of naphthalene over biochar from the pyrolysis of spruce wood in different conditions. The results showed that the activated biochar had high catalytic activity for naphthalene decomposition into carbon and hydrogen. Hu et al. [39] compared the interactions of the coal char and biomass char with the pyrolysis volatiles in a two-stage vertical reactor. The biomass char showed higher catalytic activity than the coal char due to its larger pore size and higher AAEM content, resulting in a higher H<sub>2</sub> and less CO<sub>2</sub> production. Feng et al. [23] investigated the in-situ tar removal by the biochars derived from cornstalk, rice husk, and sawdust in a two-stage fluidized-bed/fixed-bed reactor. The results showed that the biochar derived from sawdust had the highest reactivity on tar reforming when compared with the other two biochar samples.

The researches mentioned above show the potential of the utilization of woody biochars as the gasification feedstocks for H<sub>2</sub> production and the catalysts for tar conversion during the gasification process. However, researches on the co-gasification of biomass and biochar are still scarce compared with the co-gasification of biomass and coal. In our previous work [40], it was found that the gasification of raw Japanese cedarwood tended to produce larger content of tar instead of H<sub>2</sub>-rich syngas production at the lower gasification temperature. However, the syngas yield was increased significantly by further co-gasifying with the banana peel because of the synergistic effect of two different kinds of biomass feedstocks. The Japanese cedarwood exhibited the potential to be utilized as gasification feedstock for H<sub>2</sub> production. However, the proper pretreatment (carbonization) or gasification methods (catalytic gasification; co-

gasification) should be considered to decrease tar production. Thus, in this study, one kind of commercial biochar derived from regional forestry waste cedarwood in Aomori, Japan via a carbonization process was utilized as the gasification feedstock. This study aims to investigate the effect of the carbonization way on gasification reactivity for this kind of commercial biochar and evaluate the gasification performance of the biochar compared with the raw biomass. Various analyses such as ultimate analysis, proximate analysis, Brunauer-Emmett-Teller (BET) surface area analysis, thermogravimetric analysis, and scanning electron microscopy (SEM) analysis were conducted to understand the changes caused by the carbonization process. On the other hand, this study aims to explore the potential catalytic and/or synergistic effects between biomass and biochar samples during the co-gasification process. The results of this study are expected to help better understanding the variation of physicochemical characteristics of waste cedarwood after high-temperature carbonization process as well as the steam gasification/co-gasification behavior of woody biomass and its derived biochar.

## **4.2 Experimental**

### **4.2.1 Materials**

One kind of waste Japanese cedarwood and its commercial biochar were obtained from the “Aomori National Land Conservation Association” and utilized as the gasification feedstocks. The commercial biochar was produced by a carbonization process of raw cedarwood in a rotary furnace at 720 °C with a short residence time (2-3 min) in the absence of air. The ultimate analysis was performed in a Vario El cube elemental analyzer (Germany) and the proximate analysis was determined based on the thermogravimetric analysis. To avoid the evaporation of

alkaline species, the raw biomass and biochar samples were calcined in a muffle furnace at 600 °C for 2 h in the air and the chemical compositions of remaining ash residues were determined by XRF analysis (EDX-800HS, Shimadzu), and the results are shown in **Tables 4.1** and **4.2**. The surface structure and morphology of raw biomass and the biochar samples were investigated by a scanning electron microscopy (SEM, SU8010, Hitachi, Japan).

#### **4.2.2 Steam gasification processes**

The steam gasification of raw biomass and the commercial biochar as well as the steam co-gasification of their mixture samples were conducted in a lab-scale fixed-bed reactor with an inside diameter of 1.8 cm and 35 cm of total height, which has been described in our previous paper [40]. Briefly, in each gasification or co-gasification experiment, 0.5 g of biomass, biochar, or their mixture sample was put into the central part of the reactor. The height of the sample layer was around 1.5 cm. For the mixture sample, the raw biomass was physically mixed with the biochar by different weight ratios (1:1, 1:2, 2:1). Then, the reactor was slowly heated (10 °C/min) to the preset temperature (650-850 °C). The total reaction time for each experiment was fixed to 200 min in order to have a complete gasification reaction although the heating time and the residence time were varied with the reaction temperature. The steam was produced in a vaporization furnace at 250 °C by introducing the distilled water using a water pump with controllable water flow rate. The generated steam flowed into the reactor with a carrier gas (Argon) flow rate of 50 cm<sup>3</sup>/min. The gaseous products from the reactor, passed through two ice baths to remove tar and moisture and a drying column with CaCl<sub>2</sub> particles. The non-condensed gaseous products from the heating step and the holding step were collected by a 5 L gasbag and a 10 L gasbag, respectively. The two gasbags were connected with a three-way

valve at the vent part to prevent gas leakage during the gas collection. The dry and tar-free gaseous products of CO, CO<sub>2</sub>, CH<sub>4</sub>, and H<sub>2</sub> were analyzed using a gas chromatograph (GC-TCD, Agilent 7890-USA). All experiments were repeated at least 3 times to ensure reproducibility and all results shown in this study are the average results of several repeated experiments. Moreover, the predicted gas yields were calculated from the sum of yields when the raw cedarwood and its commercial biochar were gasified individually, which were compared with the experimental yields of the mixture sample.

#### 4.2.3 Estimation of carbon conversion efficiency

The following Eq. (1) was used for the calculating of carbon conversion efficiency (CCE) to gas:

$$CCE(\%) = (C \text{ content Produced} / C \text{ supplied}) \times 100 \quad (1)$$

Where, the “C content Produced” indicates the gaseous products containing carbon (i.e., CO, CO<sub>2</sub>, CH<sub>4</sub>) detected by GC. “C Supplied” is the total carbon content in dry biomass/biochar feedstock which was determined from the ultimate analysis.

### 4.3 Results and discussion

#### 4.3.1 Characteristics of raw cedarwood and its biochar samples

The ultimate analysis and proximate analysis were performed to understand the basic characteristics of the raw cedarwood (RCW) and the commercial biochar (CBC) samples. As shown in **Table 4.1**, it can be seen from the ultimate analysis that with the carbonization, the carbon content in the biochar (83.5 wt%) was almost two times larger than that in the raw biomass (48.1 wt%). The higher carbon content is desirable for the steam gasification process because it means more carbon can be supplied to react with steam for producing H<sub>2</sub>-rich gas.

Moreover, it can be seen from the proximate analysis that the fixed carbon content in the biochar increased due to the release of the volatiles during the carbonization process, which also resulted in the increase in the heating value of the biochar. The ash content indicated the amount of non-volatile and non-combustible residues in the sample after complete combustion. It can be seen that the relative ash content of the biochar was slightly higher than that of the raw biomass. The mineral composition in feedstocks could strongly affect the reactivity of gasification. Especially AAEM species (such as Na, K, and Ca) can serve as catalysts to promote the gasification process [41-43]. The XRF analyses exhibited the main inorganic compounds in the ash residues. As shown in **Table 4.2**, the ash residues of raw biomass and the biochar were dominated by K and Ca species. However, inorganic compounds are expected to be completely conserved only if the preprocessing temperature is lower than their respective volatilization temperatures. For example, the metal species such as Na and K could be volatilized and have low concentrations in the biochar if the pyrolysis temperature is higher than their melting points [44]. Therefore, the K content had a slight decrease after the carbonization process, which should be attributed to the evaporation of K species at the high carbonization temperature (720 °C) [45, 46].

TGA analyses of the RCW and CBC were performed in the nitrogen atmosphere by slowly heating (10 °C/min ) the sample to the target temperature (900 °C) in order to understand the thermal stability of the samples. The main chemical compositions of woody biomass are hemicellulose, cellulose and lignin, which have different thermal decomposition properties. Cellulose is the main component of cell walls and hemicellulose is also present in cell walls, while lignin acts as a binding agent. Different kinds of woody biomass contain different

contents of hemicellulose, cellulose, and lignin. Generally, softwood types contain a larger portion of lignin and less holocellulose (cellulose + hemicellulose) as compared to hardwood types [47]. **Fig 4.1** shows the TGA and DTG curves of individual raw cedarwood and its commercial biochar samples. The TGA/DTG curves obtained from the raw biomass could be divided into three main weight-loss stages. The first weight-loss stage indicated the water loss up to 200 °C. In the second stage, a sharp weight loss of approximately 57.7% occurred at the temperature range of 200-380 °C, which should be attributed to the initiation of the carbonization and the degradations of hemicellulose and cellulose. The final shallow decrease in mass occurred as the temperature increased from 380 to 850 °C in the final stage, which implied the degradation of lignin. The degradation feature of biochar was notably different from that of raw biomass. It can be clearly observed that the biochar was more thermally stable with negligible decomposition and retained a high amount of carbonaceous residues as the temperature was lower than 400 °C. The main degradation of biochar started from the temperature higher than 400 °C which was due to the breakdown of carbohydrate fraction maintained in the biochar structure [48]. The results revealed that although the residence time in the carbonization process for biochar production was only 2-3 min at the high temperature, the basic organic compounds from raw biomass, such as the extractive hemicellulose and cellulose, were mostly degraded.

The degradation of cellulose, hemicellulose, and lignin that occurred during the carbonization (pyrolysis) process could also lead to structural changes. Therefore, SEM analysis was carried out to compare the structures of raw cedarwood and its biochar. As shown in **Figs 4.2 a-d**, after the carbonization process, it can be seen that the original fibrillary arrangement of the wood

structure was destroyed, resulting in the honeycomb intra-pore structure on the entirety of the biochar surface. This honeycomb structure should be attributed to the release of volatile components during the carbonization process. The BET surface area of raw biomass and the biochar samples are shown in **Table 4.3**. It can be seen that the BET surface area increased considerably, from 5.0 to 360.8 m<sup>2</sup>/g due to the carbonization process. Larger surface area is always desirable in the steam gasification process because it can improve the contact between the biochar and steam, resulting in a higher gasification rate. The surface area of the biochar mainly depends upon the carbonization (pyrolysis) temperature, residence time and other parameters. James et al. [49] reported that the surface area of the *Birch pendula* increased from 5.6 m<sup>2</sup>/g to 430 m<sup>2</sup>/g by increasing the carbonization temperature from 600 to 700 °C. Moreover, it was reported by Claoston et al. [50] that the BET surface area of the biochar derived from the slow pyrolysis of rice husk at 500 °C for 2 h was 230.9 m<sup>2</sup>/g. In this study, the similar surface area increasing results were obtained by the carbonization.

**Table 4.1** Ultimate and proximate analyses of raw cedarwood and its commercial biochar samples.

|            | Ultimate Analysis<br>( wt%, d.a.f basis <sup>a</sup> ) |     |     |                | Proximate analysis<br>(wt%, dry basis) |                 |                 | Heating value<br>(MJ/kg) |      |
|------------|--|-----|-----|----------------|--|-----------------|-----------------|--------------------------|------|
|            | C  | H   | N   | O <sup>b</sup> | Ash                                    | VM <sup>c</sup> | FC <sup>d</sup> | LHV                      | HHV  |
| <b>RCW</b> | 48.1   | 6.2 | n.d | 44.6           | 1.1                                    | 87.9            | 11.0            | 14.8                     | 16.3 |
| <b>CBC</b> | 83.5   | 2.3 | n.d | 12.6           | 1.6                                    | 45.7            | 52.7            | 24.2                     | 24.5 |

<sup>a</sup> Dry and ash-free.

<sup>b</sup> By difference.

<sup>c</sup> Volatile matter

<sup>d</sup> Fixed carbon

n.d: not detected.

**Table 4.2** Main compositions of ash residues of raw cedarwood (RCW) and its biochar (CBC).

| XRF Analysis ( wt% ) |      |      |     |      |     |
|----------------------|------|------|-----|------|-----|
|                      | Ca   | K    | Si  | Al   | P   |
| <b>RCW ash</b>       | 21.4 | 37.2 | 8.4 | 21.0 | 2.9 |
| <b>CBC ash</b>       | 38.8 | 26.6 | 5.6 | 18.3 | n.d |

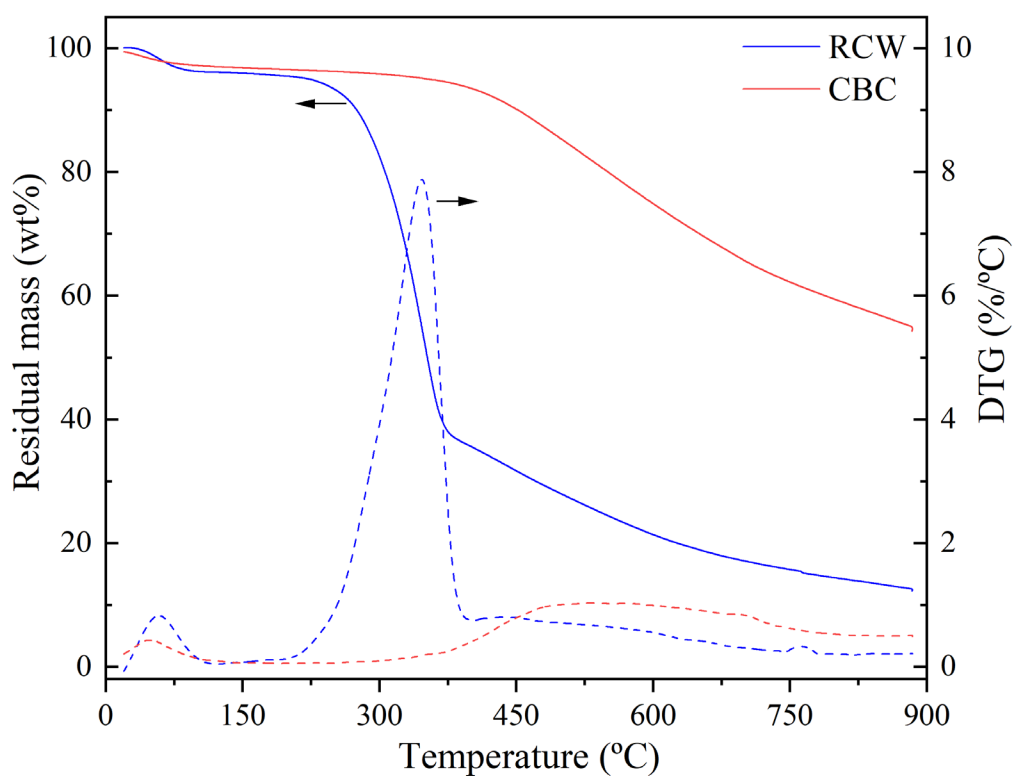


**Fig 4.1** TGA and DTG curves of raw-cedarwood (RCW) and commercial biochar (CBC) samples in N<sub>2</sub> atmosphere.

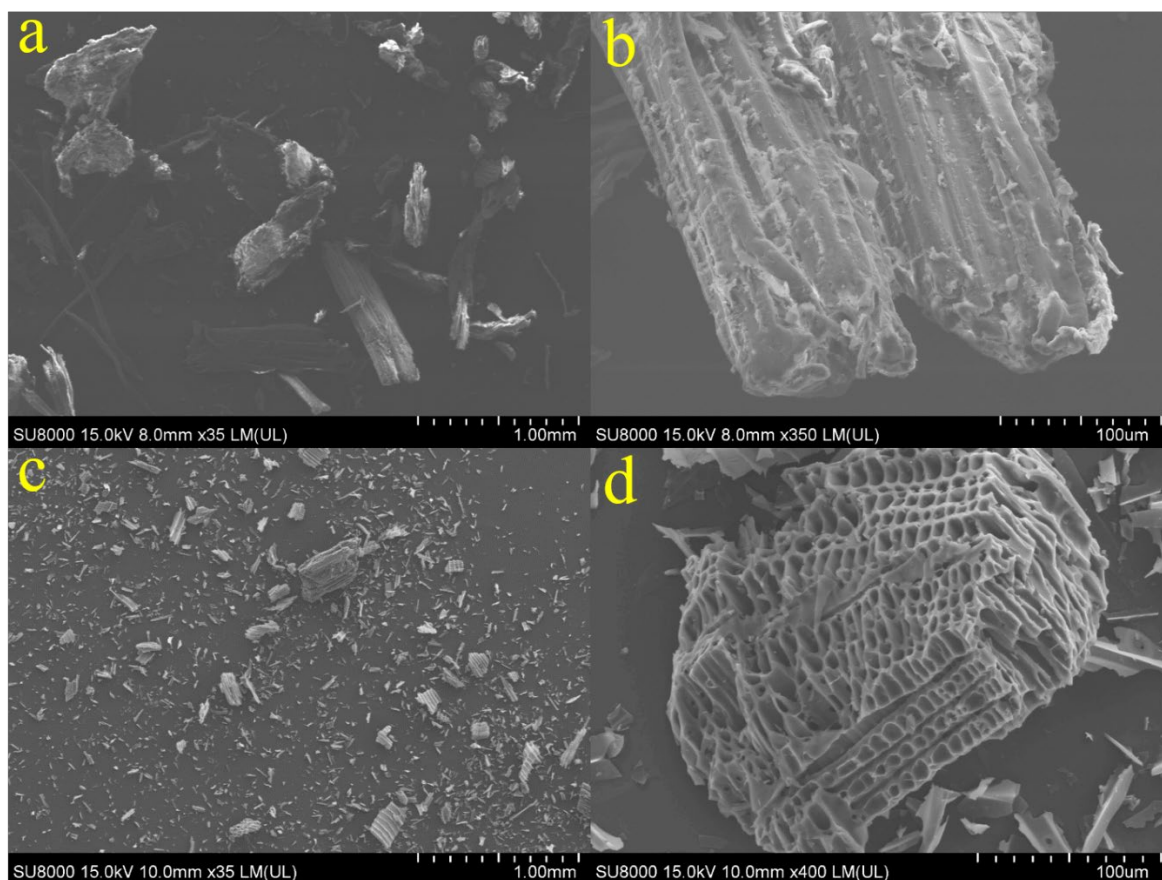


**Fig 4.2** SEM images of raw cedarwood (a, b) and its biochar (c, d).

**Table 4.3** BET surface area analysis of raw cedarwood and its biochar samples.

| Sample | BET surface area (m <sup>2</sup> /g) |
|--------|--------------------------------------|
| RCW    | 5.0                                  |
| CBC    | 360.8                                |

### 4.3.2 Steam gasification of individual raw biomass and biochar

#### 4.3.2.1 Effect of reaction temperature

The H<sub>2</sub> yield from the biomass/biochar gasification process is mainly affected by gasification temperature, steam flow rate, and catalyst addition [12]. Therefore, the steam gasification of individual samples of raw biomass as well as the biochar was carried out at three different

temperatures (i.e., 650 °C, 750 °C and 850 °C) with a water injection rate of 0.15 g/min to study the effect of gasification temperature on gas production. The gaseous products from the heating step and the setting temperature holding step at the target temperature were collected by two different gasbags and analyzed separately in order to have a better understanding of the gasification performances of biomass/biochar. Temperature is vital for biomass/biochar gasification since it directly affects the reaction rate and thermal equilibrium. As shown in **Figs 4.3a** and **b**, similar upward trends of gas production yields were observed for both the raw biomass and biochar samples. That is, with the increasing of the reaction temperature, the gas production increased considerably, especially H<sub>2</sub> production. The total gas production yield from the raw biomass increased from 10.6 mmol/g-sample at 650 °C to 55.7 mmol/g sample at 850 °C, while that from the biochar increased from 28.5 mmol/g-sample at 650 °C to 174.1 mmol/g-sample at 850 °C. Moreover, the gas production yields obtained at the heating step for both the raw biomass and biochar samples increased significantly with the increase in the reaction temperature from 750 to 850 °C, indicating the higher gasification rate at the higher temperature. It is noticeable that the total gas yields from the biochar at 850 °C was three times larger than that from the raw biomass, in which the samples were completely converted and the main reaction should be water gas reaction (WGR,  $C + H_2O \rightarrow H_2 + CO$ ). Herein, the biochar contained a higher carbon content (83.5 wt%) than the raw biomass (48.1 wt%), which means that more carbon could be provided by the biochar to react with the gasifying agent (steam), resulting in a larger H<sub>2</sub> yield from the biochar sample. More detailed results such as conversion rate, H<sub>2</sub> concentration, and carbon conversion efficiency (CCE) of steam gasification of the raw cedarwood and its biochar are shown in **Table 4.4**. It can be seen that

the H<sub>2</sub> concentration from the gasification of raw biomass at the setting temperature holding step increased from 40.3 to 65.0 wt% with the increase in the reaction temperature from 650 to 850 °C. However, the H<sub>2</sub> concentration from the biochar gasification had a slight decrease at the reaction temperature of 850 °C. Herein, the increase of the reaction temperature resulted in the increase in not only H<sub>2</sub> yield significantly but also CO and CO<sub>2</sub> gas yields, which affected the H<sub>2</sub> concentration in the obtained syngas. Acharya et al. [51] found that H<sub>2</sub> concentration decreased at the higher temperature due to the decrease of reactivity of the water gas shift reaction (WGS:  $\text{CO} + \text{H}_2\text{O} \rightleftharpoons \text{H}_2 + \text{CO}_2$ ), which means that the high temperature is more favor for the reverse water-gas shift (RWGS) reaction. Moreover, the endothermic Boudouard reaction ( $\text{C} + \text{CO}_2 \rightarrow \text{CO}$ ) also tended to be promoted at a higher temperature, and as a result, CO concentration increased sharply. The conversion rates of steam gasification of the raw biomass and biochar samples at different reaction temperatures were calculated based on the remaining solid residue amount after the reaction. It can be seen that both the raw biomass and biochar samples had higher conversion rates at the higher reaction temperature. However, the biochar showed a low conversion rate at 650 °C since the gasification temperature was lower than the prior carbonization temperature for biochar production, and as a result, the biochar showed high thermal stability and low gasification reactivity at 650 °C. On the other hand, although the raw biomass showed high conversion rates at three reaction temperatures, the carbon conversion efficiency (CCE) of raw biomass was significantly lower than that of biochar. It indicated that the raw biomass tended to produce large content of tar instead of H<sub>2</sub>-rich gas production. Thus, the application of the carbonization process prior to the gasification process

can effectively decrease the tar production and increase the purity of syngas obtained from the steam gasification.

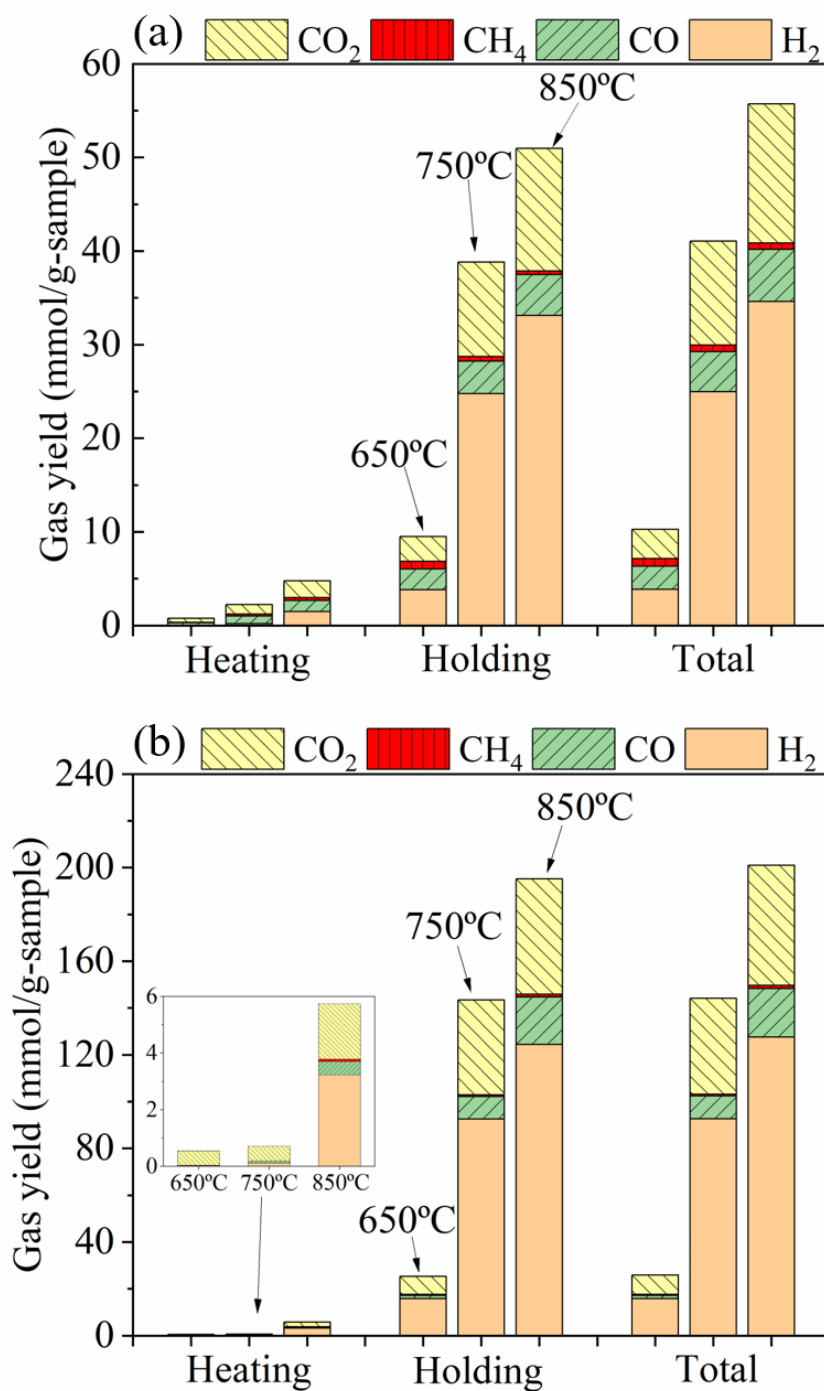


**Fig 4.3** Gas yields from raw biomass (a) and biochar (b) samples at the reaction temperatures of 650, 750, and 850 °C.

**Table 4.4** Conversion rate, H<sub>2</sub> concentration, and carbon conversion efficiency results from the gasification of the raw cedarwood and its biochar at 650, 750 and 850 °C.

|         | Temperature<br>(°C) | Conversion<br>(wt%) | H <sub>2</sub> (wt%)<br>Holding | CCE<br>(wt%) |
|---------|---------------------|---------------------|---------------------------------|--------------|
| Biomass | 650                 | 88.0                | 40.3±1.6                        | 16.0±1.1     |
| Biochar |                     | 38.0                | 62.4±1.0                        | 39.9±1.0     |
| Biomass | 750                 | 99.9                | 63.8±2.0                        | 40.2±2.7     |
| Biochar |                     | 98.0                | 64.5±0.3                        | 73.5±1.0     |
| Biomass | 850                 | 99.998.0            | 65.0±1.4                        | 52.8±4.1     |
| Biochar |                     | 99.9                | 62.7±1.6                        | 92.8±1.1     |

#### 4.3.2.2 Effect of water injection rate

The introduction of steam as the gasifying agent can enhance the H<sub>2</sub> yield from the gasification of biomass or biochar via the WGS reaction. In the present study, the effect of the water injection rate (WIR) on the gas production yield from the gasification of raw biomass or the biochar at 750 °C was investigated. Three different WIRs (i.e., 0.05, 0.15, 0.25 g/min) were applied and the results are shown in **Figs 4.4a** and **b**. As observed in **Fig 4.4a**, in the WIR range of 0.05-0.25 g/min, the gas yield from raw biomass gasification increased gradually with the increase in WIR, and reached a peak at the WIR of 0.25 g/min. However, the increase in gas yield, especially for H<sub>2</sub>, was not obvious with further increasing of WIR from 0.15 to 0.25 g/min. This result is consistent with the research conducted by Aljbouir and Kawamoto [11]. They gasified the Japanese cedarwood in a bench-scale updraft gasifier and found that the increasing of the steam supply could increase H<sub>2</sub> and CO<sub>2</sub> concentrations and decrease CO concentration. Nevertheless, the excessive increase in the steam supply tended to be

insignificant to promote the increase in the  $H_2$  concentration. The raw biomass was almost gasified completely even at a low WIR (0.05 g/min) with a high conversion rate as shown in **Table 4.5**. This is because the raw cedarwood contains a large content of volatile matter, which tends to evaporate at a low temperature. It can be observed from the TGA curve (**Fig 4.1**) that the residual mass of raw biomass at 750 °C was around 20 wt%. Thus, as the reaction temperature reached to the target temperature (750 °C) in gasification process, the long residence time (127 min) was sufficient for the low content of solid residues to be totally gasified. While, in the case of biochar, the total gas yield increased obviously with the increase of WIR from 0.05 to 0.15 g/min. However, a further increase in the WIR to 0.25 g/min resulted in a decrease in the total gas yield. Herein, the biochar has a porous structure with a large surface area, as the steam introduced into the reactor would interact with the biochar surface at first, and then diffused into the porous structure of biochar and reacted inside of pores [52]. Thus, at the low WIR (0.05 g/min), the steam might be insufficient to react with both the outer and inner parts of the biochar, and as a result, a low conversion rate and gas production yield were obtained. However, as excessive water was introduced (0.25 g/min), the biochar amount might be not sufficient to interact with all the introduced steam. Moreover, since the biochar was prepared at a pyrolysis temperature of 720 °C, the excessive steam might decrease the local temperature on the surface of the biochar, and as a result, the reaction rates of steam reforming of biochar as well as the water-gas shift reaction were decreased, thereby causing the decrease in the gas production yield [53, 54]. As shown in **Table 4.5**, the conversion rate of the biochar at the WIR of 0.15 g/min was already high (98 wt%), indicating the biochar was almost reacted completely. The further increase in the steam amount can only negatively affect the diffusion

of the product and decrease the gasification rate of the biochar, resulting in a lower conversion rate as well as a lower carbon conversion efficiency. The results indicate that the introduced steam amount plays a vital role in biochar gasification, and the proper steam amount should be applied to obtain higher H<sub>2</sub>-rich gas production. As such, in this study, the optimal WIR for the gasification of the raw biomass and its biochar were determined as 0.15 g/min.

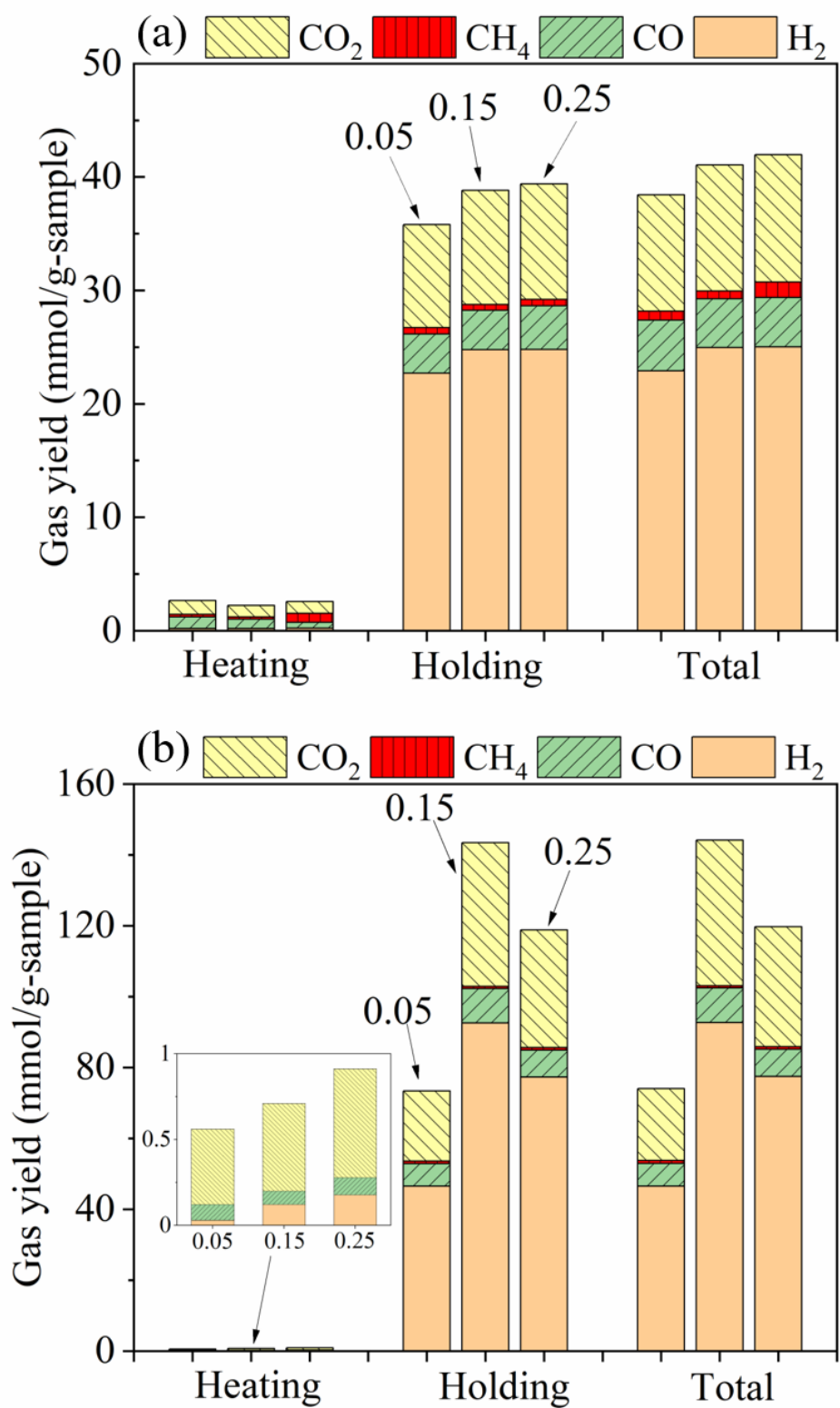


**Fig 4.4** Gas yields from raw biomass (a) and biochar (b) samples at 750 °C with three different water injection rates.

**Table 4.5** Conversion rate, H<sub>2</sub> concentration, and carbon conversion efficiency results from gasification of raw cedarwood and its biochar at 750 °C with three different water injection rates.

|         | <b>WIR</b><br><b>(g/min)</b> | <b>Conversion</b><br><b>(wt%)</b> | <b>H<sub>2</sub> (wt%)</b><br><b>Holding</b> | <b>CCE</b><br><b>(wt%)</b> |
|---------|------------------------------|-----------------------------------|--|----------------------------|
| Biomass | 0.05                         | 99.9                              | 63.4±1.9                                     | 38.8±3.0                   |
|         | 0.15                         | 99.9                              | 63.8±2.0                                     | 40.2±2.7                   |
|         | 0.25                         | 99.9                              | 63.0±1.7                                     | 42.4±3.1                   |
| Biochar | 0.05                         | 66.0                              | 63.3±0.4                                     | 39.2±1.5                   |
|         | 0.15                         | 98.0                              | 64.5±0.3                                     | 73.5±1.0                   |
|         | 0.25                         | 92.0                              | 65.1±0.4                                     | 60.4±1.4                   |

#### 4.3.3 Steam co-gasification of raw biomass and biochar

In this study, the raw cedarwood was co-gasified with the commercial biochar to investigate the catalytic effect of biochar on tar cracking/reforming and the improvement of the gas yield/quality. **Fig 4.5** compares the gas yields obtained from the mixture samples of raw biomass and the biochar at 750 °C (**a, b, c**) and 850 °C (**d, e, f**) in various biomass/biochar weight ratios (2:1, 1:1, 1:2) at a WIR of 0.15 g/min. It is obvious that the total gas yields from the co-gasification process, especially H<sub>2</sub> yield, increased with the reaction temperature. Moreover, the synergistic effect was observed at the biomass/biochar mixing ratios of 1:1 and 1:2, where the gas yields from the experimental results were larger than those predicted ones. In comparison, at the biomass/biochar weight mixing ratio at 2:1, the gas production yields obtained at two reaction temperatures were both lower than those predicted ones, indicating that the active sites on the biochar were not enough to reform all the tar produced from raw biomass in this case. At this condition, the coke deposition occurred on the biochar surface,

decreasing the reactivity of the biochar. It should be noted that the synergistic effect decreased after the reaction temperature was rose to 850 °C. This should be attributed to the evaporation of active elements such as K into the gas phase and the structural changes, leading to the decreasing in reactivity [55]. Hu et al. [56] found that the mole ratios of C/H and C/O in coal char were improved at a higher reaction temperature with a slower heating rate, which reduced the active sites in the char because the growth of char crystalline structure and the loss of functional groups were promoted. Moreover, it is always considered that the presence of AAEM spices in the fresh char and the steam atmosphere can promote the catalytic cracking reaction. Several studies found that the AAEM catalysts such as  $K_2CO_3$  and CaO can provide a catalytic effect on tar reduction [57-59]. Herein, the H/O/OH free radicals could break the bonds between K and the char matrix, resulting in the formation of active sites on the char surface, which can enhance the reforming of the tar to smaller tar components and light syngas during the  $H_2O$  or  $CO_2$  gasification reaction [60]. Fuentes-Cano et al. [29] reported the possible tar catalytic removal mechanism over char, in which the main reaction pathways consist of deposition, dehydrogenation (soot generated on char surface), and soot gasification. The gasification rate of produced soot was strongly influenced by the AAEM species in the char. During the reaction, the tar compounds initially contact with the active sites on the char surface and then the tar is adsorbed on the char matrix and undergoes the polymerization reaction, releasing gas products such as hydrogen and leaving soot on the char surface. Herein, the produced soot can block the active sites and hinder the interaction between active sites and tar, resulting in a decrease in catalytic reactivity. As shown in **Table 4.2**, both the raw cedarwood and its biochar samples contained large contents of K and Ca, which should provide the

catalytic effect during the reaction. Compared to the raw cedarwood, the high surface area and porous structure of the biochar could improve the dispersion of metal catalysts species and facilitate the transport of reactants into the inner active sites of the biochar. In the present study, however, the produced tar amount was difficult to be quantified. Therefore, TG analyses of raw cedarwood and the commercial biochar were conducted to investigate the tar adsorption by char. As mentioned before, tar can be adsorbed on the active sites of char particles and reformed into CO and H<sub>2</sub>. Raw cedarwood and the biochar with the weight ratio of 1:1 were put into the crucible up and down respectively without mixing and heated in the N<sub>2</sub> atmosphere from ambient temperature to 900 °C with a heating rate of 10 °C/min. The TGA and DTG curves are shown in **Fig 4.6**. Obviously, in the first weight-loss stage (which mainly corresponds to the water loss), almost no weight loss occurred when the biochar was placed on the top of raw cedarwood, indicating that the evaporated water might be absorbed by the biochar. This might be able to explain the good performance of the commercial biochar applied in agriculture due to its water holding capacity. As the temperature was increased to the temperature higher than 400 °C, the different decomposition behaviors were observed from the two TGA curves. The decomposition rate was getting slower and more solid residues remained at 900 °C for the case when the biochar was placed on the top of raw cedarwood. Herein, the degradation of lignin occurs at the temperature range of 380-850 °C and tar can be produced from lignin degradation due to the special molecular structure of lignin. Therefore, the low decomposition rate and high solid residues might be attributed to the adsorption of produced tar from raw cedarwood on the biochar surface. The possible mechanism is illustrated in **Fig 4.7**. That is, the volatile tar generated from raw cedarwood evaporated directly in the case when the raw cedarwood was

placed on the top of the biochar and as a result, a higher decomposition rate with less solid residues was achieved. On the other hand, as the raw cedarwood was covered with the biochar in the crucible, the tar released from the raw cedarwood would pass through the char bed and contact with the active sites on the biochar surface. As such, the tar was then adsorbed into the biochar matrix, in which the  $H_2$  was produced via polymerization reactions and leaving soot on the char surface [6]. Although more solid residues remained in TG analysis due to the absence of the gasifying agent, the solid residues with soot on the surface could be consumed by  $H_2O$  and converted into additional gases in the case with the gasifying agent of steam. Thus, the synergistic effect from the steam co-gasification of raw cedarwood and its biochar blend led to higher  $H_2$  and total syngas yields. **Table 4.6** shows the conversion rate,  $H_2$  concentration, and carbon conversion efficiency results of the co-gasification process. It can be seen that higher  $H_2$  concentrations were obtained at the condition with a mixing ratio of 1:1 at two different reaction temperatures. While, the increase in the reaction temperature or the amount of biochar in the mixture sample improved the carbon conversion efficiency, indicating that more gas production and less tar production could be obtained from the co-gasification process. Gadsbøll et al. [61] used pinned wood chips as the gasification feedstock in a two-stage gasification system, in which the pyrolysis and gasification were carried out in separate reactors. That is, the wood chips were pyrolyzed at 600 °C in the first stage and the produced biochar was directly transferred to the second stage for gasification. As such, the gaseous product such as tar vapor from the pyrolysis reactor can pass through a high-temperature oxidation zone and the char bed layer. Herein, the char bed acted as a catalyst bed for the tar removal, and as a result, 99% of the remaining tar was removed, yielding clean syngas. In the present study, as

indicated above, the raw cedarwood showed a potential to be gasified in the two-stage gasifier since the biochar derived from cedarwood can provide the catalytic effect on tar removal during the steam gasification process.

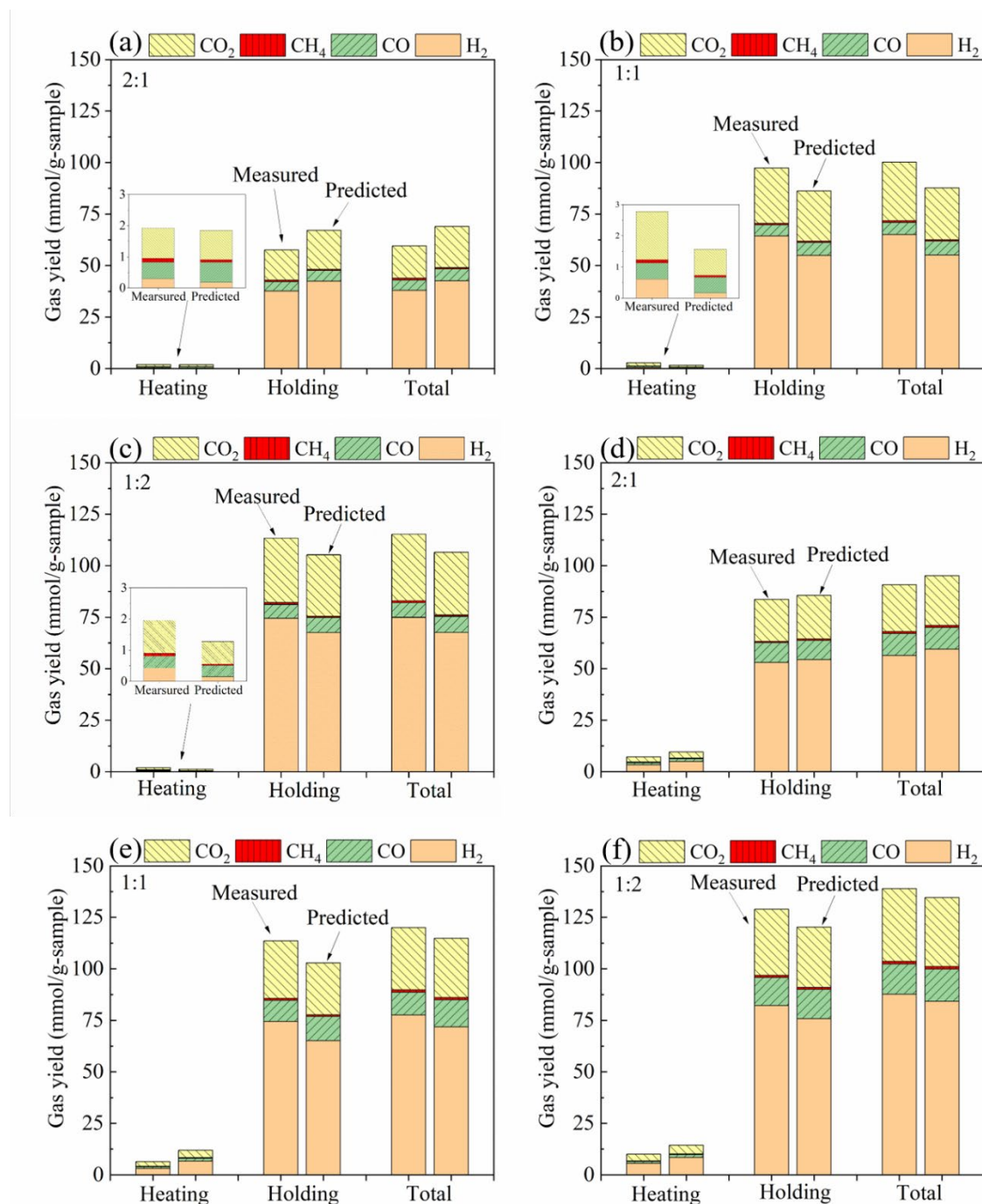


**Fig 4.5** Gas yields from the mixture samples of raw biomass and the biochar at 750 °C (a,b,c) and 850 °C (d,e,f) with three different mixing ratios (2:1, 1:1, 1:2).

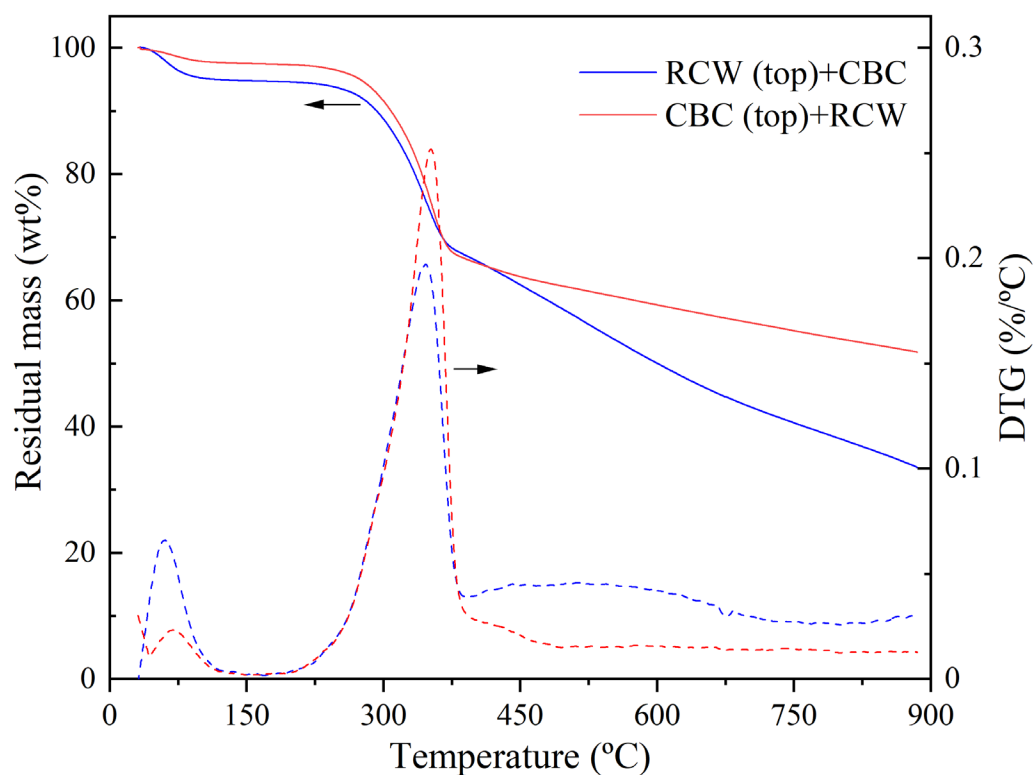


**Fig 4.6** TGA and DTG curves of raw-cedarwood (RCW) and commercial biochar (CBC) with the weight ratio of 1:1 in N<sub>2</sub> atmosphere.

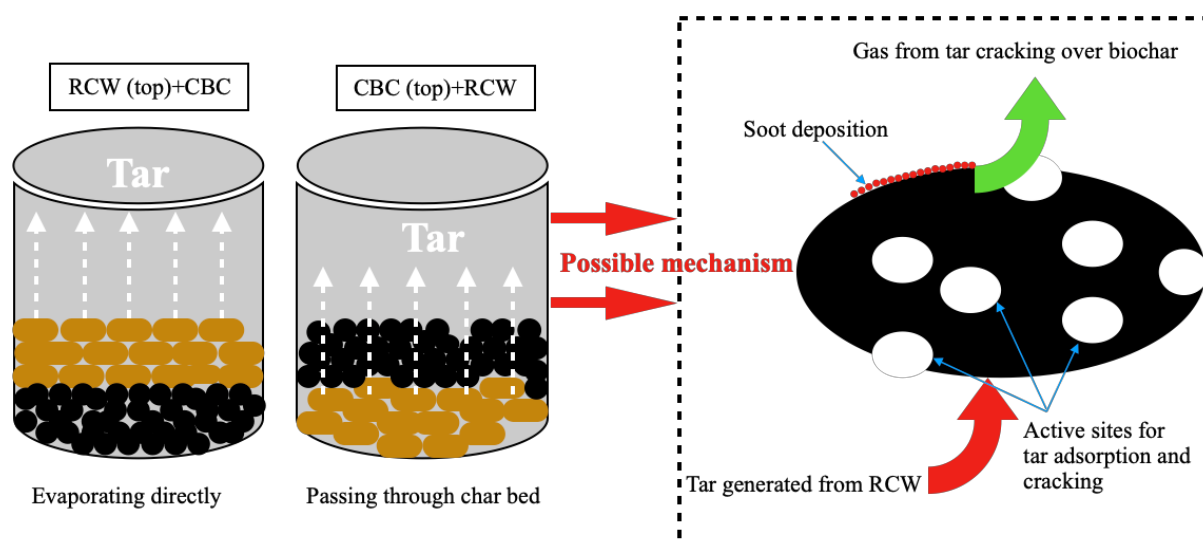


**Fig 4.7** Illustration of possible tar reforming mechanism over biochar in the crucible during the TG analysis.

**Table 4.6** Conversion rate, H<sub>2</sub> concentration, and carbon conversion efficiency results from co-gasification of raw biomass and the biochar at 750 °C and 850 °C with three different mixing ratios.

| <b>Biomass/biochar</b> | <b>Temperature<br/>(°C)</b> | <b>Conversion<br/>(wt%)</b> | <b>H<sub>2</sub> (wt%)<br/>Holding</b> | <b>CCE<br/>(wt%)</b> |
|------------------------|-----------------------------|-----------------------------|--|----------------------|
| 2:1                    | 750                         | 92.5                        | 65.4±1.2                               | 43.1±3.2             |
| 1:1                    |                             | 99.8                        | 66.1±0.7                               | 63.9±1.0             |
| 1:2                    |                             | 98.3                        | 65.7±0.5                               | 67.3±2.6             |
| 2:1                    | 850                         | 100.0                       | 63.4±0.2                               | 68.7±2.7             |
| 1:1                    |                             | 100.0                       | 65.6±0.9                               | 78.3±1.1             |
| 1:2                    |                             | 100.0                       | 63.7±0.6                               | 83.9±1.5             |

#### 4.4 Conclusions

The commercial biochar derived from Japanese cedarwood via a high-temperature carbonization process was utilized as the steam gasification feedstock. The individual sample and the mixture sample were gasified in a lab-scale vertical fixed bed reactor to investigate the feasibility of H<sub>2</sub>-rich gas production. The effects of gasification temperature and steam amount on gas production were studied. Moreover, the steam co-gasification of raw cedarwood and its biochar was studied and the synergistic effect between the two samples was observed. The following conclusions were obtained from the experimental results:

- (1) The gas production yields highly relied on the reaction temperature for both raw biomass and biochar samples. The results showed that the total gas yields from raw biomass increased from 10.6 mmol/g-sample at 650 °C to 55.7 mmol/g sample at 850 °C, while that from the biochar increased from 28.5 mmol/g-sample at 650 °C to 174.1 mmol/g-sample at 850 °C. The raw biomass sample (cedarwood) contained large content of lignin and

volatile matters leading to a high amount of tar formation during the gasification reaction.

However, with the introduction of the carbonization process prior to the steam gasification process, larger gas production and less tar production were obtained.

- (2) The water injection rate played an important role during the steam gasification process due to the steam reforming and water-gas shift reactions were enhanced by the introduction of steam, resulting in higher H<sub>2</sub> gas yield. It is found that the yields of gaseous products, especially H<sub>2</sub>, increased with the steam amount. However, the excessive amount of steam tended to be insignificant to promote a further increase in the H<sub>2</sub> concentration and led to a decrease in the yields of gaseous products.
- (3) The synergistic effect was obtained by co-gasifying the raw biomass and the biochar with the mixing ratios of 1:1 or 1:2. The synergistic effect should be attributed to the tar produced from raw biomass was catalytically reformed into the H<sub>2</sub>-rich syngas by the biochar. However, increasing the amount of raw biomass in the mixture sample led to coke deposition on the surface and cover the active sites of the biochar, decreasing the gasification reactivity of the biochar sample.

## References

- [1] Kobayashi J, Kawamoto K, Fukushima R, Tanaka S. Woody biomass and RPF gasification using reforming catalyst and calcium oxide. *Chemosphere*. 2011;83:1273-8.
- [2] Farooq A, Jang S-H, Lee SH, Jung S-C, Rhee GH, Jeon B-H, et al. Catalytic steam gasification of food waste using Ni-loaded rice husk derived biochar for hydrogen production. *Chemosphere*. 2021;280:130671.
- [3] Situmorang YA, Zhao Z, Chaihad N, Wang C, Anniwaer A, Kasai Y, et al. Steam gasification of co-pyrolysis chars from various types of biomass. *International Journal of*

Hydrogen Energy. 2021;46:3640-50.

[4] Cao L, Yu IKM, Xiong X, Tsang DCW, Zhang S, Clark JH, et al. Biorenewable hydrogen production through biomass gasification: A review and future prospects. *Environmental Research*. 2020;186:109547.

[5] Kaewpanha M, Guan G, Ma Y, Hao X, Zhang Z, Reubroychareon P, et al. Hydrogen production by steam reforming of biomass tar over biomass char supported molybdenum carbide catalyst. *International Journal of Hydrogen Energy*. 2015;40:7974-82.

[6] Zaini IN, Gomez-Rueda Y, García López C, Ratnasari DK, Helsen L, Pretz T, et al. Production of H<sub>2</sub>-rich syngas from excavated landfill waste through steam co-gasification with biochar. *Energy*. 2020;207:118208.

[7] Solarte-Toro JC, González-Aguirre JA, Poveda Giraldo JA, Cardona Alzate CA. Thermochemical processing of woody biomass: A review focused on energy-driven applications and catalytic upgrading. *Renewable and Sustainable Energy Reviews*. 2021;136:110376.

[8] World bioenergy association. Global bioenergy statistics 2020. 2020. <http://www.worldbioenergy.org/global-bioenergy-statistics/> (accessed 23 July 2021).

[9] MAFF. State of Japan's Forests and Forest Management. 2019. <https://www.maff.go.jp/e/policies/forestry/> (accessed 15 April 2021).

[10] Wu W, Kawamoto K, Kuramochi H. Hydrogen-rich synthesis gas production from waste wood via gasification and reforming technology for fuel cell application. *Journal of Material Cycles and Waste Management*. 2006;8:70-7.

[11] Aljbour SH, Kawamoto K. Bench-scale gasification of cedar wood – Part I: Effect of operational conditions on product gas characteristics. *Chemosphere*. 2013;90:1495-500.

[12] Kaewpanha M, Guan G, Hao X, Wang Z, Kasai Y, Kusakabe K, et al. Steam co-gasification of brown seaweed and land-based biomass. *Fuel Processing Technology*. 2014;120:106-12.

[13] Patel S, Kundu S, Halder P, Marzbali MH, Chiang K, Surapaneni A, et al. Production of hydrogen by catalytic methane decomposition using biochar and activated char produced from biosolids pyrolysis. *International Journal of Hydrogen Energy*. 2020;45:29978-92.

- [14] Yu T, Abudukeranmu A, Anniwaer A, Situmorang YA, Yoshida A, Hao X, et al. Steam gasification of biochars derived from pruned apple branch with various pyrolysis temperatures. *International Journal of Hydrogen Energy*. 2020;45:18321-30.
- [15] Lampropoulos A, Kaklidis N, Athanasiou C, Montes-Morán MA, Arenillas A, Menéndez JA, et al. Effect of Olive Kernel thermal treatment (torrefaction vs. slow pyrolysis) on the physicochemical characteristics and the CO<sub>2</sub> or H<sub>2</sub>O gasification performance of as-prepared biochars. *International Journal of Hydrogen Energy*. 2020.
- [16] Lv X, Xiao J, Shen L, Zhou Y. Experimental study on the optimization of parameters during biomass pyrolysis and char gasification for hydrogen-rich gas. *International Journal of Hydrogen Energy*. 2016;41:21913-25.
- [17] Klaas M, Greenhalf C, Ferrante L, Briens C, Berruti F. Optimisation of hydrogen production by steam reforming of chars derived from lumber and agricultural residues. *International Journal of Hydrogen Energy*. 2015;40:3642-7.
- [18] Zhai M, Xu Y, Guo L, Zhang Y, Dong P, Huang Y. Characteristics of pore structure of rice husk char during high-temperature steam gasification. *Fuel*. 2016;185:622-9.
- [19] Zhai M, Liu J, Wang Z, Guo L, Wang X, Zhang Y, et al. Gasification characteristics of sawdust char at a high-temperature steam atmosphere. *Energy*. 2017;128:509-18.
- [20] López-González D, Fernandez-Lopez M, Valverde JL, Sanchez-Silva L. Gasification of lignocellulosic biomass char obtained from pyrolysis: Kinetic and evolved gas analyses. *Energy*. 2014;71:456-67.
- [21] Duman G, Uddin MA, Yanik J. The effect of char properties on gasification reactivity. *Fuel Processing Technology*. 2014;118:75-81.
- [22] Guo F, Liang S, Jia X, Peng K, Jiang X, Qian L. One-step synthesis of biochar-supported potassium-iron catalyst for catalytic cracking of biomass pyrolysis tar. *International Journal of Hydrogen Energy*. 2020;45:16398-408.
- [23] Feng D, Zhao Y, Zhang Y, Zhang Z, Che H, Sun S. Experimental comparison of biochar species on in-situ biomass tar H<sub>2</sub>O reforming over biochar. *International Journal of Hydrogen Energy*. 2017;42:24035-46.
- [24] Feng D, Zhao Y, Zhang Y, Sun S. Effects of H<sub>2</sub>O and CO<sub>2</sub> on the homogeneous conversion

and heterogeneous reforming of biomass tar over biochar. *International Journal of Hydrogen Energy*. 2017;42:13070-84.

[25] Shen Y. Chars as carbonaceous adsorbents/catalysts for tar elimination during biomass pyrolysis or gasification. *Renewable and Sustainable Energy Reviews*. 2015;43:281-95.

[26] Di Blasi C. Combustion and gasification rates of lignocellulosic chars. *Progress in Energy and Combustion Science*. 2009;35:121-40.

[27] Burhenne L, Damiani M, Aicher T. Effect of feedstock water content and pyrolysis temperature on the structure and reactivity of spruce wood char produced in fixed bed pyrolysis. *Fuel*. 2013;107:836-47.

[28] Hosokai S, Kumabe K, Ohshita M, Norinaga K, Li C-Z, Hayashi J-i. Mechanism of decomposition of aromatics over charcoal and necessary condition for maintaining its activity. *Fuel*. 2008;87:2914-22.

[29] Fuentes-Cano D, Gómez-Barea A, Nilsson S, Ollero P. Decomposition kinetics of model tar compounds over chars with different internal structure to model hot tar removal in biomass gasification. *Chemical Engineering Journal*. 2013;228:1223-33.

[30] Li C, Hirabayashi D, Suzuki K. Development of new nickel based catalyst for biomass tar steam reforming producing H<sub>2</sub>-rich syngas. *Fuel Processing Technology*. 2009;90:790-6.

[31] Mašek O, Hosokai S, Norinaga K, Li C-Z, Hayashi J-i. Rapid Gasification of Nascent Char in Steam Atmosphere during the Pyrolysis of Na- and Ca-Ion-Exchanged Brown Coals in a Drop-Tube Reactor. *Energy & Fuels*. 2009;23:4496-501.

[32] Hosokai S, Norinaga K, Kimura T, Nakano M, Li C-Z, Hayashi J-i. Reforming of Volatiles from the Biomass Pyrolysis over Charcoal in a Sequence of Coke Deposition and Steam Gasification of Coke. *Energy & Fuels*. 2011;25:5387-93.

[33] Sueyasu T, Oike T, Mori A, Kudo S, Norinaga K, Hayashi J-i. Simultaneous Steam Reforming of Tar and Steam Gasification of Char from the Pyrolysis of Potassium-Loaded Woody Biomass. *Energy & Fuels*. 2012;26:199-208.

[34] Ito K, Moritomi H, Yoshiie R, Uemiya S, Nishimura M. Tar Capture Effect of Porous Particles for Biomass Fuel under Pyrolysis Conditions. *JOURNAL OF CHEMICAL ENGINEERING OF JAPAN*. 2003;36:840-5.

- [35] Namioka T, Yoshikawa K, Hatano H, Suzuki Y. High Tar Reduction with Porous Particles for Low Temperature Biomass Gasification: Effects of Porous Particles on Tar and Gas Yields during Sawdust Pyrolysis. *JOURNAL OF CHEMICAL ENGINEERING OF JAPAN*. 2003;36:1440-8.
- [36] Kuramoto K, Matsuoka K, Murakami T, Takagi H, Nanba T, Suzuki Y, et al. Cracking and Coking Behaviors of Nascent Volatiles Derived from Flash Pyrolysis of Woody Biomass over Mesoporous Fluidized-Bed Material. *Industrial & Engineering Chemistry Research*. 2009;48:2851-60.
- [37] Abu El-Rub Z. Biomass char as an in-situ catalyst for tar removal in gasification systems: University of Twente; 2008.
- [38] Nestler F, Burhenne L, Amtenbrink MJ, Aicher T. Catalytic decomposition of biomass tars: The impact of wood char surface characteristics on the catalytic performance for naphthalene removal. *Fuel Processing Technology*. 2016;145:31-41.
- [39] Hu J, Si Y, Yang H, Shao J, Wang X, Lei T, et al. Influence of volatiles-char interactions between coal and biomass on the volatiles released, resulting char structure and reactivity during co-pyrolysis. *Energy Conversion and Management*. 2017;152:229-38.
- [40] Anniwaer A, Chaihad N, Zhang M, Wang C, Yu T, Kasai Y, et al. Hydrogen-rich gas production from steam co-gasification of banana peel with agricultural residues and woody biomass. *Waste Management*. 2021;125:204-14.
- [41] Huang Y, Yin X, Wu C, Wang C, Xie J, Zhou Z, et al. Effects of metal catalysts on CO<sub>2</sub> gasification reactivity of biomass char. *Biotechnology Advances*. 2009;27:568-72.
- [42] Yip K, Tian F, Hayashi J-i, Wu H. Effect of Alkali and Alkaline Earth Metallic Species on Biochar Reactivity and Syngas Compositions during Steam Gasification. *Energy & Fuels*. 2010;24:173-81.
- [43] Dupont C, Nocquet T, Da Costa JA, Verne-Tournon C. Kinetic modelling of steam gasification of various woody biomass chars: Influence of inorganic elements. *Bioresource Technology*. 2011;102:9743-8.
- [44] Shackley S, Carter S, Knowles T, Middelink E, Haefele S, Haszeldine S. Sustainable gasification–biochar systems? A case-study of rice-husk gasification in Cambodia, Part II:

Field trial results, carbon abatement, economic assessment and conclusions. *Energy Policy*. 2012;41:618-23.

[45] Johansen JM, Jakobsen JG, Frandsen FJ, Glarborg P. Release of K, Cl, and S during Pyrolysis and Combustion of High-Chlorine Biomass. *Energy & Fuels*. 2011;25:4961-71.

[46] Kowalski T, Ludwig C, Wokaun A. Qualitative Evaluation of Alkali Release during the Pyrolysis of Biomass. *Energy & Fuels*. 2007;21:3017-22.

[47] Börcsök Z, Pásztor Z. The role of lignin in wood working processes using elevated temperatures: an abbreviated literature survey. *European Journal of Wood and Wood Products*. 2021;79:511-26.

[48] Oja V, Hajaligol MR, Waymack BE. The vaporization of semi-volatile compounds during tobacco pyrolysis. *Journal of Analytical and Applied Pyrolysis*. 2006;76:117-23.

[49] James G, Sabatini DA, Chiou CT, Rutherford D, Scott AC, Karapanagioti HK. Evaluating phenanthrene sorption on various wood chars. *Water Research*. 2005;39:549-58.

[50] Claoston N, Samsuri AW, Ahmad Husni MH, Mohd Amran MS. Effects of pyrolysis temperature on the physicochemical properties of empty fruit bunch and rice husk biochars. *Waste Management & Research*. 2014;32:331-9.

[51] Acharya B, Dutta A, Basu P. An investigation into steam gasification of biomass for hydrogen enriched gas production in presence of CaO. *International Journal of Hydrogen Energy*. 2010;35:1582-9.

[52] Sattar A, Leeke GA, Hornung A, Wood J. Steam gasification of rapeseed, wood, sewage sludge and miscanthus biochars for the production of a hydrogen-rich syngas. *Biomass and Bioenergy*. 2014;69:276-86.

[53] Yan F, Luo S-y, Hu Z-q, Xiao B, Cheng G. Hydrogen-rich gas production by steam gasification of char from biomass fast pyrolysis in a fixed-bed reactor: Influence of temperature and steam on hydrogen yield and syngas composition. *Bioresource Technology*. 2010;101:5633-7.

[54] Luo S, Xiao B, Guo X, Hu Z, Liu S, He M. Hydrogen-rich gas from catalytic steam gasification of biomass in a fixed bed reactor: Influence of particle size on gasification performance. *International Journal of Hydrogen Energy*. 2009;34:1260-4.

- [55] Zhu X, Sheng C. Evolution of the Char Structure of Lignite under Heat Treatment and Its Influences on Combustion Reactivity. *Energy & Fuels*. 2010;24:152-9.
- [56] Xu K, Hu S, Su S, Xu C, Sun L, Shuai C, et al. Study on Char Surface Active Sites and Their Relationship to Gasification Reactivity. *Energy & Fuels*. 2013;27:118-25.
- [57] Acharya B, Dutta A, Basu P. Gasification of biomass in a circulating fluidized bed based calcium looping gasifier for hydrogen-enriched gas production: experimental studies. *Biofuels*. 2017;8:643-50.
- [58] Jiang L, Hu S, Syed-Hassan SSA, Xu K, Shuai C, Wang Y, et al. Hydrogen-Rich Gas Production from Steam Gasification of Lignite Integrated with CO<sub>2</sub> Capture Using Dual Calcium-Based Catalysts: An Experimental and Catalytic Kinetic Study. *Energy & Fuels*. 2018;32:1265-75.
- [59] Kuchonthara P, Vitidsant T, Tsutsumi A. Catalytic effects of potassium on lignin steam gasification with  $\gamma$ -Al<sub>2</sub>O<sub>3</sub> as a bed material. *Korean Journal of Chemical Engineering*. 2008;25:656-62.
- [60] Feng D, Zhao Y, Zhang Y, Zhang Z, Sun S. Roles and fates of K and Ca species on biochar structure during in-situ tar H<sub>2</sub>O reforming over nascent biochar. *International Journal of Hydrogen Energy*. 2017;42:21686-96.
- [61] Gadsbøll RØ, Thomsen J, Bang-Møller C, Ahrenfeldt J, Henriksen UB. Solid oxide fuel cells powered by biomass gasification for high efficiency power generation. *Energy*. 2017;131:198-206.

## **CHAPTER 5: Utilization of fruit waste for H<sub>2</sub>-rich syngas production via steam co-gasification with brown coal**

### **5.1 Introduction**

Global energy demand is rising drastically due to the sharp increase in the world population and rapid industrial development. Fossil fuels such as coal, crude oil, and natural gas are the main energy sources for most of the countries to meet the energy demands. However, the overuse of fossil fuels is leading to serious crises such as climate change, and environmental pollution [1]. Under such circumstances, the exploration of sustainable and environmentally friendly energy alternatives is becoming urgent. Among all the renewable energy sources, biomass is considered as an important energy resource due to the environmental benefits such as renewability, carbon-neutrality, and abundant reserve [2]. Moreover, as the fuel, its utilization methods are similar to those for coal, which also include combustion, pyrolysis, and gasification. Nevertheless, the use of biomass in large-scale industrial applications is restricted due to several disadvantages such as low bulk density, low energy density, wide and thin distribution, and unstable seasonal supply [3-5]. Nowadays, coal gasification is considered as a promising technology for clean utilization of coal, which can convert solid coal into valuable syngas (i.e., H<sub>2</sub> and CO) by reacting with the gasifying agents such as steam, air and/or oxygen [6-8]. However, coal gasification has been meeting the long-term contradictions between the energy demand increasing and resource depleting [9]. Moreover, the harsh operation condition and the necessity for the reduction of greenhouse gas (GHG) and NO<sub>x</sub>/SO<sub>x</sub> pollutants of industrial coal gasification would cause ultra-high costs [10]. As such, the co-gasification of

coal with renewable biomass is believed to be a promising way to overcome the above shortcomings. Generally, even partial replacement of coal by biomass can reduce the dependence on fossil fuels and reduce the GHG emissions while co-utilization of biomass with coal can overcome the regional or seasonal availability issue of biomass. Furthermore, more gas production with less tar content could be obtained by co-gasification of different types of feedstock due to the synergistic effect. In particular, some biomasses contain high content of alkali and alkaline earth metals (AAEMs), which can act as the cheap and effective catalyst to enhance the coal gasification [7, 11, 12]. Besides, biomass also can act as an efficient hydrogen donor due to its relatively higher H/C ratio than coal, which can accelerate the gas-fossil fuel interactions, gasification, and secondary reactions during the co-gasification process [13-15]. Co-gasification of coal with biomass has been widely conducted to investigate the gasification reactivity and synergistic effect recently. Wei et al. [16] studied the synergy behaviors in the co-gasification of bituminous coal with rice straw, and found that the co-gasification reactivity increased with the increase in rice straw proportion and reaction temperature, and the synergy had a great relevance with K/Ca transformation. Cabuk et al. [17] investigated the H<sub>2</sub> production from co-gasification of lignite with sunflower seed cake, and found that H<sub>2</sub> yields mainly depended on the volatiles and AAEMs contents of biomass sample. Zhao et al. [18] confirmed that the catalytic influence of AAEMs in the wheat straw on the gasification of lignite coal was enhanced by introducing sufficient steam. Other researchers found that the potassium (K) contained in biomass commonly shows more obvious synergistic effect than other AAEM species such as calcium (Ca), sodium (Na), and magnesium (Mg), etc [11, 19-21]. On the other hand, some studies indicated that there is no synergistic effect in the co-

gasification of coal and biomass [22-24]. Considering the effects of different factors such as reaction temperature, blending method, blending ratio, and the type of biomass and coal, different synergy behaviors, either synergistic or inhibition effects, on the co-gasification reactivity could be obtained.

Woody and herbaceous are usually utilized in the co-gasification with coal due to their abundant reserves and easy obtainability. Nevertheless, it should be noticed that almost 1.3 billion tons of food waste is generated annually around the world and most of them are discarded in landfills, which has significant potential to cause air, land, and water pollution [25-27]. Fruit is one of the major fractions of food waste since a significant amount of by-products such as peels and seeds will be generated from the utilizations, especially from the fruit processing industries. Among the wide variety of fruits, banana is the second most-produced fruit in the world and grown in more than 130 countries, contributing around 16% of world fruit production and the fourth most important crop after rice, wheat, and corn [28]. India and China are the top 2 countries for banana production in the world with about 30.4 million tons and 11.6 million tons respectively in 2019 [29]. While, it is also worth mentioning that China and India are the world's two largest coal-consuming countries in 2020 [30].

Banana peel (BP) with 30-40% of the whole banana mass is always largely generated as the by-product from the fruit processing industries such as flours production, jam production, and dehydrated banana production. In our previous work [31], it was found that the banana peel had higher gasification reactivity and could produce more H<sub>2</sub>-rich syngas at a lower gasification temperature range when compared with the woody biomass (Japanese cedar) and agricultural waste (rice husk). Moreover, obvious synergistic effect was found by co-gasifying

BP with Japanese cedar and rice husk respectively at a low-temperature range. Although the BP has great potential as gasification or co-gasification feedstock, the researches on BP were mainly focused on biochemical process (fermentation) rather than thermochemical processes (e.g., pyrolysis, gasification, and combustion) [32-35]. To date, researches on the co-gasification of fruit peels with coal are still scarce. Therefore, in this work, BP was utilized as the gasification feedstock to co-gasify with brown coal for exploring the feasibility of mixing them to produce H<sub>2</sub>-rich syngas at a relatively low gasification temperature range and the potential synergistic effect between the two samples. It is expected to provide a useful way for the effective application of fruit wastes to reduce coal consumption in the industrial-scale gasification process.

## **5.2 Materials and methods**

### **5.2.1 Materials**

Brown coal (BC, Adaro) from Indonesia and BP from Ecuador were used as the feedstock. Both samples were pulverized and sieved into a size below 1 mm. Prior to use, they were dried at 105°C in the oven for 24 h. The ultimate and proximate analysis results of the BC and BP are listed in **Table 5.1**. Ash compositions of them (**Table 5.2**) were analyzed by X-ray fluorescence (XRF, EDX-800HS, Shimadzu, Japan). Thermogravimetry analyses (TGA) of the two samples were conducted in nitrogen (N<sub>2</sub>) atmosphere with a slow heating rate of 10°C/min to understand the thermal decomposition behaviors of two different samples and the results are shown in **Fig 5.1**. Three different samples with mixing ratios of 4:1, 1:1, and 1:4 (BP:BC) were prepared by physical mixing of them.

**Table 5.1** Ultimate and proximate analyses of BP and BC.

| Ultimate Analysis<br>( wt%, d.a.f basis <sup>a</sup> ) |      |     |     |                | Proximate analysis<br>(wt%, dry basis) |                 |                 |
|--|------|-----|-----|----------------|--|-----------------|-----------------|
|  | C    | H   | N   | O <sup>b</sup> | Ash                                    | VM <sup>c</sup> | FC <sup>d</sup> |
| <b>BP</b>  | 44.3 | 4.9 | 1.3 | 49.5           | 9.7                                    | 66.1            | 24.4            |
| <b>BC</b>  | 64.0 | 5.3 | 0.8 | 29.9           | 2.1                                    | 46.9            | 50.1            |

<sup>a</sup> Dry and ash-free.<sup>b</sup> By difference.<sup>c</sup> Volatile matter<sup>d</sup> Fixed carbon**Table 5.2** Main elemental compositions of ash residues of BP and BC.

| XRF Analysis ( wt% ) |      |      |      |      |      |
|----------------------|------|------|------|------|------|
|                      | Ca   | K    | Si   | Al   | Fe   |
| <b>BP ash</b>        | 3.5  | 67.3 | 2.8  | 21.0 | n.d  |
| <b>BC ash</b>        | 20.1 | 0.3  | 13.7 | 17.7 | 23.4 |

n.d: not detected.

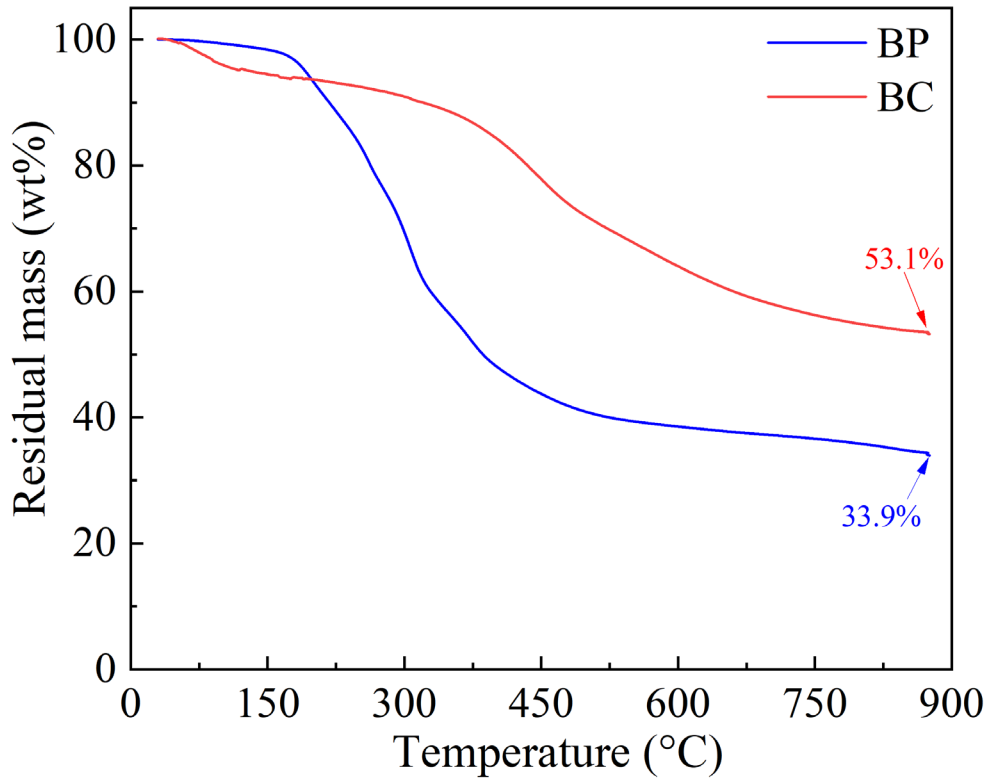


**Fig 5.1** Thermogravimetry analysis (TGA) of BP and BC in N<sub>2</sub> atmosphere.

### 5.2.2 Apparatus and procedure

Steam gasification of a single sample and co-gasification were conducted in a vertical fixed-bed reactor, which has been illustrated in our previous studies [36, 37]. Briefly, in each experiment, 0.5 g of BP, BC, or their mixture sample was located in the middle of the tube reactor (18 mm inner diameter, 350 mm in length). Then, the gasification was carried out at the preset temperature (650, 700, 750, or 800 °C) for 60 min, and the heating rate from the ambient temperature to the target one was 10 °C/min, in which Argon (Ar) was used as the carrier gas with a flow rate of 50 cm<sup>3</sup>/min. When the temperature of the reactor reached 200 °C, the water steam with a temperature of 250 °C was introduced into it with a controllable water flow rate.

The products carried by the Ar gas passed through two ice baths to collect the condensable tar and water, and the non-condensable gaseous products were passed through a CaCl<sub>2</sub> particles filled dry cylinder and finally collected by a 10 L gasbag. The gaseous products were analyzed by the Agilent 7890 gas chromatography (GC-TCD, America). The same experiment was retested and the average value was used for the analysis. While in order to investigate the synergistic effect, the theoretical gas yield of the co-gasification was determined by the sum of yields from the gasification of BP and BC separately.

### 5.2.3 Carbon conversion efficiency

Carbon conversion efficiency (CCE) to gas was calculated by:

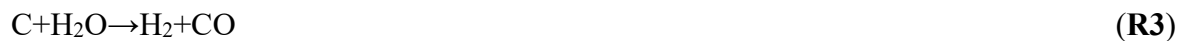
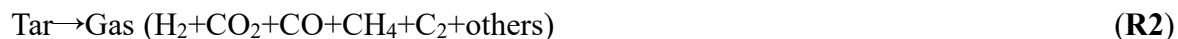
$$CCE(\%) = (C \text{ content Produced} / C \text{ supplied}) \times 100 \quad (1)$$

where, the “C content Produced” is determined by the amount of those gas products containing carbon (i.e., CO, CO<sub>2</sub> and CH<sub>4</sub>), and “C Supplied” is the total carbon content in the feedstock based on the ultimate analysis.

## 5.3 Results and discussion

### 5.3.1 Effect of reaction temperature

The reaction temperature is important for the endothermic steam gasification since it directly affects the reaction rate and thermal equilibrium [38]. Generally, the steam gasification of biomass or coal can be divided into two main steps: (1) pyrolysis step, where biomass or coal was decomposed into char, volatiles, and gases; and followed by a reforming step (2), where these intermediate products were further reformed into gaseous products mainly including H<sub>2</sub>, CO, CO<sub>2</sub> and CH<sub>4</sub> in the presence of steam. The main possible chemical reactions occurred during the steam gasification process are listed as follows:



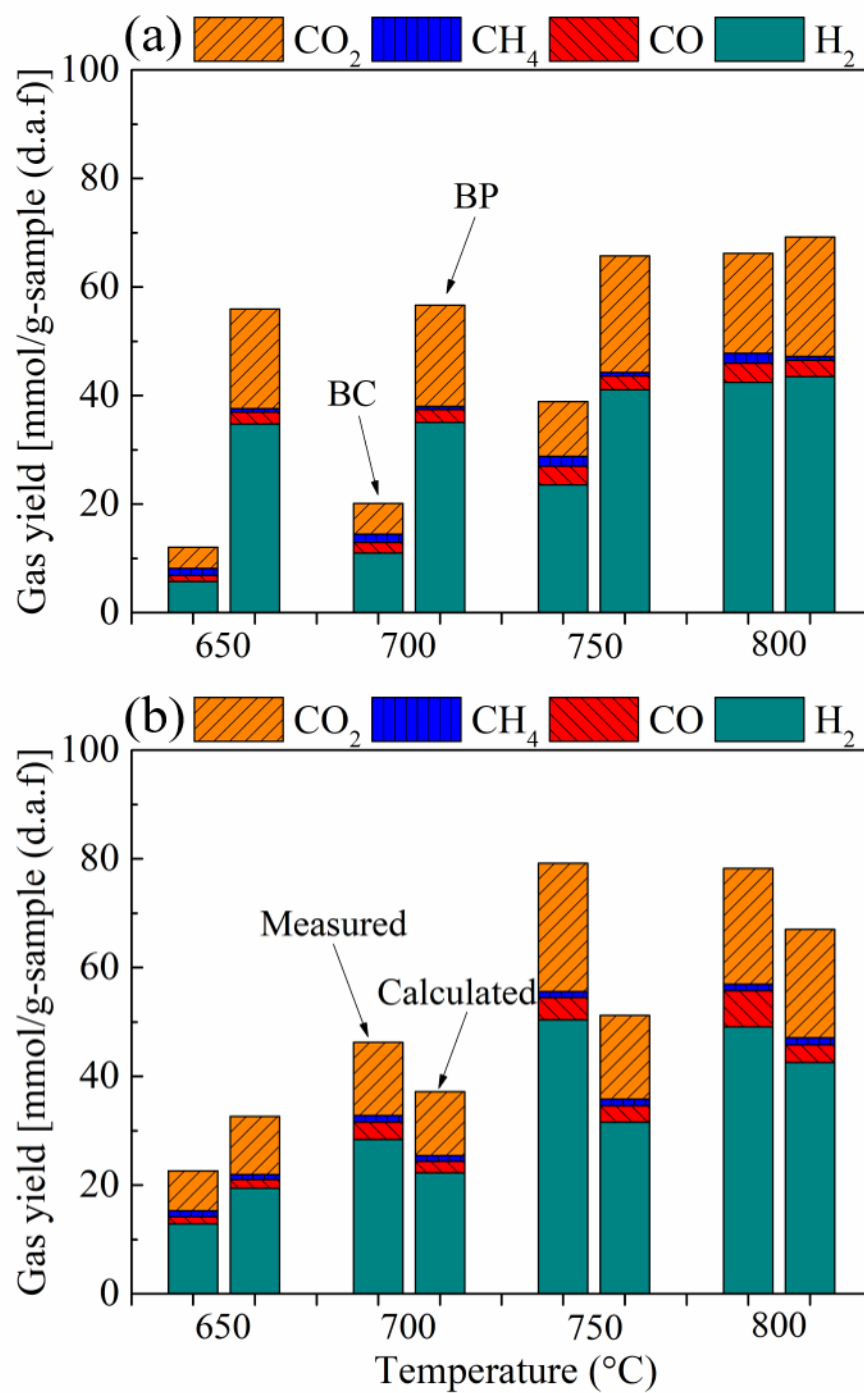
In the present work, four reaction temperatures were selected (i.e., 650 °C, 700 °C, 750 °C, 800 °C) to investigate the effect of temperature on gas yields. Moreover, prior to the co-gasification, in order to investigate the interaction between BP and BC, the gasification of the individual sample was carried out at first. **Fig 5.2a** shows the results for the gasification of individual BC and BP at the four different temperatures with a steam flow rate of 0.15 g/min. One can see that they had a similar increasing trend with the increase in the gasification temperature. That is, the total gas yield from the gasification of BC raised from 12.0 (650°C) to 66.2 (800°C) mmol/g-sample whereas that from the BP raised from 55.9 (650°C) to 69.2 (800°C) mmol/g-sample. Obviously, comparing with BC, BP had much higher gasification reactivity, which was almost completely gasified even at 650 °C with a significantly higher content of H<sub>2</sub>. This might be firstly attributed to the higher volatile content of BP than that of BC (**Table 5.1**). Generally, gasification conversion rate is affected by the volatile matter content in the sample, and the sample with higher volatile matter is always more reactive and easier to be gasified with less char production [39, 40]. Secondly, as summarized in **Table 5.2**, BP contains a large amount of potassium, which can act as the catalyst to promote tar cracking as well as char reforming during the steam gasification process, enhancing the gasification

reactivity, thereby generating more syngas [41-44]. Jiang et al. [45] proposed that the promotion of  $H_2$  and  $CO_2$  production should be related to the heterogeneous char gasification (**R3**), homogeneous water-gas shift reaction (**R4**), and hydrocarbon reforming reactions (**R2**), which can be promoted by the inherent AAEM species in biomass. Similarly, in the present work, the large content of K in the BP should provide promoting effects on these reactions during the steam gasification process. Those solid K compounds contained in the biochar phase could provide promoting effect on the heterogeneous reactions to convert the fixed carbon whereas the gaseous K compounds vaporized from BP could promote the homogeneous reactions. As a result, the gas production and carbon conversion from gasification of BP were significantly higher than those of BC. However, the gap of gas yields between the two samples decreased as the temperature increased up to  $800^\circ C$  since the unreactive char residues from coal could start to react with steam at the higher temperature even in the absence of catalysts. The conversion rate of BC was increased from 64.8 to 84.0 wt% with the increase of temperature from 750 to  $800^\circ C$ , indicating the strong influence of reaction temperature on the coal gasification. However, although the total gas yields from the two samples at  $800^\circ C$  were almost identical, the carbon conversion efficiency (CCE) of BC (42.6%) was still lower than that of BP (70.2%), which implied that a larger content of tar should have produced from BC during the steam gasification at the high temperature. These results are consistent with the research conducted by Rizkiana et al. [39], in which the same BC was also performed at a low reaction temperature range ( $500\text{--}750^\circ C$ ) in a fixed-bed reactor.

After understanding the gasification performances of two individual samples, the co-gasification of them was conducted in the same condition with a mixing weight ratio of 1:1. As

shown in **Fig 5.2b**, it can be observed that the total experimental gas yields were all higher than those calculated ones except the case at 650 °C, indicating that there were the synergistic effect at a co-gasification temperature higher than 700 °C. The excess growth rates in total gas yields were 19.6%, 35.2%, and 14.4% at 700 °C, 750 °C, 800 °C respectively. It should be noted that the highest excess growth rate on the gas yield was obtained at 750°C and the experimental result at 750 °C was almost identical with that at 800 °C. Besides, considering the total reaction time for the co-gasification at 800 °C (137 min) was longer than that at 750 °C (132 min) due to the longer heating time, the gasification temperature of 750 °C should be the optimum co-gasification temperature in this work. While, it should be mentioned that more than 30 wt% of char still remained after the BC was gasified at 750°C individually whereas the mixture sample was almost gasified completely at 750 °C with a gasification conversion rate of 94.1 wt%, indicating that the existence of BP greatly enhanced the gasification of BC, in which the water-gas reaction (**R3**) should be especially enhanced with almost no char remaining finally. Moreover, it is obvious that the yields of H<sub>2</sub> and CO<sub>2</sub> at 750 °C were higher than the calculated ones, implying that the water-gas shift reaction (**R4**) was promoted with the addition of BP. In addition, the measured CCE results of the mixture sample, as shown in **Fig 5.2c**, increased sharply from 21.6 wt% to 64.8 wt% while those calculated CCEs increased steadily from 29.5 wt% to 54.4 wt% with the increase of temperature from 650 to 800°C. It is reported that the synergistic effect on co-gasification reactivity was mainly related to the active AAEM transformation since the active AAEM could provide catalytic effect on the gasification of carbonaceous feedstock with a promotion effect on the gasification reactivity of those samples with lower reaction activity [46]. In this work, the main active AAEM species in the mixture

sample was K from BP, and the synergistic effect obtained from co-gasification of BP and BC should be mainly affected by the mobility of K. During the co-gasification, after the complete gasification of fixed carbon in BP, those K species in BP might transfer to the surface of adjacent BC particles, providing the catalytic effect on coal gasification [45, 47]. The inhibition effect obtained at 650 °C might be attributed to the low reactivity and conversion rate of BC at this low reaction temperature even in the presence of K species, and a large amount of unreactive BC particles could get in the interspaces among the BP particles, leading to the resistance on the mass transfer [9, 48].



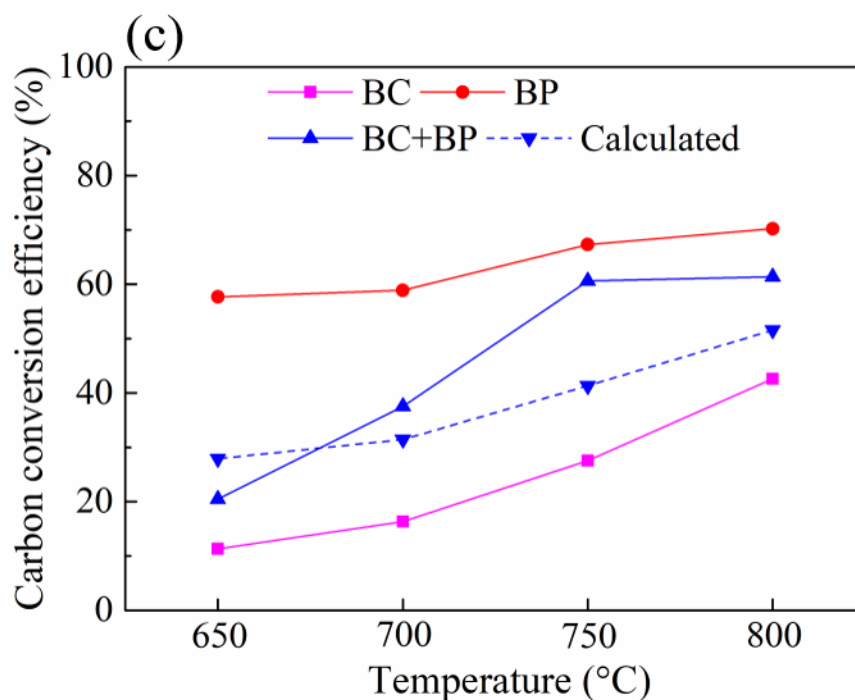


**Fig 5.2** Gas yields from steam gasifications of individual samples (a) and mixture sample (b); (c) carbon conversion efficiency to gas.

### 5.3.2 Effects of blending ratio and reaction time

#### 5.3.2.1 Effect of blending ratio

**Fig 5.3a** compares the experimental results with the calculated values for the co-gasification of BP and BC with three different blending ratios (i.e., 1:1, 1:4, 4:1). Based on the above results, the mixture samples were all co-gasified at 750 °C with a steam flow rate of 0.15 g/min. One can see that the gas yields from experimental results were all higher than those calculated values in all three cases, indicating that the synergistic effect between BC and BP was obtained even with a little amount of the addition of BP. However, the extents of promoting effect with various blending ratios were different. The blending ratio of 1:1 showed not only the highest gas yield but also the highest promoting effect. The excess growth rates of total gas yields for

blending ratios of 1:4, 4:1 and 1:1 were 28.8%, 16.3% and 37.3%, respectively. While, as shown in **Fig 5.3b**, the experimental CCEs were higher than the calculated values in all blending ratios and showed the highest CCE at the ratio of 1:1 (66.5%). Some reported results also exhibited that the co-gasification reactivity of coal and biomass can be promoted with the increase in the biomass amount in the mixture sample since more inherent AAEMs with high catalytic activity are contained in the biomass [16, 49]. However, it is also found that the co-gasification reactivity decreased with the increase in biomass proportion due to the reaction of active AAEMs with some elements in the coal [19, 50]. Xu et al. [51] conducted the gasifications of coal, biomass, and their mixture samples by TG-FTIR in the presence of CO<sub>2</sub>, and found that the most intense synergistic interaction on co-gasification reactivity was obtained as the blending ratio of lignite (high ash, 18.4%) with sawdust (low ash and AAEM content) at 4:1. In this case, the high ash in the coal might play the key role in the co-gasification reactivity, especially for high coal proportion in the mixture samples. Therefore, the types of coal and biomass will also affect the co-gasification results. In this work, as shown in **Tables 5.1** and **5.2**, the ash content of BC was only 2.1% with a relatively low amount of Al and Si species in the ash whereas the ash content of the BP was 9.7% with a large amount of K in the ash. It is reported that more obvious synergistic effect can be obtained for the mixture sample with higher K/Si as well as higher K/Al molar ratio in the blends [11, 52] since the K species could react with Si and Al species to generate unreactive and stable potassium aluminosilicates, which would cause the disappearance of catalytic effect provided by K species, resulting in the inhibition effect instead of synergistic effect during the co-gasification process [31, 53]. Thus, the synergistic effect could be obtained in the present study even as the blending ratio of BP

and BC at 1:4 due to the significantly higher content of K in BP than the Si and Al species in BC. In addition, it should be noted that BC ash was enriched in Ca, which might weaken the deactivation of biomass-derived K since Si and Al preferred to react with Ca rather than K [54, 55].

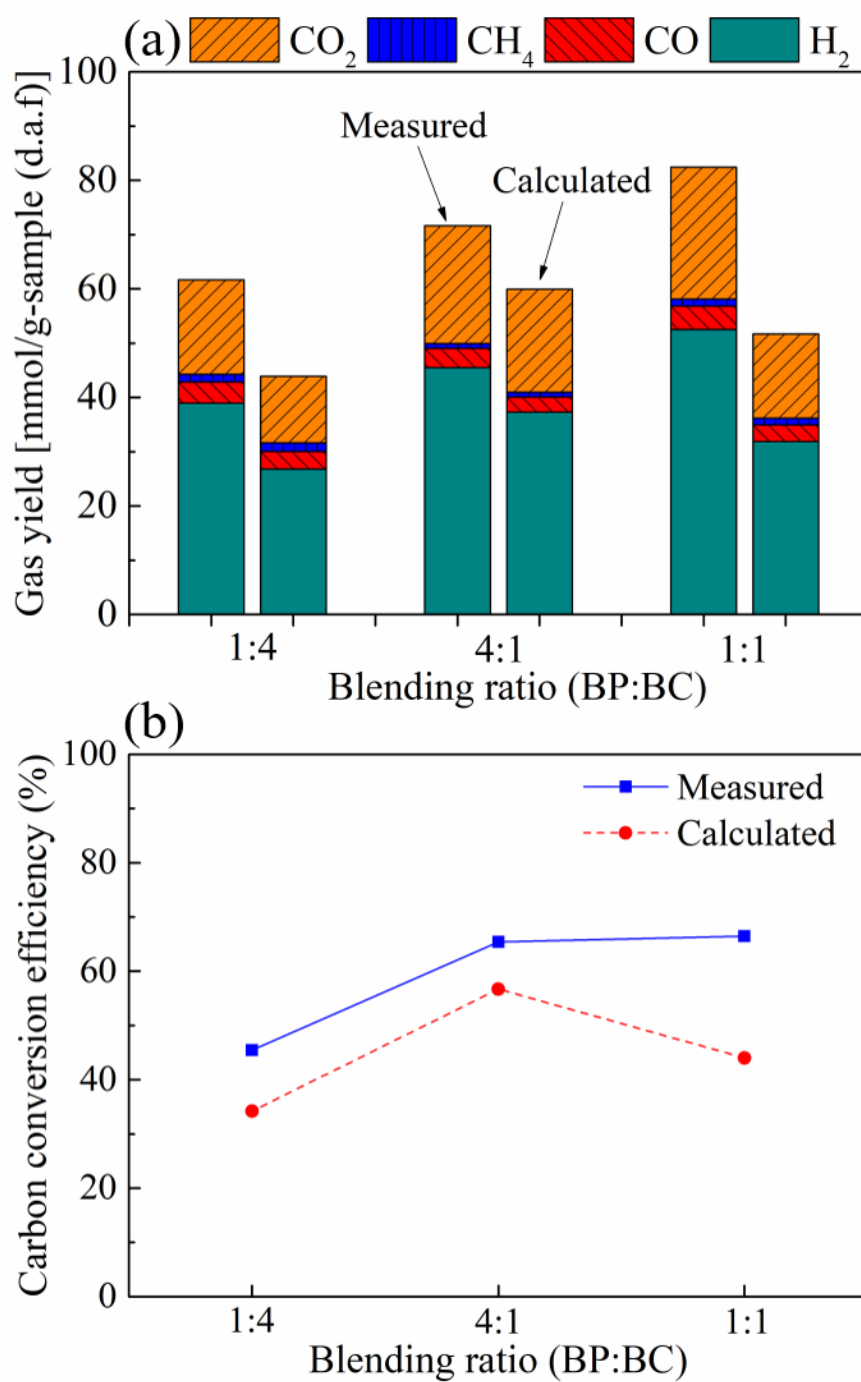


**Fig 5.3** Gas yields (a) and carbon conversion efficiencies (b) from co-gasifications of BP and BC with three different blending ratios at 750 °C.

### 5.3.2.2 Effect of reaction time

In the present work, the co-gasifications of BP and BC with the different blending ratios (1:1, 1:4, 4:1) were also conducted in a shorter reaction time (30 min) in order to further investigate the effects of the blending ratio on co-gasification reactivity and total gas yields. **Figs 5.4a** and **b** display the gas yields and CCEs obtained from experiments compared with those calculated values in a shorter reaction time. As displayed in **Fig 5.4a**, the experimental gas yields were also higher than the calculated values for all blending ratios, which means that synergistic effect existed after the reaction occurred in a short period. The largest gas yield was from the blending ratio of 4:1 due to the existence of more BP with higher reactivity. However, it should be noted that the biggest excess growth rate of gas yield over the calculated results was obtained at the blending ratio of 1:1 (30.1%), which was much higher than that in the cases of 4:1 (16.2%) and 1:4 (15.3). While, the total gas yield obtained from the blending ratio of 1:1 was 49.1 mmol/g-sample in **Fig 5.4a**, which was almost identical with the calculated value (51.7 mmol/g-sample) in **Fig 5.3a**, indicating that the gasification reactivity and gasification rate were significantly enhanced by blending BP and BC even with the ratio of 1:1 due to the synergistic effect. As shown in **Fig 5.4b**, both experimental CCEs and calculated ones showed a linear relationship with the increase in the proportion of BP in the blends, which means that the CCE increased with the addition of more BP. Comparing the gas yields from different reaction time (**Figs 5.3a** and **5.4a**), the total gas yields for blending ratios of 1:4, 1:1 and 4:1 were increased from 28.8, 49.1, and 52.4 to 61.7, 82.4, and 71.6 mmol/g-sample respectively with the increase in the residence time from 30 to 60 min. Thus, it can be concluded that the reaction time also plays an important role in the co-gasification process, especially for the mixture sample with higher

coal proportion which contains a higher carbon content and lower AAEM content since it required a longer reaction time to convert fixed carbon and tar into H<sub>2</sub>-rich syngas via promoting the reactions **R2**, **R3**, and **R4** by the AAEM species in the biomass.

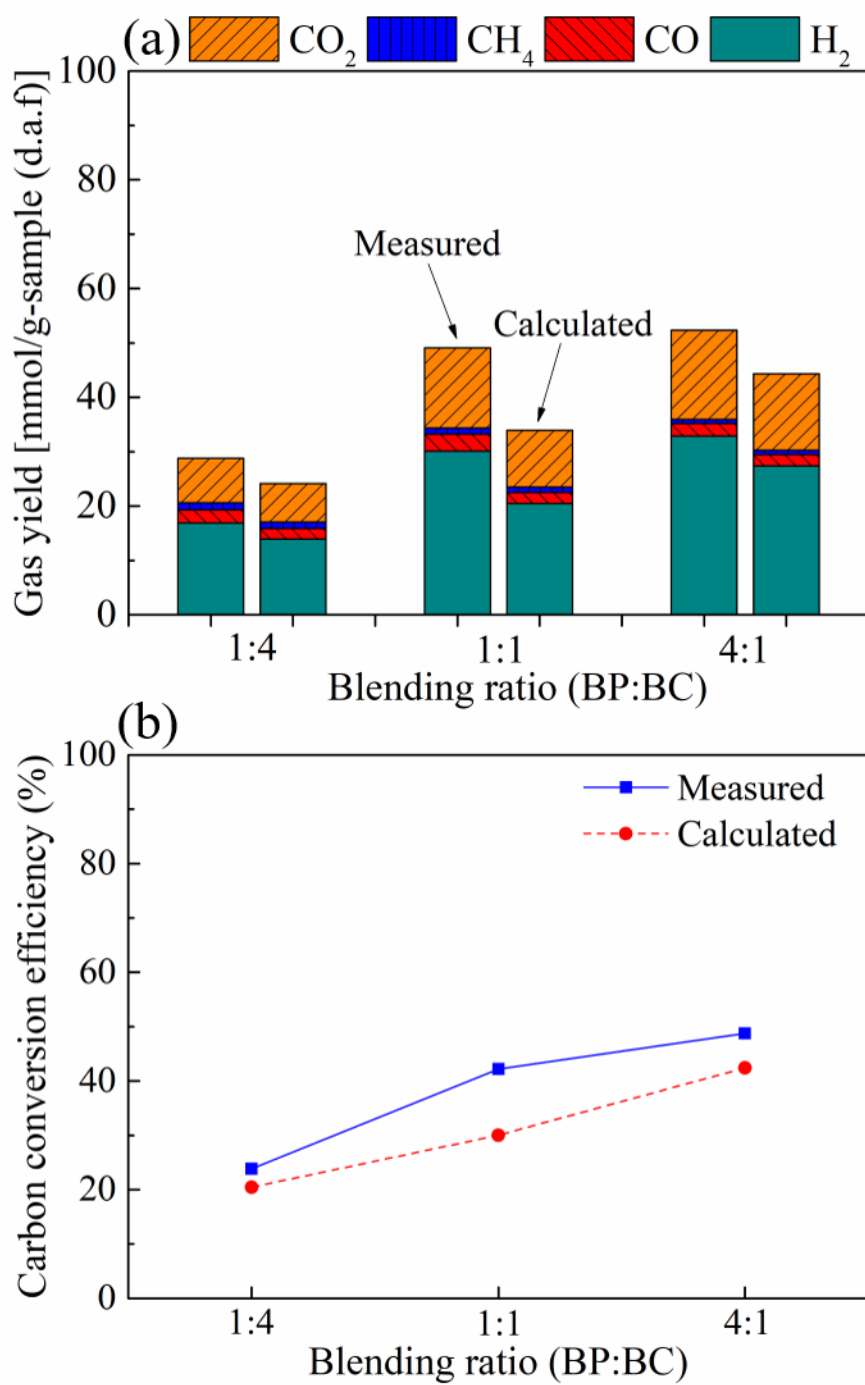


**Fig 5.4** Gas yields (a) and carbon conversion efficiency (b) from co-gasification of BP and BC with three different blending ratios at 750 °C in a shorter reaction time (30 min).

### 5.3.3 Effect of steam flow rate

During the gasification process, the application of steam as gasifying agent can efficiently increase the hydrogen production in the syngas due to the water-gas shift reaction (**R4**) [56, 57]. However, it is vital to investigate the reasonable steam flow rate since the excessive amounts of steam will not only lead to energy waste but also cause the real reaction temperature in the reactor to be lower than the preset temperature, resulting in a negative effect during the gasification process. In the present study, three different steam flow rates of 0.05, 0.15, and 0.25 g/min corresponding to total amounts of water introduced into the reactor of 5.75, 17.25, and 28.75 g, respectively, were applied. However, the amounts of the biomass, coal, or their blends for each experiment were the same (i.e., 0.5g). As such, the weight ratios of the feedstock and water were 1:12, 1:35, and 1:58, respectively. In addition, the pyrolysis experiments of BP, BC and their mixture sample were also conducted respectively in order to have a better understanding on the effect of steam by comparing pyrolysis and gasification results.

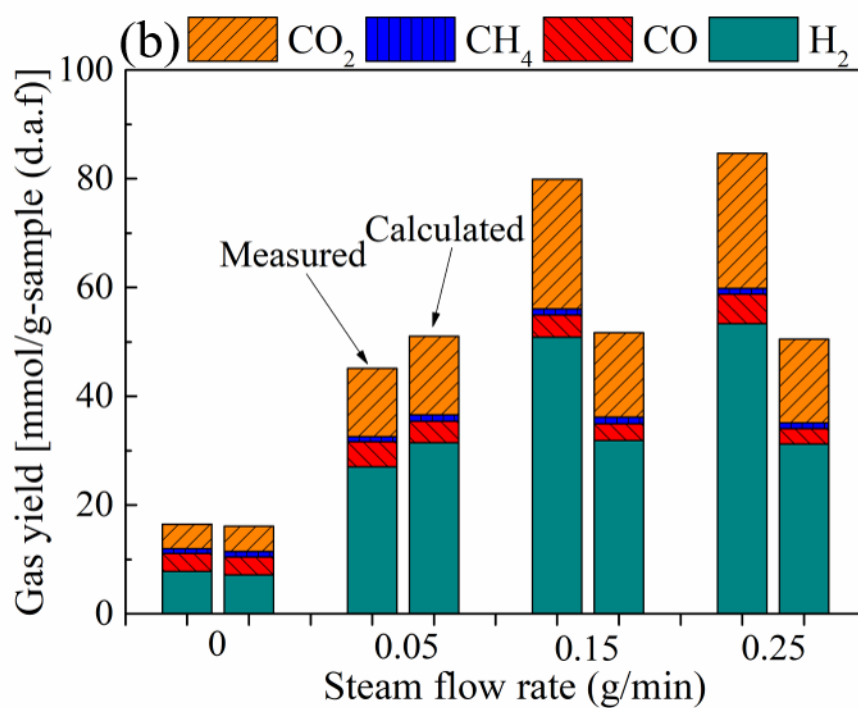
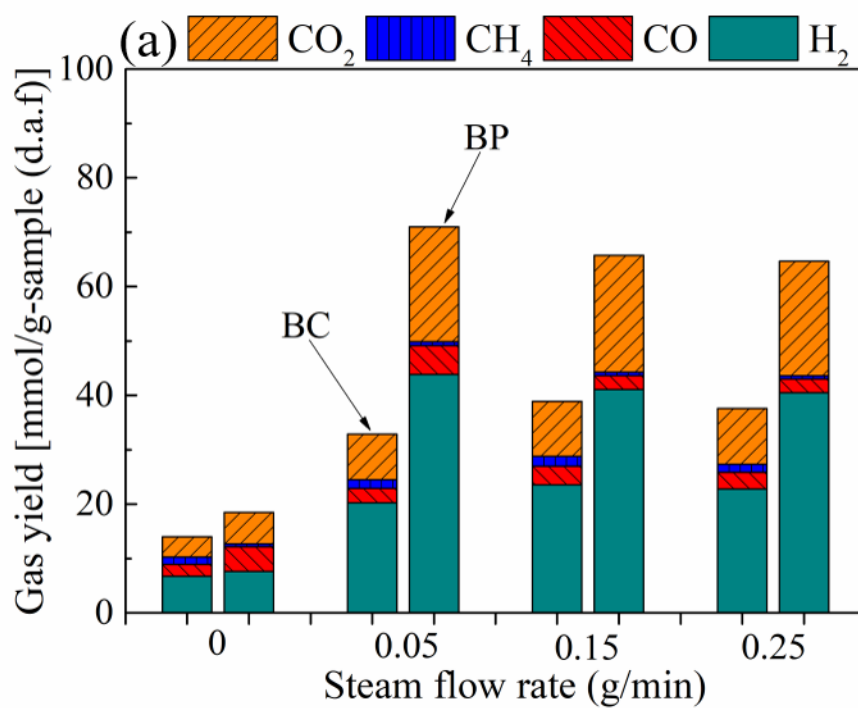
As shown in **Fig 5.5a**, the gas yields from individual BP and BC showed different trends with the increase of the steam flow rate. In the case of BC, the gas yield from pyrolysis process was only 14.0 mmol/g-sample with 46 wt% of solid residues (char) remaining in the reactor. While, by introducing steam into the reactor with a steam flow rate of 0.05 g/min, the total gas yield was increased to 32.9 mmol/g-sample with a decreased char yield of 42 wt%. The total gas production from BC gasification increased with increasing the steam flow rate from 0.05 to 0.15 g/min, but showed a slight decrease with the further increasing steam flow rate to 0.25 g/min. Herein, the low gas yield and high char yield should be mainly attributed to the low

gasification reactivity of BC at the low gasification temperature (750 °C). In comparison, the gas yield, especially H<sub>2</sub> yield from BP increased significantly with the introduction of steam. That is, 18.5 mmol/g-sample of total gas production from the pyrolysis at 750°C, but the total gas production was increased to 71.0 mmol/g-sample from the steam gasification of BP with a steam flow rate of 0.05 g/min. Moreover, the total gas production decreased only slightly with further increasing the steam flow rate. In addition, the largest gas production from BP was obtained from the case with the lowest steam flow rate, which might be attributed to the low content of fixed carbon and the high content of K. Furthermore, about 27 wt% of biochar was derived from BP in the absence of steam, which is much less than that from BC, however, almost no solid residues remained after applying steam into the reactor, indicating that the reaction **R3** was highly enhanced with the addition of steam. It also should be mentioned that the gas productions from the two samples were almost identical in the absence of steam, implying a larger amount of tar generated from BP during the pyrolysis process. Generally, the addition of steam can also enhance the tar cracking/reforming by dissociating the compounds to form a large number of H/O/OH free radicals, which are further adsorbed by the active sites on the char surface to promote tar catalytic decomposition [58, 59], resulting in a great increase in gas production, especially H<sub>2</sub> production. While, it was reported that K compounds in the biomass could reduce the bond energy of the aromatic ring to promote homogeneous steam tar reforming, thus reducing the tar yield [40, 60].

**Fig 5.5b** compares the experimental data in the co-gasifications of BP and BC with different steam flow rates and the corresponding calculated values. For the pyrolysis process, the gas yields from the pyrolysis process were almost identical with those calculated values while the

yields of char were higher than those predicted results. This might be attributed to the adsorption of the volatiles with H and OH free radicals on the coal char surface [48, 61, 62]. The similar co-pyrolysis behaviors were observed by Zhao et al [18], in which they co-pyrolyzed the mixture sample of wheat straw and lignite at a temperature range of 700-900°C but did not obtain obvious synergy effect at a temperature lower than 800°C. The Elemental and XRF analyses were conducted for the obtained char residues since the large contents of chars were produced during the pyrolysis process in the present work. As summarized in **Table 5.3**, the carbon contents of chars derived from BP and BC were both higher than that of their raw samples (**Table 5.1**). While, the carbon content of the char obtained from co-pyrolysis process was also higher than expected, indicating the volatiles from BP might be adsorbed by coal char. In addition, as can be seen in **Table 5.4**, BC char and BP char were dominated by Fe and K respectively, but the mixture char was dominated only by K, which also indicated that the K species evaporated with the tar should be adsorbed on the generated mixture char. Although the mixture char formed in the absence of steam contained high carbon content and high K content, the gas yield and carbon conversion were both low. Nevertheless, the gas yield from the mixture sample increased significantly after introducing the steam to the reactor. Although the inhibition effect occurred at the low steam flow rate (0.05 g/min), the more obvious synergistic effect was observed by further increasing the steam flow rate. The total syngas yields were increased from 16.5 to 85.7 mmol/g-sample with the increasing of the steam flow rate from 0 to 0.25 g/min, which increased more than 5 times larger with introducing a sufficient amount of steam. The biggest excess growth rate was obtained at the steam flow rate of 0.25 g/min, with 40.3% of more syngas generated from the experiment when compared with

the calculated values. This implied the necessity of the steam introduction for promoting the interaction between BP and BC and also promoting the catalytic effect of AAEM species. The different trends obtained from the steam gasifications of individual and mixture samples indicated that BP could provide catalytic effect to enhance the steam gasification reactivity of BC by promoting the **R3**, but a larger steam amount was required due to the high carbon content of mixture char. Moreover, as shown in **Fig 5.5c**, the CCE of the co-gasification process increased sharply with the increase in steam flow rate. It almost reached 70% at the steam flow rate of 0.25 g/min, which was significantly higher than the corresponding calculated value (42%). The tar produced during the co-gasification process at the higher steam flow rates (0.15 and 0.25 g/min) should be catalytically reformed since the high K content in the mixture sample could not only enhance the gasification reactivity of BC but also provide catalytic effect on tar reforming, resulting in a higher H<sub>2</sub>-rich syngas production.



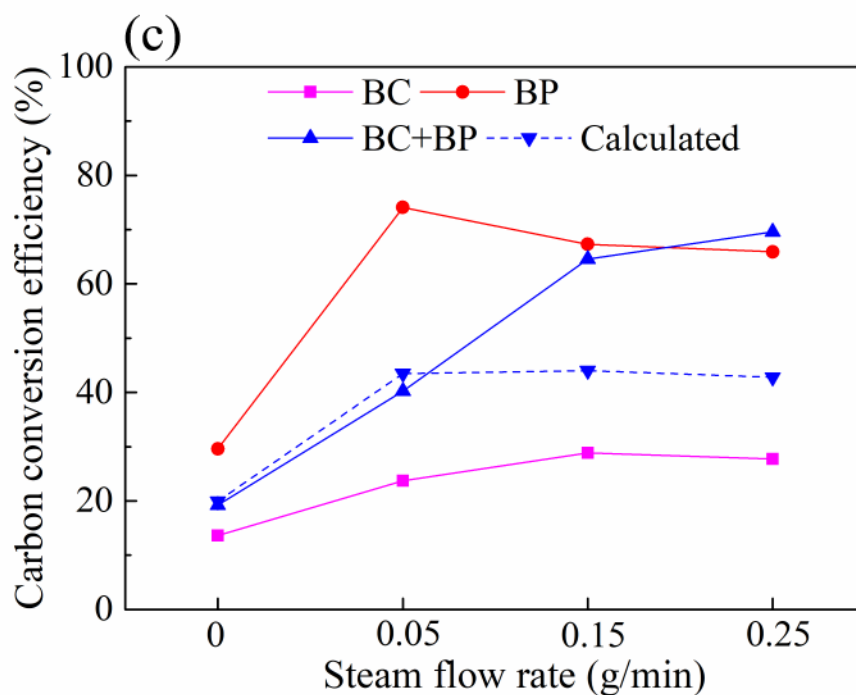


**Fig 5.5** Gas yields from the steam gasifications of individual samples (a) and mixture sample (b) at 750 °C with different steam flow rates ; (c) carbon conversion efficiency to gas.

**Table 5.3** Elemental analysis results of chars derived from pyrolysis of BP, BC, and their mixture sample at 750 °C.

| Ultimate Analysis ( wt% ) |      |     |     |
|---------------------------|------|-----|-----|
|                           | C    | H   | N   |
| <b>BP-char</b>            | 46.3 | 2.1 | 0.8 |
| <b>BC-char</b>            | 86.1 | 2.2 | 0.9 |
| <b>Mixture-char</b>       | 76.6 | 1.7 | 0.8 |

**Table 5.4** Main components of chars derived from pyrolysis of BP, BC, and their mixture sample at 750 °C.

| <b>XRF analysis (wt%)</b> |          |           |           |           |           |           |
|---------------------------|----------|-----------|-----------|-----------|-----------|-----------|
|                           | <b>K</b> | <b>Al</b> | <b>Cl</b> | <b>Ca</b> | <b>Si</b> | <b>Fe</b> |
| <b>BC char</b>            | 6.9      | 17.1      | n.d       | 9.1       | n.d       | 53.2      |
| <b>BP char</b>            | 51.1     | 18.1      | 20.9      | 1.9       | 3.3       | 1.8       |
| <b>Mixture char</b>       | 52.9     | 18.6      | 18.1      | 3.6       | 2.4       | 2.2       |

## 5.4 Conclusion

Steam co-gasification of waste BP and BC was performed in order to investigate the feasibility for H<sub>2</sub>-rich gas production by using waste fruit and low-rank coal. The effects of reaction temperature, mixing ratio, reaction time, and steam flow rate on gas yields were studied. It is found that gasification reactivity of BP and the related gas production yields were significantly higher than those of BC at a temperature lower than 800 °C due to the high content of potassium species in BP. Although BC had a low gasification reactivity and produced a larger amount of char at the low reaction temperature (750 °C), the gasification reactivity can be enhanced efficiently with the addition of BP, resulting in a high H<sub>2</sub>-rich gas production yield with less char yield. The synergistic effect between BP and BC was observed in all investigated three blending weight ratios (i.e., 1:1, 1:4, 4:1), which may provide a more flexible option for the large-scale application. Especially, the blending ratio of 1:1 resulted in the largest excessive gas production compared with the calculated values. In addition, no obvious synergistic effect

can be obtained in the absence of steam, indicating that steam should be an important factor to promote the synergistic effect and H<sub>2</sub>-rich gas production.

## References

- [1] Sharma A, Pareek V, Zhang D. Biomass pyrolysis—A review of modelling, process parameters and catalytic studies. *Renewable and Sustainable Energy Reviews*. 2015;50:1081-96.
- [2] Chen X, Liu L, Zhang L, Zhao Y, Qiu P. Gasification reactivity of co-pyrolysis char from coal blended with corn stalks. *Bioresource Technology*. 2019;279:243-51.
- [3] Balat M, Balat M, Kırtay E, Balat H. Main routes for the thermo-conversion of biomass into fuels and chemicals. Part 1: Pyrolysis systems. *Energy Conversion and Management*. 2009;50:3147-57.
- [4] Wu Z, Wang S, Zhao J, Chen L, Meng H. Synergistic effect on thermal behavior during co-pyrolysis of lignocellulosic biomass model components blend with bituminous coal. *Bioresource Technology*. 2014;169:220-8.
- [5] Chen X, Zhao Y, Liu L, Zhang L, Zhang Z, Qiu P. Evaluation of chemical structure, pyrolysis reactivity and gaseous products of Shenmu coal of different particle sizes. *Journal of Analytical and Applied Pyrolysis*. 2018;130:294-304.
- [6] Seçer A, Fakı E, Türker Üzden Ş, Hasanoğlu A. Hydrothermal co-gasification of sorghum biomass and çan lignite in mild conditions: An optimization study for high yield hydrogen production. *International Journal of Hydrogen Energy*. 2020;45:2668-80.
- [7] Masnadi MS, Grace JR, Bi XT, Lim CJ, Ellis N, Li YH, et al. From coal towards renewables: Catalytic/synergistic effects during steam co-gasification of switchgrass and coal in a pilot-scale bubbling fluidized bed. *Renewable Energy*. 2015;83:918-30.
- [8] Masnadi MS, Grace JR, Bi XT, Lim CJ, Ellis N. From fossil fuels towards renewables: Inhibitory and catalytic effects on carbon thermochemical conversion during co-gasification of biomass with fossil fuels. *Applied Energy*. 2015;140:196-209.
- [9] Wei J, Guo Q, He Q, Ding L, Yoshikawa K, Yu G. Co-gasification of bituminous coal and

hydrochar derived from municipal solid waste: Reactivity and synergy. *Bioresource Technology*. 2017;239:482-9.

[10] Ding L, Zhou Z, Huo W, Wang Y, Yu G. In Situ Heating Stage Analysis of Fusion and Catalytic Effects of a  $\text{Na}_2\text{CO}_3$  Additive on Coal Char Particle Gasification. *Industrial & Engineering Chemistry Research*. 2014;53:19159-67.

[11] Zhang Y, Zheng Y, Yang M, Song Y. Effect of fuel origin on synergy during co-gasification of biomass and coal in  $\text{CO}_2$ . *Bioresource Technology*. 2016;200:789-94.

[12] Jeong HJ, Park SS, Hwang J. Co-gasification of coal–biomass blended char with  $\text{CO}_2$  at temperatures of 900–1100°C. *Fuel*. 2014;116:465-70.

[13] Masnadi MS, Grace JR, Bi XT, Ellis N, Lim CJ, Butler JW. Biomass/coal steam co-gasification integrated with in-situ  $\text{CO}_2$  capture. *Energy*. 2015;83:326-36.

[14] Li S, Chen X, Liu A, Wang L, Yu G. Study on co-pyrolysis characteristics of rice straw and Shenfu bituminous coal blends in a fixed bed reactor. *Bioresource Technology*. 2014;155:252-7.

[15] Chen C, Ma X, He Y. Co-pyrolysis characteristics of microalgae *Chlorella vulgaris* and coal through TGA. *Bioresource Technology*. 2012;117:264-73.

[16] Wei J, Guo Q, Chen H, Chen X, Yu G. Study on reactivity characteristics and synergy behaviours of rice straw and bituminous coal co-gasification. *Bioresource technology*. 2016;220:509-15.

[17] Cabuk B, Duman G, Yanik J, Olgun H. Effect of fuel blend composition on hydrogen yield in co-gasification of coal and non-woody biomass. *International Journal of Hydrogen Energy*. 2020;45:3435-43.

[18] Zhao S, Yang P, Liu X, Zhang Q, Hu J. Synergistic effect of mixing wheat straw and lignite in co-pyrolysis and steam co-gasification. *Bioresource Technology*. 2020;302:122876.

[19] Zou X, Ding L, Gong X. Study on the Co-gasification Reactivity and Interaction Mechanism of Coal with Different Components of Daily Food Waste. *Energy & Fuels*. 2020;34:1728-36.

[20] Yip K, Tian F, Hayashi J-i, Wu H. Effect of Alkali and Alkaline Earth Metallic Species on Biochar Reactivity and Syngas Compositions during Steam Gasification. *Energy & Fuels*.

2010;24:173-81.

[21] Situmorang YA, Zhao Z, Chaihad N, Wang C, Anniwaer A, Kasai Y, et al. Steam gasification of co-pyrolysis chars from various types of biomass. *International Journal of Hydrogen Energy*. 2021;46:3640-50.

[22] Kumabe K, Hanaoka T, Fujimoto S, Minowa T, Sakanishi K. Co-gasification of woody biomass and coal with air and steam. *Fuel*. 2007;86:684-9.

[23] Zhu W, Song W, Lin W. Catalytic gasification of char from co-pyrolysis of coal and biomass. *Fuel Processing Technology*. 2008;89:890-6.

[24] McLendon TR, Lui AP, Pineault RL, Beer SK, Richardson SW. High-pressure co-gasification of coal and biomass in a fluidized bed. *Biomass and Bioenergy*. 2004;26:377-88.

[25] Lorenz BA-S, Hartmann M, Langen N. What makes people leave their food? The interaction of personal and situational factors leading to plate leftovers in canteens. *Appetite*. 2017;116:45-56.

[26] Xu Z, Zhang Z, Liu H, Zhong F, Bai J, Cheng S. Food-away-from-home plate waste in China: Preference for variety and quantity. *Food Policy*. 2020;97:101918.

[27] Su G, Ong HC, Fattah IMR, Ok YS, Jang J-H, Wang C-T. State-of-the-art of the pyrolysis and co-pyrolysis of food waste: Progress and challenges. *Science of The Total Environment*. 2021:151170.

[28] Alzate Acevedo S, Díaz Carrillo ÁJ, Flórez-López E, Grande-Tovar CD. Recovery of Banana Waste-Loss from Production and Processing: A Contribution to a Circular Economy. *Molecules*. 2021;26.

[29] FAO. Banana Market Review 2019. Rome, Italy: FAO; 2020. <https://www.fao.org/publications/card/en/c/CB0168EN/> (accessed 10 November 2021)

[30] IEA. Global Energy Review. Paris: IEA; 2021. <https://www.iea.org/reports/global-energy-review-2021> (accessed 10 November 2021)

[31] Anniwaer A, Chaihad N, Zhang M, Wang C, Yu T, Kasai Y, et al. Hydrogen-rich gas production from steam co-gasification of banana peel with agricultural residues and woody biomass. *Waste Management*. 2021;125:204-14.

[32] Saeed S, Ur Rehman Baig U, Tayyab M, Altaf I, Irfan M, Raza SQ, et al. Valorization of

banana peels waste into biovanillin and optimization of process parameters using submerged fermentation. *Biocatalysis and Agricultural Biotechnology*. 2021;36:102154.

[33] Mishra RR, Samantaray B, Chandra Behera B, Pradhan BR, Mohapatra S. Process optimization for conversion of Waste Banana peels to biobutanol by A yeast Co-Culture fermentation system. *Renewable Energy*. 2020;162:478-88.

[34] Nathoa C, Sirisukpoca U, Pisutpaisal N. Production of Hydrogen and Methane from Banana Peel by Two Phase Anaerobic Fermentation. *Energy Procedia*. 2014;50:702-10.

[35] Maity S, Das S, Mohapatra S, Tripathi AD, Akthar J, Pati S, et al. Growth associated polyhydroxybutyrate production by the novel *Zobellella tiwanensis* strain DD5 from banana peels under submerged fermentation. *International Journal of Biological Macromolecules*. 2020;153:461-9.

[36] Anniwaer A, Yu T, Chaihad N, Situmorang YA, Wang C, Kasai Y, et al. Steam gasification of marine biomass and its biochars for hydrogen-rich gas production. *Biomass Conversion and Biorefinery*. 2020.

[37] Anniwaer A, Chaihad N, Zahra ACA, Yu T, Kasai Y, Kongparakul S, et al. Steam co-gasification of Japanese cedarwood and its commercial biochar for hydrogen-rich gas production. *International Journal of Hydrogen Energy*. 2021;46:34587-98.

[38] Pandey B, Prajapati YK, Sheth PN. Recent progress in thermochemical techniques to produce hydrogen gas from biomass: A state of the art review. *International Journal of Hydrogen Energy*. 2019;44:25384-415.

[39] Rizkiana J, Guan G, Widayatno WB, Hao X, Huang W, Tsutsumi A, et al. Effect of biomass type on the performance of cogasification of low rank coal with biomass at relatively low temperatures. *Fuel*. 2014;134:414-9.

[40] Yu T, Abudukeranmu A, Anniwaer A, Situmorang YA, Yoshida A, Hao X, et al. Steam gasification of biochars derived from pruned apple branch with various pyrolysis temperatures. *International Journal of Hydrogen Energy*. 2019.

[41] Mitsuoka K, Hayashi S, Amano H, Kayahara K, Sasaoaka E, Uddin MA. Gasification of woody biomass char with CO<sub>2</sub>: The catalytic effects of K and Ca species on char gasification reactivity. *Fuel Processing Technology*. 2011;92:26-31.

- [42] Wang J, Jiang M, Yao Y, Zhang Y, Cao J. Steam gasification of coal char catalyzed by  $K_2CO_3$  for enhanced production of hydrogen without formation of methane. *Fuel*. 2009;88:1572-9.
- [43] Nzihou A, Stanmore B, Sharrock P. A review of catalysts for the gasification of biomass char, with some reference to coal. *Energy*. 2013;58:305-17.
- [44] Lv X, Xiao J, Shen L, Zhou Y. Experimental study on the optimization of parameters during biomass pyrolysis and char gasification for hydrogen-rich gas. *International Journal of Hydrogen Energy*. 2016;41:21913-25.
- [45] Jiang L, Hu S, Wang Y, Su S, Sun L, Xu B, et al. Catalytic effects of inherent alkali and alkaline earth metallic species on steam gasification of biomass. *International Journal of Hydrogen Energy*. 2015;40:15460-9.
- [46] Wei J, Guo Q, Gong Y, Ding L, Yu G. Synergistic effect on co-gasification reactivity of biomass-petroleum coke blended char. *Bioresource Technology*. 2017;234:33-9.
- [47] Fernandes R, Hill JM, Kopyscinski J. Determination of the Synergism/Antagonism Parameters during Co-gasification of Potassium-Rich Biomass with Non-biomass Feedstock. *Energy & Fuels*. 2017;31:1842-9.
- [48] Yuan S, Dai Z-h, Zhou Z-j, Chen X-l, Yu G-s, Wang F-c. Rapid co-pyrolysis of rice straw and a bituminous coal in a high-frequency furnace and gasification of the residual char. *Bioresource Technology*. 2012;109:188-97.
- [49] Satyam Naidu V, Aghalayam P, Jayanti S. Synergetic and inhibition effects in carbon dioxide gasification of blends of coals and biomass fuels of Indian origin. *Bioresource Technology*. 2016;209:157-65.
- [50] Zhang Z, Pang S, Levi T. Influence of AAEM species in coal and biomass on steam co-gasification of chars of blended coal and biomass. *Renewable Energy*. 2017;101:356-63.
- [51] Xu C, Hu S, Xiang J, Zhang L, Sun L, Shuai C, et al. Interaction and kinetic analysis for coal and biomass co-gasification by TG–FTIR. *Bioresource Technology*. 2014;154:313-21.
- [52] Wei J, Wang M, Wang F, Song X, Yu G, Liu Y, et al. A review on reactivity characteristics and synergy behavior of biomass and coal Co-gasification. *International Journal of Hydrogen Energy*. 2021;46:17116-32.

- [53] Habibi R, Kopyscinski J, Masnadi MS, Lam J, Grace JR, Mims CA, et al. Co-gasification of Biomass and Non-biomass Feedstocks: Synergistic and Inhibition Effects of Switchgrass Mixed with Sub-bituminous Coal and Fluid Coke During CO<sub>2</sub> Gasification. *Energy & Fuels*. 2013;27:494-500.
- [54] Tang J, Wang J. Catalytic steam gasification of coal char with alkali carbonates: A study on their synergic effects with calcium hydroxide. *Fuel Processing Technology*. 2016;142:34-41.
- [55] Jiang M-Q, Zhou R, Hu J, Wang F-C, Wang J. Calcium-promoted catalytic activity of potassium carbonate for steam gasification of coal char: Influences of calcium species. *Fuel*. 2012;99:64-71.
- [56] Kaewpanha M, Guan G, Ma Y, Hao X, Zhang Z, Reubroychareon P, et al. Hydrogen production by steam reforming of biomass tar over biomass char supported molybdenum carbide catalyst. *International Journal of Hydrogen Energy*. 2015;40:7974-82.
- [57] Kalinci Y, Hepbasli A, Dincer I. Biomass-based hydrogen production: A review and analysis. *International Journal of Hydrogen Energy*. 2009;34:8799-817.
- [58] Feng D, Zhao Y, Zhang Y, Zhang Z, Sun S. Roles and fates of K and Ca species on biochar structure during in-situ tar H<sub>2</sub>O reforming over nascent biochar. *International Journal of Hydrogen Energy*. 2017;42:21686-96.
- [59] Feng D, Zhao Y, Zhang Y, Sun S. Effects of H<sub>2</sub>O and CO<sub>2</sub> on the homogeneous conversion and heterogeneous reforming of biomass tar over biochar. *International Journal of Hydrogen Energy*. 2017;42:13070-84.
- [60] Li CZ, Sathe C, Kershaw JR, Pang Y. Fates and roles of alkali and alkaline earth metals during the pyrolysis of a Victorian brown coal. *Fuel*. 2000;79:427-38.
- [61] Krerkkaiwan S, Fushimi C, Tsutsumi A, Kuchonthara P. Synergetic effect during co-pyrolysis/gasification of biomass and sub-bituminous coal. *Fuel Processing Technology*. 2013;115:11-8.
- [62] Sonobe T, Worasuwanarak N, Pipatmanomai S. Synergies in co-pyrolysis of Thai lignite and corncob. *Fuel Processing Technology*. 2008;89:1371-8.

## CHAPTER 6: Conclusions and Future Perspective

### 6.1 Conclusions

Steam gasification is a promising technology to utilize and convert the energy content of biomass resources into the syngas product enriched in  $H_2$  and CO, which has higher efficiency and less GHG gas emissions compared with the direct combustion process. Moreover, the producer syngas with high content of  $H_2$  provides more options to utilize the syngas products from biomass gasification such as chemical or bio-oil synthesis other than electricity. However, the utilization of biomass resources in large-scale industrial applications is limited due to several disadvantages such as low bulk density, low energy density, wide and thin distribution, and unstable seasonal supply. The combination of different types of biomass is considered as a sustainable way to use biomass in large-scale applications. Nevertheless, different types of biomass have different physicochemical properties resulting in different gasification reactivity and optimum gasification conditions. In other words, the lab-scale preliminary investigations on the compatibility of mixture feedstock and feasibility of  $H_2$ -rich syngas production are necessary in order to use co-feedstock efficiently in large-scale applications. In this study, biomass wastes were combined with different types of carbon-based solid materials such as biomass, biochar, and coal to investigate compatibility and the potential synergy effect via the steam co-gasification process. The effects of operating parameters including feedstock types, reaction temperature, reaction time, steam flow rate, mixing ratios, catalyst loading amount on gasification reactivity and  $H_2$ -rich syngas yields were investigated in detail.

**In Chapter 1**, research motivation, basic principles of biomass gasification, and the major effect factors on gasification performances and gas yields in the steam gasification process were introduced.

**In Chapter 2**, the gasification feedstock and the catalyst used in this research were described. The various types of characterization apparatuses used in this study were also listed.

**In Chapter 3**, the common biomass wastes including fruit waste (banana peel), woody biomass (cedarwood), and agricultural residues (rice husk) were selected as the steam co-gasification feedstock in order to investigate the compatibility of mixture samples and synergistic effect of

different biomass with different inorganic species. It is found that banana peel (BP) is easier to be gasified at a low gasification temperature and produces a significantly higher content of H<sub>2</sub>-rich syngas compared with rice husk (RH) and cedarwood (CW) in the steam gasification process. The ash content and inorganic compounds show a strong influence on gasification reactivity. The ash contents of the three samples are as follows RH>BP>CW (18 wt%>10 wt%>2 wt%), containing high content of Si, K, and Ca respectively. BP contains a large content of K species in its ashes which can provide a self-catalytic effect during the steam gasification process, resulting in a high gasification reactivity and H<sub>2</sub> production. While RH contains a large content of Si species shows a low gasification reactivity which is difficult to be fully gasified at a lower gasification temperature and produce large content of biochar instead of H<sub>2</sub>-rich gas production. CW, on the other hand, with a low ash content but high Ca species in its ash can be easily gasified at a low reaction temperature with almost no solid residues remaining. But the gas yield is really low from steam gasification of CW, which means large content of tar is generated instead of H<sub>2</sub>-rich syngas production. From the results of steam gasification of three different samples individually, the importance of biomass types and physicochemical characteristics are emphasized. By applying the co-gasification process, the low gasification reactivity of RH and the tendency of tar production of CW are highly improved. The co-gasification of RH and CW with BP shows a positive synergistic effect, resulting in a higher co-gasification reactivity and higher H<sub>2</sub>-rich syngas yields compared with the predicted results. Moreover, the addition of calcined seashells as the CaO catalyst is found to be able to offset the negative effect of Si species in the RH, further improving the H<sub>2</sub> production yield.

**In Chapter 4**, Japanese cedarwood and its commercial biochar obtained from a high-temperature carbonization process were utilized as the steam gasification feedstock. In the last work as described in **Chapter 3**, cedarwood (CW) contained large content of lignin and volatile matters leading to a high amount of tar formation during the steam gasification process. Therefore, carbonization as a pretreatment process is applied prior to the steam gasification process, as a result, significantly larger gas production and less tar production can be obtained from the commercial biochar compared with the raw cedarwood. The carbonization process not only leads to the evaporation of volatile matters but also leads to structural changes. The

collapse of the surface structure increases the surface area and exposes the inner porous structures, which can improve the contact between biochar with the gasifying agent, resulting in a higher gas production yield. As mentioned in **Chapter 1**, biochar can be utilized as a catalyst for tar cracking/reforming. It is found that the catalytic effect and the synergistic effect can be obtained by co-gasifying the raw biomass and the biochar with the mixing ratios of 1:1 or 1:2 in this work. The synergistic effect should be attributed to the tar produced from raw biomass is catalytically reformed into the H<sub>2</sub>-rich syngas by the biochar. However, increasing the amount of raw biomass in the mixture sample leads to coke deposition on the surface and covers the active sites of the biochar, decreasing the gasification reactivity of the biochar sample.

In **Chapter 5**, steam co-gasification of waste banana peel and brown coal was performed in order to investigate compatibility and feasibility for H<sub>2</sub>-rich syngas production by using fruit waste and low-rank coal. In the previous work as described in **Chapter 3**, banana peel shows great potential to be utilized as the gasification feedstock, which not only has a high gasification reactivity but also can provide catalytic effect during the co-gasification process with rice husk and cedarwood. Therefore, in this work, the co-gasification performances and the potential synergistic effect with brown coal were investigated. The effects of reaction temperature, mixing ratio, reaction time, and steam flow rate on gas yields were studied. It is found that the synergistic effect between BP and BC can be obtained in all investigated three blending weight ratios (i.e., 1:1, 1:4, 4:1), which may provide a more flexible option for the large-scale application. Especially, the blending ratio of 1:1 resulted in the largest excessive gas production compared with the calculated values. In addition, no obvious synergistic effect can be obtained in the absence of steam, indicating that steam should be an important factor to promote the synergistic effect and H<sub>2</sub>-rich gas production. The combination of waste fruit and coal not only provides a better way of waste treatment but also decreases the dependency and usage amount of fossil fuels, potentially reducing GHG emissions.

## 6.2 Future perspective

With the increase in the global human population, not only the demand for energy increased, the global food demand also increased significantly in recent years. As mentioned in **Chapter**

5, Food and Agriculture Organizations (FAO) reported that one-third of the food produced for human consumption (1.3 billion tons) is wasted in the food supply chains including harvest, processing, transportation, and consumption, and it is estimated that the food waste generated in the urban area will increase to 138 million tons by 2025. The increasing and uncontrolled production of food waste is arousing a global concern about the sustainability of the food supply and the environmental problem. The majority of food wastes are discarded in landfills, contributing about 8% of total GHG emissions to the environment. The concept of circular bioeconomy is considered as a viable solution to reduce the losses caused by food waste disposal and also maximize the value of food. The main target of the circular bioeconomy is to utilize and convert waste into wealth. As shown in **Fig. 6-1**, the food wastes generated from industries or households are recycled instead of discarded in landfills. The recycled food waste then can be utilized as gasification feedstock for hydrogen production or power generation after adopting appropriate pretreatment such as size reduction, drying, torrefaction, and palletization. The power and heat generated from the gasification plant using food waste as the feedstock can supply energy to agricultural fields, food processing industries, and also the households. As mentioned in **Chapter 1**, biomass energy can be considered as “Carbon Neutral”, since the emission of CO<sub>2</sub> from the gasification plant can be absorbed by the growing biomass in the farmland such as banana, orange, rice, wheat, and so on. Therefore, the utilization of biomass energy can not only contribute to circular economy but also the carbon-neutral society. In this study, banana peel as a typical food waste was selected as the gasification feedstock for hydrogen production. From the results described in **Chapter 3** and **Chapter 5**, the gasification reactivity and total syngas yields of banana peel were obviously higher than that of common biomass gasification feedstock (i.e., cedarwood, rice husk) and common coal gasification feedstock (brown coal), especially at a low reaction temperature. Moreover, banana peel also showed a great performance in the co-gasification process by providing a catalytic effect on enhancing co-gasification reactivity and hydrogen production due to the high content of AAEM in its ash residues. This study also can be considered as a part of circular bioeconomy, applying one kind of waste biomass (banana peel) enriched in AAEM compounds in it to improve co-gasification reactivity and hydrogen gas production from rice husk, cedarwood, and brown coal.

The waste amount and reaction temperature were decreased and syngas production was increased by utilizing food waste and applying co-gasification process. In addition, as noted in **Chapter 5**, India and China are the top two countries for banana production and also the top two countries for energy consumption. Therefore, it might be a good way to utilize food waste such as banana peel, collecting the banana peel from food processing industries and co-gasifying it with coal in the energy sector. Utilization of banana peel in this experimental study is an example for achieving circular bioeconomy in near future. The other types of food waste or fruit waste are also worth to investigating the feasibility of hydrogen production via the co-gasification process (e.g., citrus peel, apple peel, kiwi peel, etc).

On the other hand, gasification of raw biomass has exposed some disadvantages, such as low heating value due to the high moisture content and oxygen content, high storage and transportation costs due to the low density, and biological degradation risks. Therefore, pretreatment methods are important to improve the conditions of biomass feedstock for enhancing the gasification reactivity. As described in **Chapter 4**, the raw biomass sample (cedarwood) containing large content of lignin and volatile matters always leads to a high amount of tar formation during the gasification reaction. However, with the introduction of the carbonization process prior to the steam gasification process, larger gas production and less tar production were obtained. From various analysis results, both chemical and physical characteristics of cedarwood were improved via the carbonization process, increasing the gasification reactivity and total syngas production. However, the high energy input for high-temperature carbonization process needs to be considered and further studied. Torrefaction, otherwise, may be a feasible pretreatment method for biomass feedstock. Torrefaction is a mild thermal degradation process conducted in an inert atmosphere with a temperature range of 200-300 °C. Torrefaction process also can improve the properties of biomass feedstock in several ways such as reduction in moisture content and light volatile matter, and increase in heating value and carbon content, resulting in higher ignitability and reactivity. The effects of the torrefaction process on the physicochemical properties of biomass have been widely studied in recent years. However, the investigation of co-gasification performances of torrefied biochar derived from different types of biomass is still scarce, requiring more in-depth studies to utilize

biochar efficiently.

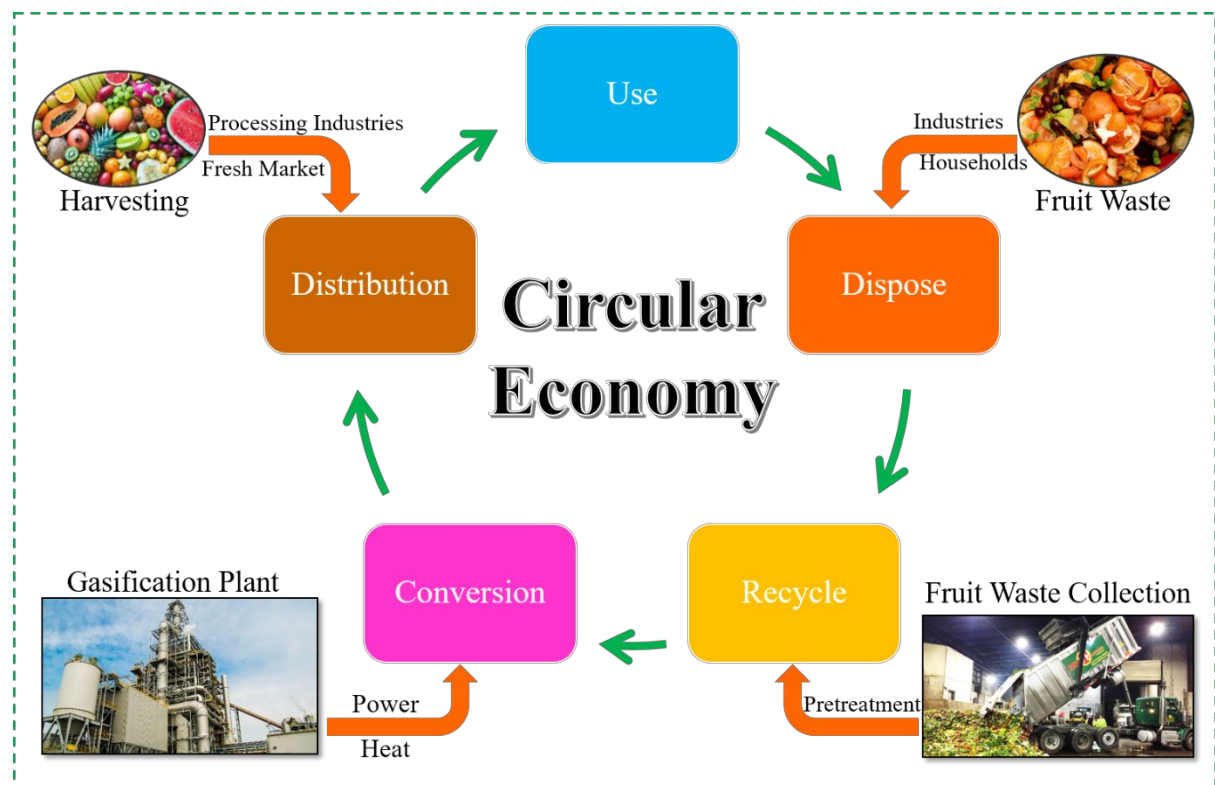


**Fig 6.1** Utilization of waste biomass for achieving the circular economy.